Load and Resistance Factor Design of Drilled Shafts in Shale Using SPT and TCP Measurements

---

A Thesis presented to
the Faculty of the Graduate School
at the University of Missouri-Columbia

In Partial Fulfillment
of the Requirements for the Degree

Master of Science

---

by

MARK D. PIERCE

Dr. J. Erik Loehr Thesis Supervisor

DECEMBER 2013

The undersigned, appointed by the dean of the Graduate School, have examined the thesis entitled

LOAD AND RESISTANCE FACTOR DESIGN OF DRILLED SHAFTS IN SHALE USING SPT AND TCP MEASUREMENTS

presented by Mark Pierce,

a candidate for the degree of master of civil engineering,

and hereby certify that, in their opinion, it is worthy of acceptance.

Professor J. Erik Loehr, P.E.

Professor John J. Bowders, P.E.

Professor Douglas E. Smith, P.E.

Dedicated to my wife for her never-failing support and patience during the completion of this thesis.

ACKNOWLEDGEMENTS

This research and thesis would not have been successfully completed without the assistance and hard work of many individuals. I would like to thank my supervising professor Dr. J. Erik Loehr for sharing his knowledge, expertise, and time while completing my research and thesis. I would also like to thank Dr. John J. Bowders and Dr. Douglas E. Smith for their comments and guidance while reviewing this thesis.

I would also like to thank Mr. Alan Miller, Jennifer Harper, and many others at MoDOT for providing the opportunity to perform this research. I would like to thank Mr. Bill Ryan, Mr. Andy Skiffington, and others from Loadtest Inc. for their assistance in successfully completing the load test program. Also, thank you to Mr. Luke Schuler from Hayes Drilling, Inc., and Mark and Bruce Murphy from Drilling Services Co. for their support and services during the drilled shaft construction.

Finally, I would like to thank Sarah Grant, Kyle Murphy, and many other University of Missouri graduate and undergraduate students, for their assistance during the drilled shaft construction and load testing.

TABLE OF CONTENTS

LIST OF ILLUSTRATIONS

Figure

LIST OF TABLES

Table

Abstract

Missouri Department of Transportation (MoDOT) designers currently follow American Association of State Highway and Transportation Officials (AASHTO) design methods for design of drilled shafts in shale and other weak rock. These methods are generally based on Load and Resistance Factor Design (LRFD) methods that relate uniaxial compressive strength measurements of rock cores to the side and tip resistance for drilled shafts. However, shale and other weak rock can be notoriously difficult to effectively sample and test, which poses practical problems for those tasked with designing drilled shafts in such materials.

The difficulty in sampling shale has lead geotechnical engineers to consider in-situ tests, such as the Standard Penetration Test (SPT) and the Texas Cone Penetration test (TCP), as surrogates for conventional coring and laboratory testing. In order to utilize results of in-situ tests for design of drilled shafts using Load and Resistance Factor Design (LRFD), it is necessary to correlate in-situ test measurements with side and tip resistance and to establish calibrated resistance factors that account for the reliability of the correlations and the in-situ test measurements. This thesis describes efforts undertaken to develop improved correlations among in-situ test measurements and drilled shaft capacity and to develop resistance factors that produce established target reliabilities for different classes of roadways.

Twenty-five drilled shafts were constructed and load tested at two shale sites in Missouri to support development of improved design methods. Ten shafts ranging from 3 to 5 feet in diameter and 20 to 35 feet in length were constructed and tested at a site near

Frankford Missouri. Fifteen, 3-foot diameter shafts ranging from 30 to 50 feet in length were constructed and tested at a site near Warrensburg Missouri. Each shaft was load tested using the Osterberg Cell (O-cell™) load testing technique to establish the ultimate side and tip resistance for each shaft. SPT and Modified Texas Cone Penetration tests (MTCP) were also conducted at each site. Results of these tests were utilized in conjunction with results of several historical load tests conducted in Missouri shales to develop correlations among side and tip resistance and SPT and MTCP measurements and to establish calibrated resistance factors for use with these techniques.

Two design methods were developed to relate ultimate unit tip and side resistance to SPT and MTCP measurements. The SPT relation for tip resistance is a linear relationship: $q_p = 0.95 \cdot \overline{N_{eq-60}}$; resistance factors for this relation range from 0.025 to 0.34. The SPT side resistance relationship is $q_s = \frac{\overline{N_{eq-60}}}{15}$ with resistance factors ranging from 0.02 to 0.26. The MTCP relationship for tip resistance is a power function, $q_p = 500 \cdot \overline{MTCP}^{-1.22}$, with resistance factors ranging from 0.04 to 0.65. The MTCP side resistance relationship is $q_p = 29 \cdot \overline{MTCP}^{-1.14}$ with resistance factors ranging from 0.03 to 0.27. The resulting design methods are expected to produce more cost effective foundations for MoDOT bridges while still achieving established target reliabilities for bridge foundations.

Chapter 1 - Introduction

An introduction of the purpose and organization of this thesis is presented in this chapter. Background information regarding the reasons for the research is first provided followed by the project objective. The scope of this research is then described followed by the organization of the thesis.

1.1 Background

Designing drilled shafts in shale in Missouri has proven to be a challenge. The challenge comes primarily from the generally low strength of many shales, the presence of secondary features (fractures, weak bedding planes, etc), and the often rapid degradation of the shale that occurs following sampling. Combined, these issues make acquisition and testing of samples that are both intact and representative difficult. In-situ testing, such as Standard Penetration Tests (SPT) and Texas Cone Penetration (TCP) tests can be used as an effective surrogate to conventional coring and laboratory testing if in-situ test measurements can be correlated to shaft capacity.

Although design methods utilizing SPT and MTCP measurements are currently available, the Missouri Department of Transportation (MoDOT) does not currently design drilled shafts using in-situ test measurements. Available design methods include an SPT-based design method utilized by the Colorado Department of Transportation (CDOT) and a TCP-based design method used by the Texas Department of

Transportation (TxDOT), respectively. The appropriateness of these design methods for use by MoDOT is currently unknown since no comparisons of measured shaft capacity and the in-situ test measurements have been made. Regardless of the appropriateness of these methods, there is need to develop resistance factors that appropriately reflect the variability of drilled shaft capacity experienced by MoDOT since this variability may vary among different agencies because of different construction practices. This provides motivation to develop "MoDOT specific" SPT and TCP design methods. Such methods can be developed from analysis of in-situ test measurements in Missouri and corresponding load test measurements.

1.2 Objectives

The objectives of this research are to: (1) develop "MoDOT specific" design relations for predicting side and tip resistance for drilled shafts in shale from SPT and TCP measurements and (2) establish appropriate resistance factors for these methods that achieve target levels of reliability established by MoDOT. Satisfying these objectives will, in turn, lead to potentially reducing the size and/or number of drilled shafts when designing from SPT and TCP measurements, which will reduce the costs of foundations for bridges founded on drilled shafts while still achieving target reliability values established by MoDOT.

1.3 Scope

To develop SPT and TCP design relationships and resistance factors, a number of load test sites were characterized using SPT and TCP measurements. These characterizations were completed for two "new" sites as well as five sites where load tests have been performed previously. The "new" load tests were performed on twenty five test shafts at two different sites. Unit side and tip resistance measurements from load tests performed at these two sites and five other historical load test sites were related to corresponding SPT and TCP measurements to develop "MoDOT specific" design relations. Resistance factors for the new MoDOT relations were then calibrated based on the variability and uncertainty in the relations to produce the target reliabilities established by MoDOT for different classes of roadways.

1.4 Organization of Thesis

This thesis is organized into nine chapters. Chapter 2 provides a review of relevant design methods for drilled shafts. Current MoDOT methods for design of drilled shafts are described along with available methods for design of drilled shafts in weak rock from in-situ test measurements.

The in-situ testing performed at the respective field test sites is described in Chapter 3 along with a summary of the load test program. Detailed descriptions of drilled shaft construction, instrumentation, and load testing are provided.

The SPT and TCP measurements taken at each site are provided in Chapter 4. Site profiles established from the SPT and TCP measurements are also presented along with summaries of the general geological conditions for each site. The variability of measurements for each site is also provided.

The proposed design relations established from analysis of the load test and in-situ test data are presented in Chapter 5. The variability and uncertainty for the respective design relations established from analysis of the load test and in-situ test data is presented in Chapter 6.

The methods used for determining resistance factor for the respective design relations are presented in Chapter 7 along with the resulting resistance factors. An example utilizing the new design methods is presented in Chapter 8 to illustrate their application. Chapter 8 also includes a comparison of the anticipated costs for shafts designed using the proposed design methods and current methods utilizing SPT and TCP measurements. Finally, Chapter 9 provides a summary of the thesis, along with a series of conclusions and recommendations drawn from the work performed.

Chapter 2 - Literature Review

2.1 Introduction

Several methods used for design of drilled shafts in shale and other weak rock are described in this chapter. The Missouri Department of Transportation's (MoDOT's) current methods for prediction of side and tip resistance for drilled shafts in shale and weak rock are first described. Methods that can be used for design of drilled shafts in weak rock from results of SPT tests are then summarized. Finally, two available methods for design of drilled shafts from results of TCP measurements are presented.

2.2 MoDOT Drilled Shaft Design Methods

MoDOT does not currently design drilled shafts based on SPT or TCP measurements, but rather designs drilled shafts from results of uniaxial compression tests on intact rock core. In 2009, MoDOT's Engineering Policy Guide (EPG) recommended that unit side resistance for drilled shafts be estimated as (MoDOT, 2009):

$$q_{s-ult} = 0.65 \cdot \alpha_E p_a \cdot \left({}^{q_u}/_{p_a}\right)^{0.5} < 7.8 \cdot p_a \cdot \left({}^{f'_c}/_{p_a}\right)^{0.5} \quad (2.1)$$

where q_{s-ult} is the predicted ultimate unit side resistance (in ksf), α_E is a dimensionless reduction factor to account for jointing in rock (O'Neill and Reese, 1999), p_a is

atmospheric pressure (=2.12 ksf), q_u is the uniaxial compressive strength of intact rock core (in ksf), and f'_c is the concrete compressive strength (in ksi).

In most cases, past MoDOT practice has been to neglect any tip resistance provided by drilled shafts. However, in cases where tip resistance is considered, the 2009 EPG recommended that unit tip resistance be estimated as

$$q_{p-ult} = 2.5 * q_u \text{ (ksf)} \quad (2.2)$$

where q_{p-ult} is the predicted ultimate unit tip resistance, and q_u is the uniaxial compressive strength of rock core (in ksf).

Although MoDOT does not routinely design drilled shafts based on SPT measurements, such methods have been used on occasion for specific MoDOT projects. In particular, SPT-based methods were used for design of drilled shafts for the I-64/US40 design-build project in St. Louis (URS Corporation, 2007). In this case, the methods used were derived from local experience and methods described in the following section.

2.3 Methods for Design of Drilled Shafts from SPT Measurements

Like Missouri, bridges in Colorado are commonly supported on drilled shafts founded in weak rock. Since the 1960's, the Colorado Department of Transportation (CDOT) has used empirical methods and "rules of thumb" to correlate Standard Penetration Test (SPT) measurements to side and tip resistance for drilled shafts. Two different versions of this method are described in the literature as summarized in this section.

2.3.1 Original Colorado SPT-based (CSB) Method

In the "original" Colorado SPT-based (CSB) method, the allowable unit tip resistance is predicted as

$$q_{p-all\cdot} = 0.5 \cdot N \quad (2.3)$$

where q_{p-all} is the allowable unit tip resistance (ksf), and N is the corrected SPT N-value (blows/ft). Similarly, the allowable unit side resistance is predicted as

$$q_{s-all} = 0.05 * N \quad (2.4)$$

where q_{s-all} is the allowable unit side resistance (ksf), and N is the corrected SPT N-value (blows/ft).

The SPT measurements expressed in Equations 2.3 and 2.4, and in subsequent equations, are expressed in blows per foot and are corrected for hammer efficiency. Equations 2.3 and 2.4 produce "allowable" values for unit tip and side resistance and include an unknown factor of safety inherent in the equations (Abu-Hejleh, et al. 2003). This factor of safety is frequently presumed to be equal to 3, due to the lack of information (Abu-Hejleh, et al. 2003). If the factor of safety is taken as being equal to 3, the ultimate unit tip and side resistance can respectively be predicted as

$$q_p = 1.5 \cdot N \quad (2.5)$$

and

$$q_s = 0.15 \cdot N \quad (2.6)$$

where q_p is the predicted ultimate unit tip resistance (ksf), q_s is the predicted ultimate unit side resistance (ksf), and N is the corrected SPT N-value (blows/ft).

2.3.2 Updated Colorado SPT-based (UCSB) Method

While the "original" Colorado SPT based method (CSB) described above has reportedly been used for many years without notable problems, there is also little direct evidence available to demonstrate its accuracy (Abu-Hejleh, et al. 2003). Abu-Hejleh, et al. (2003) therefore utilized results from several load test programs conducted in Colorado to develop the Updated Colorado SPT-based (UCSB) method. In the UCSB method, the allowable unit tip and side resistance are respectively predicted as

$$q_{p-all} = 0.46 * N \quad (2.7)$$

and

$$q_{s-all} = 0.037 * N \quad (2.8)$$

where q_{p-all} is the predicted allowable unit tip resistance (ksf), q_{s-all} is the predicted allowable unit side resistance (ksf), and N is the corrected SPT N-value (blows/ft).

Based on results of the load tests analyzed, Abu-Hejleh, et al. (2003) determined that the CSB method produced a factor of safety of approximately 2 for tip resistance and a factor of safety in the range of 1.3 – 1.8 for side resistance. They also found that the UCSB design method predicts side and tip resistance values that inherently have a factor of safety of approximately 2. The difference in the factors of safety can simply be attributed to the fact that the accuracy of the CSB design method was never really determined (Abu-Hejleh, et al. 2005).

Presuming a factor of safety of 2, the ultimate unit tip and side resistance for the UCSB method can be estimated as

$$q_p = 0.92 * N \quad (2.9)$$

and

$$q_s = 0.075 * N \quad (2.10)$$

where both relations produce values in units of ksf.

2.4 Methods for Design of Drilled Shafts from TCP Measurements

The Texas Department of Transportation (TXDOT) developed methods for design of drilled shafts based on Texas Cone Penetration (TCP) test measurements to address difficulties with acquiring suitable samples of shale and weak rock. The TCP test is similar to the SPT test except that a special 3-inch diameter cone is used instead of the Standard (split spoon) sampler. TCP measurements also differ from SPT measurements in that they are recorded as penetration values (measured in inches or mm) per 100 blows rather than as a number of blows for a given penetration as is done for SPT measurements.

Two alternative TCP-based design methods are presented in this section. The first method is the one currently used by TXDOT (TXDOT, 2006) and the other is a recently developed revision of the method proposed by Nam and Vipulanandan (2010) based on evaluations performed for several load tests.

2.4.1 TXDOT TCP Design Method

The TXDOT TCP Design method is implemented using design curves to predict ultimate unit side and tip resistance based on a nominal TCP value. The design curve used to predict the ultimate unit side resistance is presented in Figure 2.1 (dashed line); the ultimate unit tip resistance is predicted using the curve (dashed line) presented in Figure 2.2. The TXDOT method is appropriate for cases where the TCP value is less than twelve inches for 100 blows.

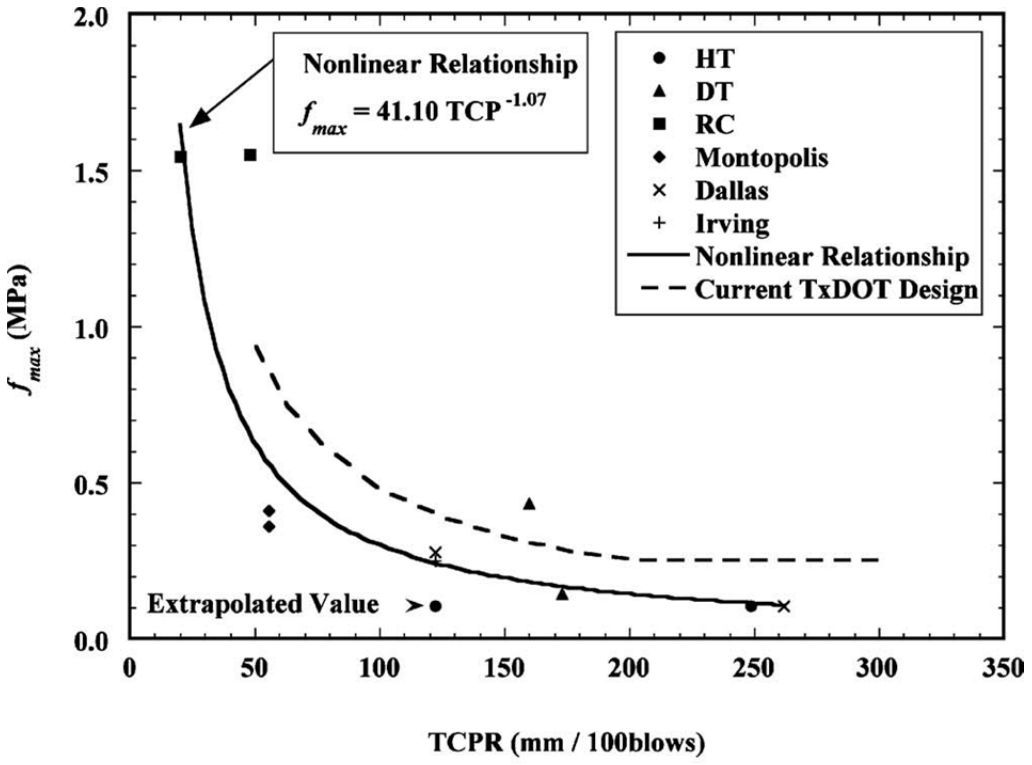

Figure 2.1- Relationship between ultimate unit side resistance (f_{max}) and TCP values proposed by Nam and Vipulanandan. (from Nam and Vipulanandan, 2010). [1 MPa = 21 ksf, 25 mm = 1 inch]

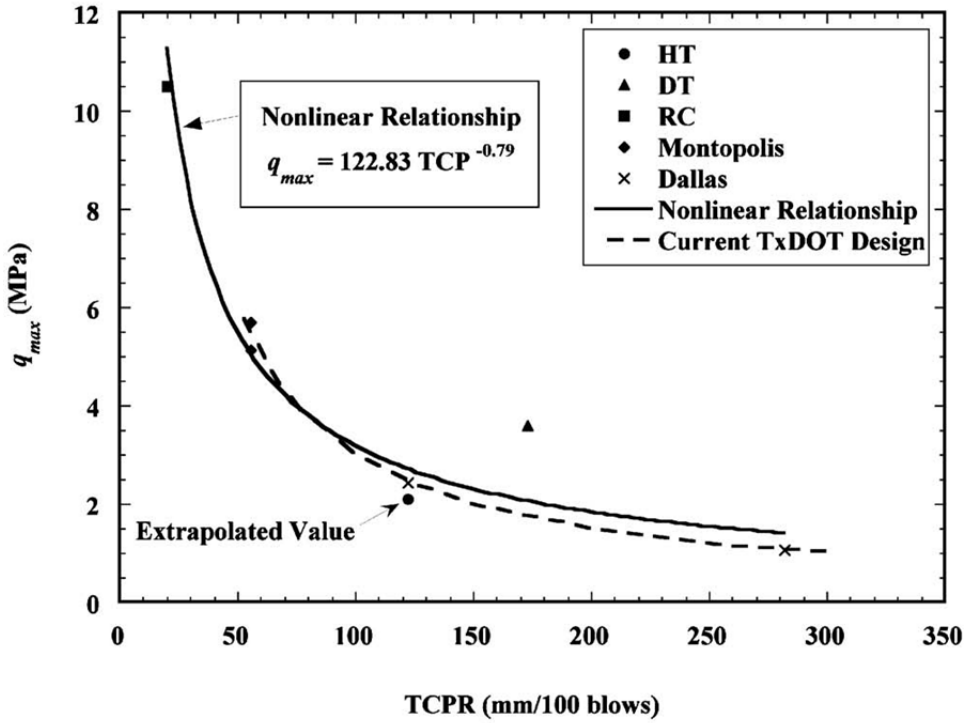

Figure 2.2- Relationship between ultimate unit tip resistance (q_{max}) and TCP values, proposed by Nam and Vipulanandan (from Nam and Vipulanandan, 2010). [1 MPa = 21 ksf, 25 mm = 1 inch]

2.4.2 Nam and Vipulanandan (2010) Method

Nam and Vipulanandan (2010) proposed revisions to the TXDOT TCP design method based on evaluation of several load tests performed in shale. The proposed method is applied similarly to the TXDOT method, but using different relations between the TCP value and unit side and tip resistance as shown using solid lines in Figures 2.1 and 2.2, respectively. The proposed design methods by Nam and Vipulanandan predict ultimate unit tip and side resistance in MPa using TCP measurements reported in millimeters per 100 blows . Therefore, the predicted relations presented in Figures 2.1 and 2.2 should be converted to predict unit tip and side resistance in ksf using TCP

measurements reported in inches per 100 blows to be consistent with the units in the remainder of this thesis. The Nam and Vipulanandan design relation for ultimate unit tip resistance, in equivalent English units, is:

$$q_{p-ult} = 500 \cdot TCP^{-0.79} \quad (2.11)$$

where q_{p-ult} is the predicted ultimate unit tip resistance (ksf), and TCP is the Texas Cone Penetration measurement (in/100 blows). The Nam and Vipulanandan design relation for ultimate unit side resistance is:

$$q_{s-ult} = 26.95 \cdot TCP^{-1.07} \quad (2.12)$$

where q_{s-ult} is the predicted ultimate unit side resistance (ksf), and TCP is the Texas Cone Penetration measurement (in/100 blows).

Both the TXDOT and Nam and Vipulanandan methods are shown in Figures 2.1 and 2.2. The solid lines indicate the relation proposed by Nam and Vipulanandan and the dashed lines indicate the current TxDOT (2006) design relations. The Nam and Vipulanandan relation predicts unit side resistance values that are generally lower than the TXDOT method. The magnitude of the difference changes due to the power function but the Nam and Vipulanandan model predicts unit side resistance values ranging from 40% to 30% less than the current (2006) TxDOT method. The Nam and Vipulanandan relation for tip resistance predicts unit tip resistance values that are similar to those produced using the TxDOT method.

Direct comparisons of the UCSB and Vipulanadan & Nam methods are not available since there is seldom both SPT and TCP measurements available for the same load test sites. The information presented in this thesis will accomplish just that, by

respectively relating SPT and TCP measurements to tip and side resistance for the same shafts.

2.5 Summary

Three different methods for prediction of drilled shaft capacity in shale and weak rock were described in this chapter. The current (2009) method used by MoDOT relates unit side and tip resistance to uniaxial compressive strength of the intact rock measured from cores. The CSB and UCSB methods utilize SPT measurements in shale and weak rock to determine unit side and tip resistance. The UCSB produces virtually the same unit tip resistance as the CSB model but predicts unit side resistance values more than 20 percent lower than predicted using the CSB method. The TXDOT and Nam and Vipulanandan methods utilize results from TCP measurements to establish unit side and tip resistance. The Nam and Vipulanandan model predicts lower unit side resistance than the TxDOT method but both predict similar unit tip resistance.

Chapter 3 - Field Testing Procedures

3.1 Introduction

In this chapter, the procedures followed for performing Standard Penetration Tests (SPT) and modified Texas Cone Penetration tests (MTCP) to characterize all load test sites are described. Procedures for construction and load testing of twenty five drilled shafts at two of these sites are then presented and relevant characteristics of the test shafts are summarized. Finally, the instrumentation and load testing methods used to establish shaft performance are described.

3.2 In-Situ Testing at Field Load Test Sites

Standard Penetration Tests (SPT) and modified Texas Cone Penetration Tests (MTCP) were performed at two new load test sites and five historical load test sites to characterize each site. Test holes were drilled using either truck-mounted or track-mounted drill rigs. SPT and MTCP tests were generally conducted using a 140 lb automatic hammer with a 30-inch drop distance and measured hammer efficiencies between 76 and 80 percent. Each type of testing was generally conducted at five- foot intervals within the boreholes, commonly alternating between SPT and MTCP tests every 2.5 feet. The procedures followed for performing the SPT and MTCP tests are described in this section.

3.2.1 Standard Penetration Tests

Standard Penetration tests were performed following common ASTM testing procedures (ASTM D1586, 2008) modified to account for the fact that the tests were conducted in shale and weak rock. SPT tests were performed at five-foot intervals in each borehole using a Standard, 2-inch O.D., split spoon sampler (Figure 3.1) that was driven into the base of the boring using an automatic 140-lb hammer. Standard penetration measurements were recorded as the number of hammer blows to penetrate the sampler in each of three 6-inch increments. The measured SPT *N*-value, denoted N_{meas}, was taken to be the sum of the number of blows over the last two 6-inch increments and recorded in blows per foot. An energy correction was applied to these measurements to arrive at the standardized N_{60}-value as:

$$N_{60} = (E_f/60) * N_{meas} \quad (3.1)$$

where E_f is the measured energy efficiency of the hammer system (in percent).

Current MoDOT practice is to cease SPT testing when 50 blows are applied over a 6-inch interval. In such cases, measurements were reported as the penetration that occurred for those 50 blows. This penetration was then converted to an "equivalent" *N*-value according to

$$N_{eq} = 12 \cdot \left(\frac{N_{meas}}{p}\right) \quad (3.2)$$

where N_{eq} is the "equivalent" *N*-value, N_{meas} is the measured number of blows, and p is the measured penetration for that number of blows in inches. Energy corrections were applied to the calculated N_{eq}-values according to Equation 3.1 to arrive at equivalent N_{eq-60} values. In cases where the Standard sampler could not be penetrated the full 6

inches during the first or second intervals, the value for N_{meas} was taken as the number of hammer blows over that interval and the value for p was taken as the penetration over that interval. In cases where the Standard sampler was penetrated a full 6 inches during the second interval but then could not be penetrated the full 6 inches during the third interval, the value for N_{meas} in Equation 3.2 was taken as the total number of blows over the second and third intervals and the value for p was taken to be the cumulative penetration over those same intervals.

Figure 3.1- In situ test devices used to characterize field load test sites: Texas Cone Penetrometer (left) and Standard split spoon sampler (right).

3.2.2 Modified Texas Cone Penetration Tests

Modified Texas Cone Penetration (MTCP) tests were performed using a 3-in diameter, heat-treated steel cone with a 60 degree apex (Figure 3.1). The standard

TXDOT procedure calls for use of a 170-lb hammer with a 24-inch drop distance (TXDOT, 2006). Since MoDOT did not have access to such a hammer, a conventional 140-lb automatic hammer, with a 30-inch drop, was used for the Texas Cone Penetration tests. Use of the conventional SPT hammer for TCP tests imparts in a nominal hammer energy of 350 ft-lbs per blow, which is slightly greater than the 340 ft-lbs per blow that is specified for TCP tests in the TXDOT Geotechnical Manual (TXDOT, 2006). TCP test measurements acquired for this research are therefore referred to as "Modified" Texas Cone Penetration (MTCP) test measurements to distinguish the measurements from those that might be obtained using the specified TCP hammer. It is presumed that measurements made following the "modified" procedure will be similar to those that would be made using the specified TXDOT hammer since the nominal hammer energy for the two hammers is similar. However, no direct comparison data is available to confirm this presumption. MTCP measurements were recorded as a penetration distance, in inches, per 100 hammer blows.

3.3 Drilled Shaft Construction

Twenty-five drilled shafts were constructed at two test sites in Missouri as a part of this research project. Ten shafts were constructed at the Frankford load test site with diameters ranging from 3 to 5 feet and lengths ranging from 20 to 35 feet. Fifteen shafts were constructed at the Warrensburg load test site, all being 3 feet in diameter and ranging from 30 to 50 feet in length. The test shafts at both sites were constructed with permanent casing through the overburden material. All shafts were constructed using the

"dry" method without slurry, although a number of test shafts had minor seepage into the base of the shaft prior to concreting. Construction details and differences among the shafts at the two test sites are described subsequently.

3.3.1 Construction of Test Shafts at Warrensburg Load Test Site

The Warrensburg Load Test Site is located near the city of Warrensburg, in west-central Missouri approximately 60 miles east of Kansas City (Figure 3.2). The site is composed of approximately 15 feet of silty clay overburden soil overlying shale formations with highly variable strength along with sporadic sandstone. The test shafts were constructed in the right-of-way for U.S. Highway 50, near the intersections with a new bypass for Missouri Highway 13 and State Highway HH (Figure 3.3). The test shafts were constructed in three rows of five shafts between U.S. 50 and the westbound entrance ramp to U.S. 50 from the new MO 13 bypass as shown in Figure 3.4. A summary of test shaft characteristics is provided in Table 3.1.

All test shafts at the Warrensburg Load Test Site were constructed by Hayes Drilling, Inc., using a LoDrill model number LLMHTFB50 rig shown in Figure 3.5. The typical drilling process followed for construction of the test shafts started with use of a 36-inch diameter auger bit to drill to a depth of approximately 10 to 15 feet. A 42-inch core barrel (Figure 3.6) was then used to expand the hole for placement of permanent casing through the overburden material. The 42-inch diameter, ¼-inch thick, 16-ft long permanent steel casing was then placed in the hole and sighted to the target elevation. Drilling then continued using the 36 inch auger to excavate the rock socket. The rock

sockets were excavated to the desired elevation and each hole was cleaned out using the rock auger.

Figure 3.2 – Location of Warrensburg Load Test Site. (Google Earth, 2011a)

Figure 3.3 – Location of Warrensburg Load Test Site east of Warrensburg, MO on U.S. Highway 50 near the intersection with State Highway HH. (Google Earth, 2011b)

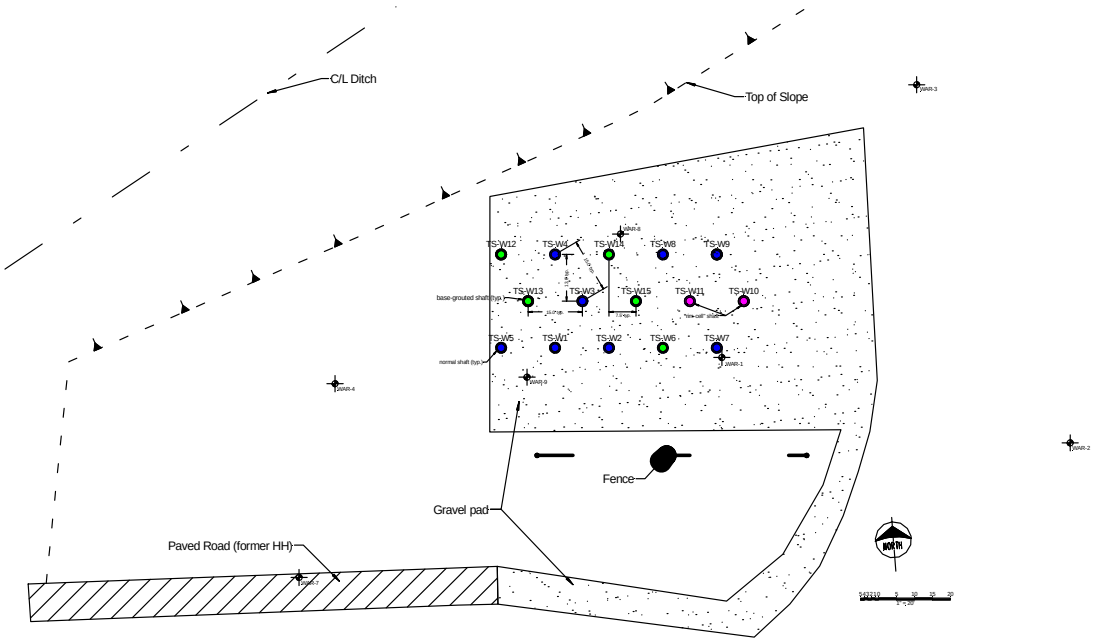

Figure 3.4 – Layout of test shafts at the Warrensburg Load Test Site.

Table 3.1- Summary of Test Shaft Characteristics for Warrensburg Load Test Site.

Test Shaft	Nominal Diameter (in)	Shaft Length (ft)	Permanent Casing Length (ft)	Post Grouted (yes/no)	SCC† (yes/no)	Load Test Method
W1	36	32.5	16	No	No	O-Cell
W2	36	33.4	16	No	No	O-Cell
W3	36	47.1	16	No	No	O-Cell
W4	36	49.4	16	No	No	O-Cell
W5	36	27.1	16.5	No	No	O-Cell
W6	36	33.1	16	Yes	No	O-Cell
W7	36	36.6	16	No	Yes	O-Cell
W8	36	48.1	16	No	No	O-Cell
W9	36	47.8	16	No	Yes	O-Cell
W10	36	36.8	16	No	No	RIM Cell
W11	36	39.6	16	No	No	RIM Cell
W12	36	33.6	16	Yes	No	O-Cell
W13	36	32.9	16	Yes	No	O-Cell
W14	36	32.8	16	Yes	No	O-Cell
W15	36	33.3	16	Yes	No	O-Cell

† self-consolidating concrete

Figure 3.5- LoDrill (model number LLMHTFB50) rig used at the Warrensburg Load Test Site.

Figure 3.6- Core barrel used at Warrensburg Load Test Site.

Following excavation and cleanout of each shaft, the reinforcing cage was carefully lifted using a boom truck and the drill rig to bring it to a vertical alignment

(Figure 3.7). Approximately eighteen inches of concrete was generally placed into the hole prior to placement of the reinforcing cage to ensure good seating of the O-Cell™. The reinforcing cage was then lowered into the hole and secured at the desired elevation. Wheel spacers were placed on the cage as it was lowered into the hole to keep the cage centered within the hole.

Following placement of the reinforcing cage, concrete was placed in the shaft using a pump truck. The concrete used was MoDOT Class B-2 concrete with aggregate gradation D, which has a maximum aggregate size of 1 inch. Class B-2 concrete is a relatively "rich" concrete that includes at least 705 pounds of cement per cubic yard. The specified minimum compressive strength of the concrete is 4000 psi.

Figure 3.7- Reinforcement cage picked by the crane and drill rig.

Prior to placement, the concrete slump was adjusted using super plasticizer to achieve a slump of 9 to 10 inches. Concrete slump and entrained air tests were performed for each shaft according to AASHTO standard methods T119 and T152 (AASHTO, 2010), respectively. Concrete cylinders were taken for each shaft to establish the concrete strength and to help in establishing the concrete modulus for interpretation of load test results. In all cases, concrete was placed on the same day that the shaft excavation was completed.

Self-consolidating concrete (SCC) was used in test shafts W7 and W9. For these shafts, on-site concrete testing included J-ring tests and slump tests for each concrete truck. The J-ring tests followed the ASTM Standard C1621M-09b (ASTM, 2009) to evaluate the placement condition of the self-consolidating concrete.

Test shafts W6, W12, W13, W14, and W15 were post-grouted shafts. For these shafts, a post-grout plate and grouting tubes were attached to the reinforcing cage prior to the cage being lowered into the hole (Figure 3.8). The cage was then lowered into the hole until the post-grout plate rested on the base of the hole, prior to placement of concrete. Since the annular space between the O-Cell™ and the side of the hole was not large enough for the concrete tremie pipe to be extended below the O-Cell™, neat cement grout with a water-cement ratio of 0.45 was placed into the shaft using a grout hose until the grout reached a level just above the O-cell™ top plate. "Normal" Class B-2 shaft concrete was then placed to complete the shaft following the same procedure used for the other test shafts.

Figure 3.8 - Photograph of post-grouting plate being attached to the reinforcing cage prior to placement in the hole.

3.3.2 Construction of Shafts at Frankford Load Test Site

The Frankford Load Test Site is located near Frankford, Missouri along U.S. Highway 61 northwest of St. Louis, Missouri (Figure 3.9). The site is composed of weathered shale overlying unweathered shale, which in turn overlies competent limestone. The strength of the shale at the Frankford site varies somewhat with the degree of weathering, but is quite consistent and uniform across the site. The test shafts were constructed along the ditch line of the outer gravel road on the west side of U.S. 61, just south of the intersection with Pike County Road 58 (Figure 3.10). The test shafts were arranged in a straight line, parallel with U.S. 61 as shown in Figure 3.11.

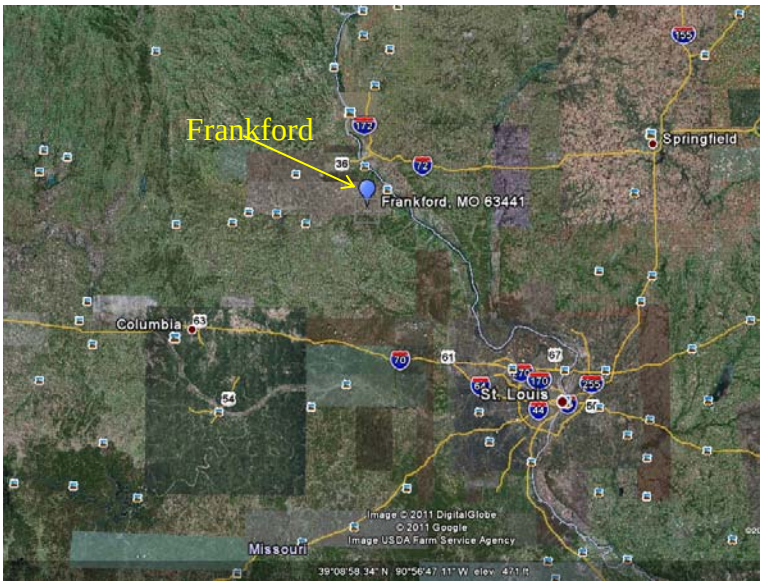

Figure 3.9 - Location of Frankford Load Test Site. (Google Earth, 2011c)

Figure 3.10 - Location of Frankford Load Test Site south of Frankford, MO along U.S. Highway 61 near the intersection with Pike County Road 58. (Google Earth, 2011d)

All test shafts at the Frankford Load Test site were installed by Drilling Service Company, Inc. using a Watson-3100 CM rig (Figure 3.12). The typical construction procedure at the Frankford site was to first use a 60-inch or 36-inch auger (Figures 3.13 and 3.14) to excavate to a depth of approximately 5 feet. A short, oversized section of temporary casing was then placed in the hole to prevent sloughing of surficial soil and gravel into the hole during excavation. The rock sockets were then excavated to the desired depth using the 36-inch or 60-inch augers (as appropriate for the desired shaft size) and cleaned using either the augers or a cleanout bucket. Finally, permanent steel casing was hung in the middle of the temporary casing at the desired target elevation (Figure 3.15). Table 3.2 summarizes the characteristics of the test shafts.

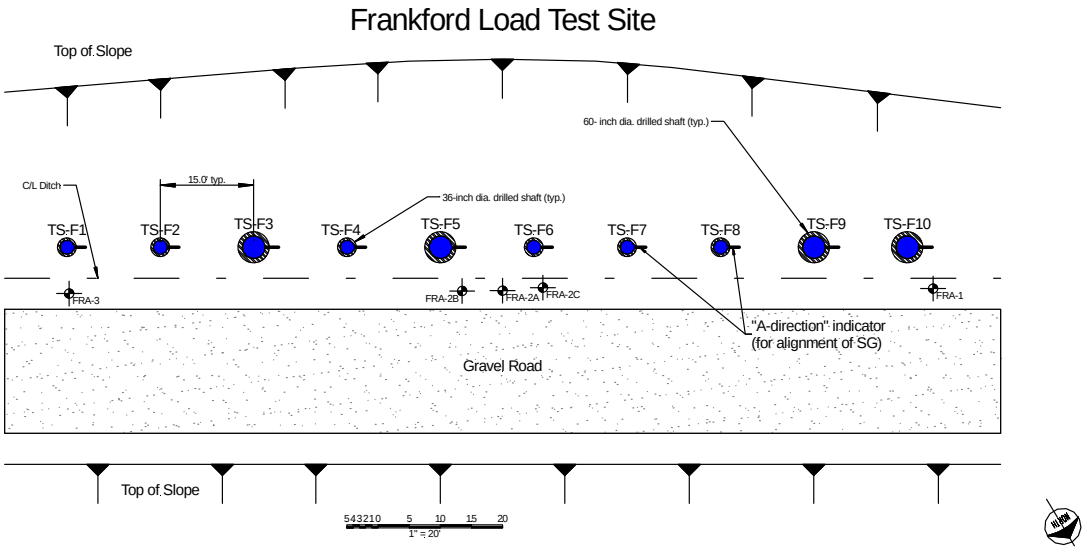

Figure 3.11 – Layout of test shafts at Frankford Load Test Site.

Figure 3.12- Watson-3100 CM rig used to construct test shafts at the Frankford Load Test Site.

Figure 3.13- The 60-inch auger used to excavate 60-inch diameter shafts at the Frankford Load Test Site

Figure 3.14- The 36-inch auger used to excavate the 36-inch diameter shafts at the Frankford Load Test Site.

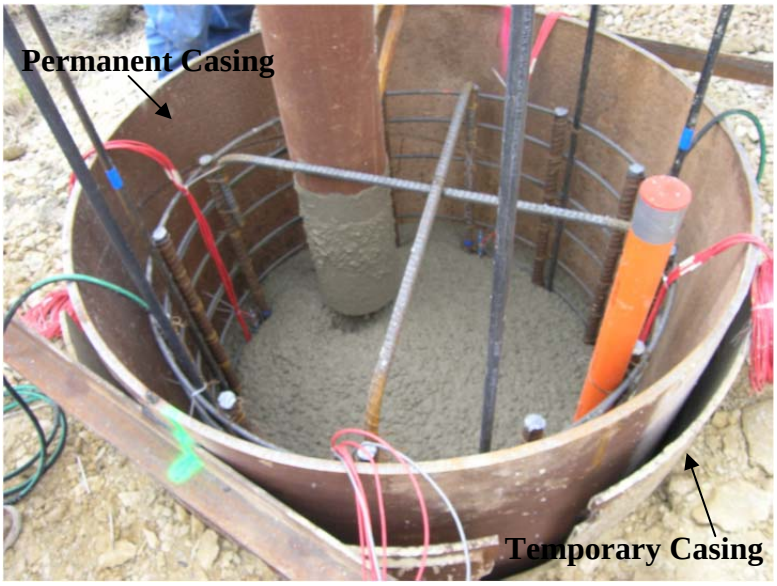

Figure 3.15- Drilled shaft with temporary and permanent casing. The temporary casing was removed following concrete placement.

Table 3.2- Summary of Test Shaft Characteristics for Frankford Load Test Site.

Test Shaft	Nominal Diameter (in)	Length (ft)	Permanent Casing Length (ft)	Post Grouted (yes/no)	SCC (yes/no)	Load Test Method
F1	36	20.5	5.0	No	No	O-Cell
F2	36	22.8	6.0	No	No	RIM Cell
F3	60	25.2	5.8	No	No	O-Cell
F4	36	26.3	5.7	No	No	O-Cell
F5	60	33.6	5.0	No	No	O-Cell
F6	36	27.3	5.7	No	No	O-Cell
F7	36	34.7	6.0	No	No	O-Cell
F8	36	23.3	5.0	No	No	RIM Cell
F9	60	16.7	6.0	No	No	O-Cell
F10	60	18.6	6.8	No	No	O-Cell

Reinforcing cages were hoisted using the drill rig and a loader to raise the cages to a vertical alignment (Figure 3.16). For all 3-ft diameter shafts, several feet of concrete was placed into the hole prior to placement of the reinforcing cage to bring the concrete level just above the planned elevation of the O-Cells. This process was followed to ensure intimate contact between the base plate of the O-Cell and the concrete beneath the O-Cell since there was not sufficient space for the tremie pipe to extend past the O-cells. The reinforcing cages where then placed into the hole and hanged at the appropriate elevation while the remainder of concrete was placed. Wheel spacers were placed on the cages of all shafts to maintain the alignment of the reinforcing cage in the center of the shaft. A similar process was followed for the 5-ft diameter shafts except that no concrete was placed in the bottom of the hole prior to hanging the reinforcing cage because there was sufficient room to extend the tremie pipe past the O-Cells.

Figure 3.16 - Hoisting of reinforcing cage using the drilling rig at the top of the cage and front end loader at the O-cell™.

The concrete used at the Frankford Load Test Site was MoDOT class B-2 concrete with a minimum compressive strength of 4000 psi and a maximum aggregate size of ¾ inches. The concrete generally arrived on site with a slump of 4 to 8 inches. The concrete slump was adjusted prior to placement using super plasticizer to achieve a slump of 9 to 10 inches. Concrete cylinders were made and slump and entrained air tests performed for each concrete batch. Concrete was placed using a "ported" tremie pipe.

3.4 Osterberg Cell™ and Instrumentation

Each test shaft was instrumented with six levels of vibrating wire strain gauges, four to five tell-tale rods and one inclinometer casing. Two geophones were also installed in most of the shafts to allow for evaluation of small strain concrete modulus.

Cross-hole sonic logging (CSL) pipes were installed in four of the test shafts (two at each site) to allow for evaluation of shaft quality. Osterberg Cell loading devices (O-cells™) were installed in twenty one of the test shafts. Alternative RIM Cells™ were installed in the remaining four test shafts.

The Osterberg cell (O-cell™) is commonly used for full-scale load testing of drilled shafts. The O-cell™ is a sacrificial jack that is usually attached to the base of the reinforcing cage (Figure 3.17). During a load test, the O-cell™ is pressurized to apply "bi-directional" load to the respective portions of the shaft above and below the O-cell™. Tell-tale pipes were attached to the bottom and top plates to allow for measurement of movement of the upper and lower plates.

The RIM Cell™ (Figure 3.18) is an alternative, proprietary, sacrificial load testing device developed by Loadtest, Inc. that can be used in a manner similar to the more common O-Cell. RIM Cells were used to load four of the twenty five test shafts (two at each site).

Figure 3.17 - Osterberg Cell™ attached to the base of a reinforcing cage.

Figure 3.18 - RIM Cell™ attached to the base of a reinforcing cage.

Strain gauges were installed at six levels to allow the distribution of load along the test shafts to be determined at different applied loads. The strain gauges were

vibrating wire, concrete embedment gauges (Geokon Model 4200) attached to u-brackets welded inside the rebar cage (Figure 3.19). Most shafts were instrumented with four gauges at each level for a total of 24 gauges per shaft. The post-grouted shafts at the Warrensburg Test Site (shafts W6, W12, W13, W14, and W15) were instrumented with two gauges at each level.

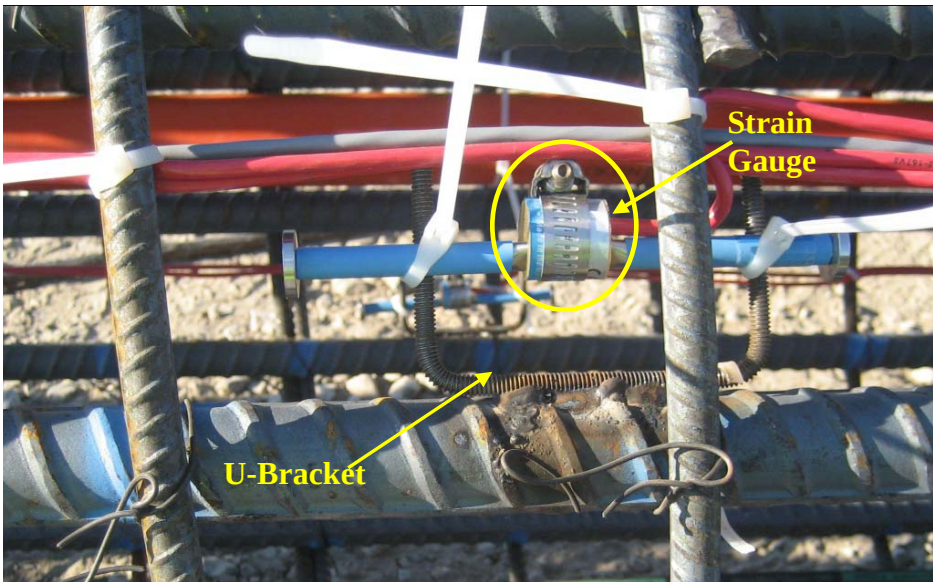

Figure 3.19- Vibrating wire strain gauge mounted on reinforcing cage.

Two geophones were also placed in most shafts; one just above the level of the O-Cell and one near the middle of the shaft to allow for measurement of wave propagation velocity and correlation of these measurements to small strain concrete modulus. The geophones were attached directly to the vertical reinforcing bars using either zip ties or pipe clamps with foam material placed between the geophones and the reinforcing bars to isolate the geophones from the reinforcing bar.

Steel Crosshole Sonic Logging (CSL) pipes were also installed in drilled shafts F5, F7, W1 and W2 to allow for CSL measurements to evaluate the condition of the shafts and to provide an alternative means to assess concrete modulus in select shafts. Six CSL tubes were installed in test shaft F5 while four CSL tubes were installed in shafts F7, W1 and W2.

Tell-tale pipes were installed in all test shafts to allow for the upward and downward movement of the top and bottom plates of the O-cell™ to be monitored during testing. Prior to performing each load test, metal rods were lowered into the pipes and attached to fittings at the bottom of each pipe. Upward and downward movements were then measured during each test using LVDTs attached to tops of the tell-tale rods. Tell-tale pipes for measuring the movement of the bottom plates were scored at the O-cell™ fracture plane to force the pipe to fracture at that location so that the pipes would not restrict O-cell™ expansion.

A single inclinometer casing was installed in each test shaft for future lateral load testing. The inclinometer casings were not used as part of the axial load testing program considered in this thesis.

3.5 Summary

The subsurface investigations for each of the test sites included Standard Penetration Test and modified Texas Cone Penetration Test measurements. SPT measurements were converted to an "equivalent" N-value, denoted as N_{eq-60}. MTCP testing followed TxDOT standard procedures except for modifications to the hammer

weight and drop distance, which resulted in slightly greater nominal hammer energy than is traditionally used.

Twenty-five drilled shafts were constructed at two test sites in Missouri, fifteen at a site near Warrensburg and ten at a site near Frankford. The shafts were instrumented with six levels of vibrating wire strain gauges and tell-tale rods to allow for establishing both load transfer along the shaft and the ultimate side and tip resistance for each shaft. All test shafts were socketed into shale and load tested using the Osterberg Cell^{TM} load test method.

Chapter 4 - In-situ Test Measurements at Field Load Test Sites

4.1 Introduction

Standard Penetration tests (SPT) and modified Texas Cone Penetration tests (MTCP) were completed at seven test sites where full scale load tests have been performed on drilled shafts in shale. The field test sites include "new" test sites located near the cities of Frankford and Warrensburg and "historical" load test sites located in or near the cities of Grandview, Kansas City, Lexington, Waverly, and Dearborn. Results of SPT and MTCP tests performed at each of these sites are presented in this chapter along with descriptions of the general geology of the respective sites. Site "models" developed to reflect the in-situ test measurements for each site are also presented.

4.2 Frankford Load Test Site

The Frankford Load Test Site is located south east of Frankford, Missouri on U.S. Highway 61 (Figure 4.1). Figure 4.2 shows a plan view of the site with locations of the test shafts and boring locations. The boreholes are labeled FRA-1, FRA-2A, FRA-2B, FRA-2C, and FRA-3. Shale cores from borings FRA-1, FRA-2A and FRA-3 were extracted and tested to evaluate the uniaxial compressive strength (UCS) of the shale. SPT and MTCP testing was performed in boring FRA-2B.

Figure 4.1- Location of Frankford Load Test Site on U.S. Highway 61 southeast of Frankford, Missouri. (Google Earth, 2011d)

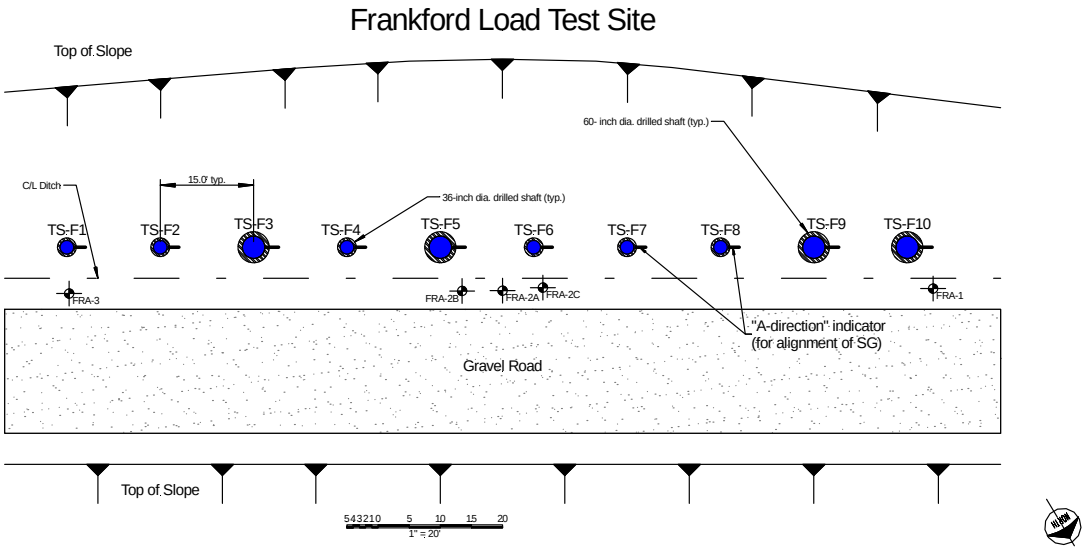

Figure 4.2 – Plan view of Frankford Load Test Site showing locations of the test shafts and boring locations. U.S. Highway 61 is located on the north side of the gravel road, at the bottom of the schematic.

4.2.1 Geology of Frankford Site

The soil and rock at the Frankford site is Ordovician in age and from the Maquoketa shale formation, which is typically laminated, silty, calcareous or dolomitic shale (Thompson, 1995). The Maquoketa Formation was divided into three strata designated as A, B and C. Stratum A and Stratum B are composed of a dull green, dark gray and brown, weathered shale with UCS ranging from approximately 3 to 30 ksf. Stratum C is a hard gray shale with UCS ranging from 40 to 100 ksf. The Maquoketa formation is underlain by competent limestone.

4.2.2 SPT Measurements at Frankford Site

Values for N_{eq-60} from SPT measurements at the Frankford site are provided in Table 4.1 and plotted versus elevation in Figure 4.3. Maquoketa Stratum A was encountered between approximate elevations 660 and 655 ft. A single SPT test was performed in this stratum that produced an N_{eq-60}-value of 29 blows/ft. Maquoketa Stratum B was encountered between elevations 655 and 645.8 ft. The measured SPT N_{eq-60}-values in this stratum ranged from 47 to 101 blows/ft. Stratum C was encountered between elevations 645.8 and 620.9 ft. The measured N_{eq-60}-values in this stratum ranged from 203 to 304 blows/ft.

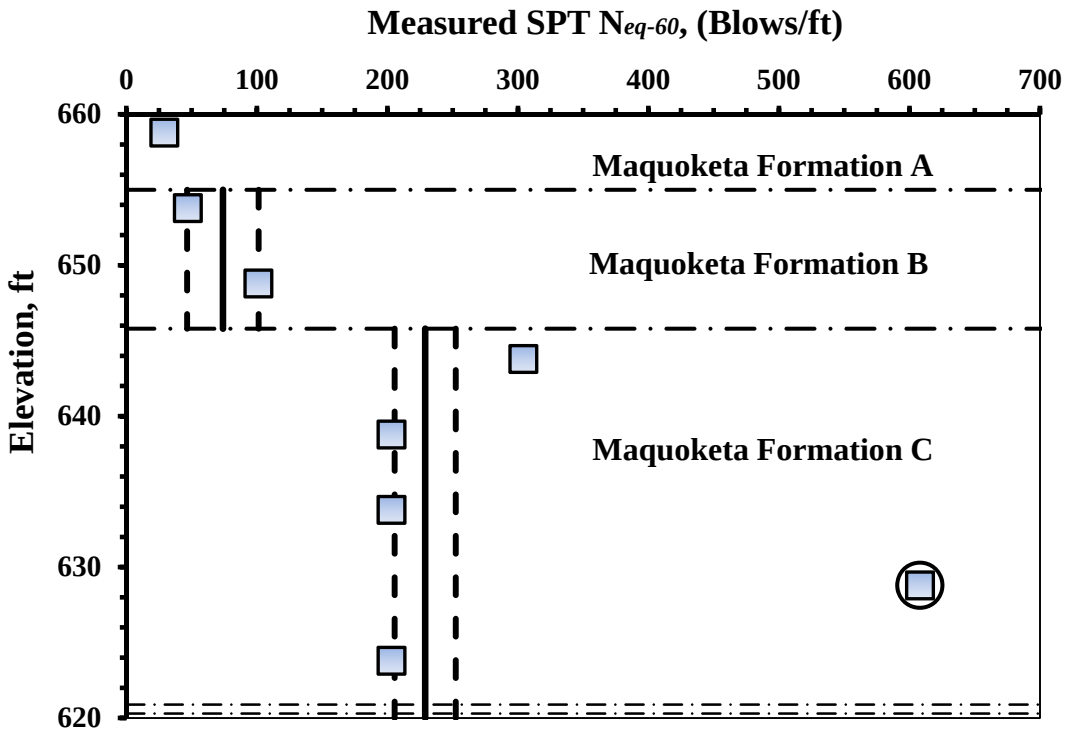

Figure 4.3- Measured N_{eq-60} values from Frankford site shown with interpreted "model" values. The horizontal dash-dot lines indicate approximate boundaries between shale strata.

Table 4.1- Measured SPT N_{eq-60}-values for Frankford Site.

Elevation (ft)	SPT Measurements	
	Blows/6"	N_{eq-60} (blows/ft)
658.8	6-8-14	29
653.8	2-14-21	47
648.8	25-38 in 6"	101
643.8	38 in 2"	304
638.8	38 in 3"	203
633.8	38 in 3"	203
628.8	38 in 1"	608
623.8	38 in 3"	203

Mean, or "model" values of N_{eq-60} in each stratum are also shown in Figure 4.3 as solid vertical lines. The dashed vertical lines shown reflect the mean value plus or minus one standard deviation of the mean, i.e. the "model" standard deviation. Numeric values for the mean and the standard deviation of the mean for each stratum are provided in Table 4.2. The mean values for each stratum were established by fitting probability distributions to the measured data using the distribution fitting tool in MATLAB®. The mean value was taken to be the mean of the best fit probability distribution. The standard deviation of the mean (or the "model standard deviation") was in turn calculated as:

$$\sigma_{\overline{N_{eq}}} = \frac{\sigma_{\widehat{N_{eq}}}}{\sqrt{n}} \tag{4.1}$$

where $\sigma_{\overline{N_{eq}}}$ is the standard deviation of the mean value of N_{eq-60}, n is the number of measurements used to establish the best fit distribution, and $\sigma_{\widehat{N_{eq}}}$ is the standard deviation of best fit distribution to the N_{eq-60} values. Model standard deviation values were used because they reflect the variability and uncertainty in the *mean* value of N_{eq-60} rather than the standard deviation of the measurements. The model standard deviation reflects the confidence in the mean value of N_{eq-60} based on the available measurements, which is generally appropriate for use in design.

The standard deviation of the N_{eq-60} measurements in Equation 4.1 was also established from the best fit probability distribution to the measurements in each stratum. This is the common standard deviation that most people determine from experimental data, which can be computed as

$$\sigma_{\widehat{N_{eq}}} = \sqrt{\frac{\sum_{i=1}^{n}\left(\widehat{N_{eq}} - \overline{N_{eq}}\right)^2}{n-1}} \tag{4.2}$$

where $\widehat{N_{eq}}$ is a measured value of N_{eq-60}, and $\overline{N_{eq}}$ is the mean or "model" value of N_{eq-60}.

Table 4.2 - Summary of characteristics for best fit probability distributions for N_{eq-60} values at the Frankford site.

Stratum	Upper Elevation Limit (ft)	Lower Elevation Limit (ft)	Number of Tests	Best Fit Distribution	Mean Value (blows/ft)	Model Standard Deviation (blows/ft)
Maquoketa Stratum A	660+	655	1	--	29	--
Maquoketa Stratum B	655	645.8	2	Normal	74	27.4
Maquoketa Stratum C	645.8	620	4	Lognormal	229	23.4

The circled data point shown in Maquoketa Formation C in Figure 4.3 (i.e. the point corresponding to 608 blows/ft at elevation 625 ft) was judged to be an outlier. This point was not used when establishing the best fit distribution to the measured data.

4.2.3 MTCP Measurements at Frankford Site

Measured *MTCP* values for the Frankford test site are provided in Table 4.3 and plotted in Figure 4.4. No MTCP tests were performed in Maquoketa Stratum A. Two MTCP tests were conducted in Maquoketa Stratum B, both producing a *MTCP* value of 3.5 in/100 blows. *MTCP* values in Maquoketa Stratum C ranged from 1.75 to 2.0 in/100 blows. It is important to note that MTCP measurements reflect penetration while SPT

measurements reflect the inverse of penetration so higher $MTCP$ values reflect softer material while higher N_{eq-60} values reflect stiffer material.

Best fit distributions were determined for the *MTCP* measurements in each stratum, from which values for the mean and standard deviation of the mean were established following procedures similar to that described previously for N_{eq-60} measurements. Table 4.4 summarizes the relevant characteristics of the best fit distributions for each stratum.

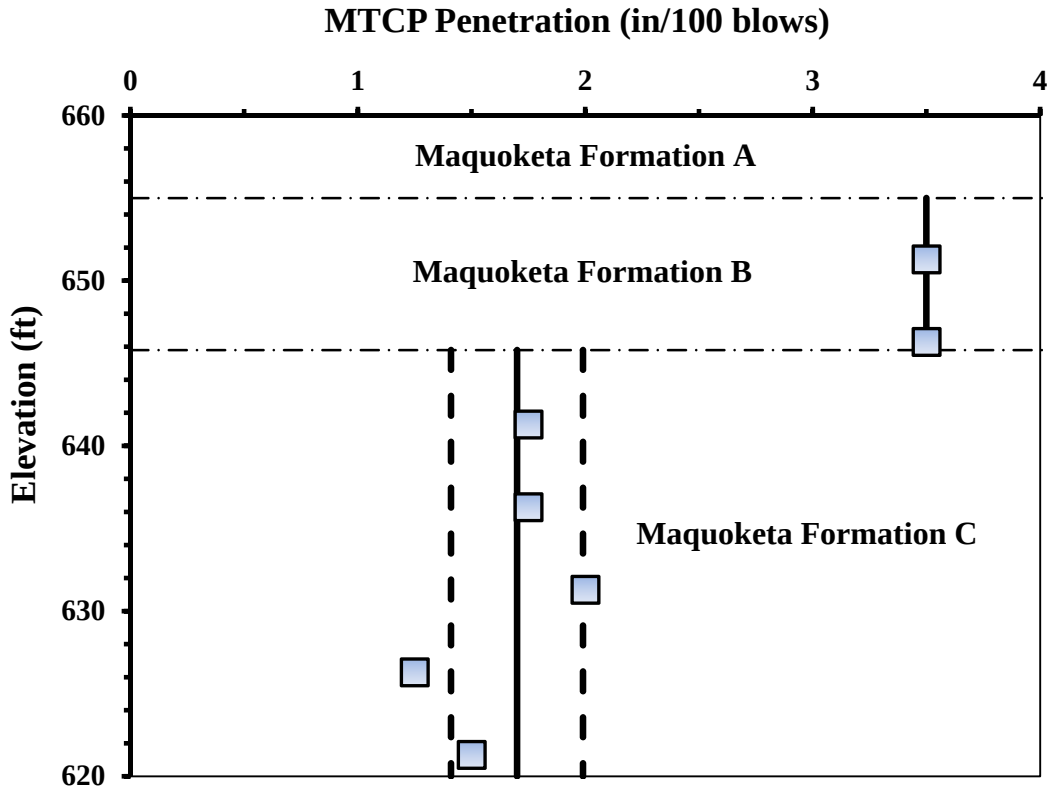

Figure 4.4- Measured *MTCP* values from Frankford site shown with interpreted "model" values for each stratum. The horizontal dash-dot lines indicate approximate boundaries between shale strata.

Table 4.3- Measured *MTCP* values for Frankford Site.

Elevation (ft)	MTCP Measurements	
	Blows/6”	(in/100 blows)
651.3	50 in 2.5”, 50 in 1”	3.5
646.3	50 in 3”, 50 in 0.5”	3.5
641.3	50 in 1.5”, 50 in 0.25”	1.75
636.3	50 in 1.5”, 50 in 0.25”	1.75
631.3	50 in 1.5”, 50 in 0.5”	2.0
626.3	50 in 1”, 50 in 0.25”	1.25
621.3	50 in 1.5”, 50 in 0”	1.5

Table 4.4- Summary of characteristics for best fit probability distributions for MTCP measurements at the Frankford site.

Stratum	Upper Elevation Limit (ft)	Lower Elevation Limit (ft)	Number of Tests	Best Fit Distribution	Mean Value (in/100 blows)	Model Standard Deviation (in/100 blows)
Maquoketa Stratum A	660+	655	0	NA	NA	NA
Maquoketa Stratum B	655	645.8	2	Normal	3.5	0
Maquoketa Stratum C	645.8	620	5	Normal	1.7	0.29

4.3 Warrensburg Load Test Site

The Warrensburg Load Test Site is located east of Warrensburg, Missouri on US 50 (Figures 4.5 and 4.6). Figure 4.7 shows a plan view of the site with locations of the test shafts and borings. SPT and MTCP tests were conducted at the boring location labeled WAR-1. Soil and rock cores were taken from the remaining boring locations shown.

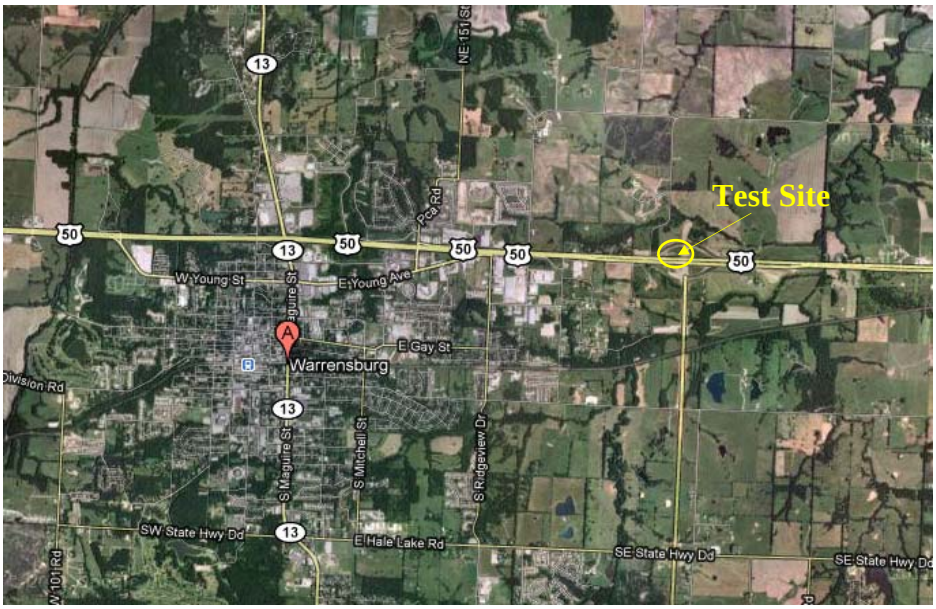

Figure 4.5- Location of Warrensburg Load Test Site on US Highway 50 east of Warrensburg, Missouri. (Google Earth, 2011b)

Figure 4.6- Warrensburg Load Test Site showing location of the SPT and MTCP test borehole. (Google Earth, 2011e)

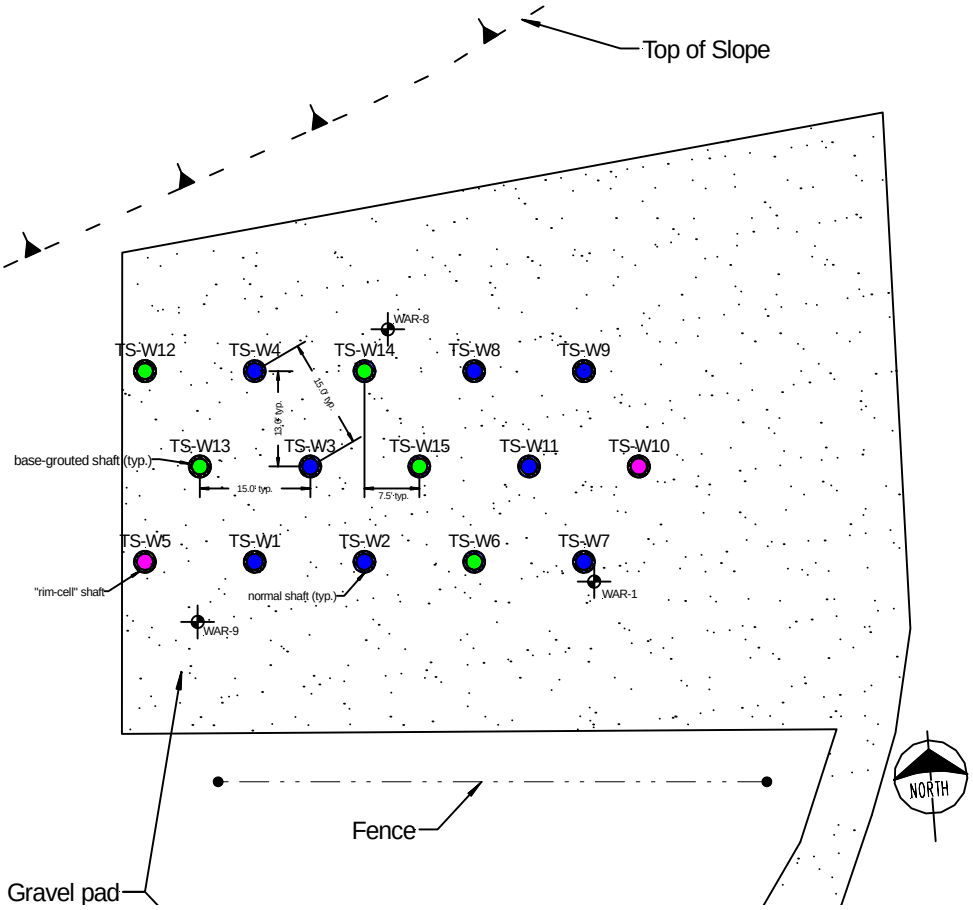

Figure 4.7- Plan view of Warrensburg Load Test Site showing locations of the test shafts and borings. US 50 is located on the south side of the test site, at the bottom of the figure.

4.3.1 Geology of Warrensburg Site

The bedrock found at the Warrensburg site is of Pennsylvanian age and includes sandstone, siltstone, underclay, limestone, and coal beds. The formations present within the range of depths of the test shafts are the Croweburg and Fleming formations. Uniaxial compressive strengths (UCS) for the Croweburg Formation ranged from 3to 80 ksf while uniaxial strengths for the Fleming Formation ranged from 5 to 240 ksf.

The Croweburg Formation was encountered from elevation 767 feet to elevation 745 feet with an approximate thickness of 22 feet. The formation was divided into three strata, denoted as A, B and C, and Stratum A was not encountered in the SPT and MTCP borings. Therefore SPT and MTCP measurements are only available in Strata B and C, with the interface between these strata located at elevation 750 ft. Stratum B is a weathered zone in the Croweburg Formation, which was captured in the MTCP measurements. Both Croweburg strata are composed of olive green and reddish sandstone, siltsone, and shale.

The Fleming Formation was encountered from elevation 745 to approximate elevation 713 feet. This formation is composed of more competent gray shale.

4.3.2 SPT Measurements at Warrensburg Site

Measured values for N_{eq-60} from the Warrensburg site are plotted in Figure 4.8 and provided in Table 4.5. Measured N_{eq-60} values ranged from 47 to 243 blows/ft in Croweburg Formation B. In Croweburg Formation C, SPT N_{eq}-values ranged from 93 to 122 blows/ft. In the Fleming Formation, N_{eq-60} values ranged from 122 to 304 blows per foot. As shown in Figure 4.8, there is considerably more scatter in N_{eq-60} at the Warrensburg site than at the Frankford site. However, this scatter is generally consistent with observations for UCS and $MTCP$ measurements so it is believed to reflect actual site variability.

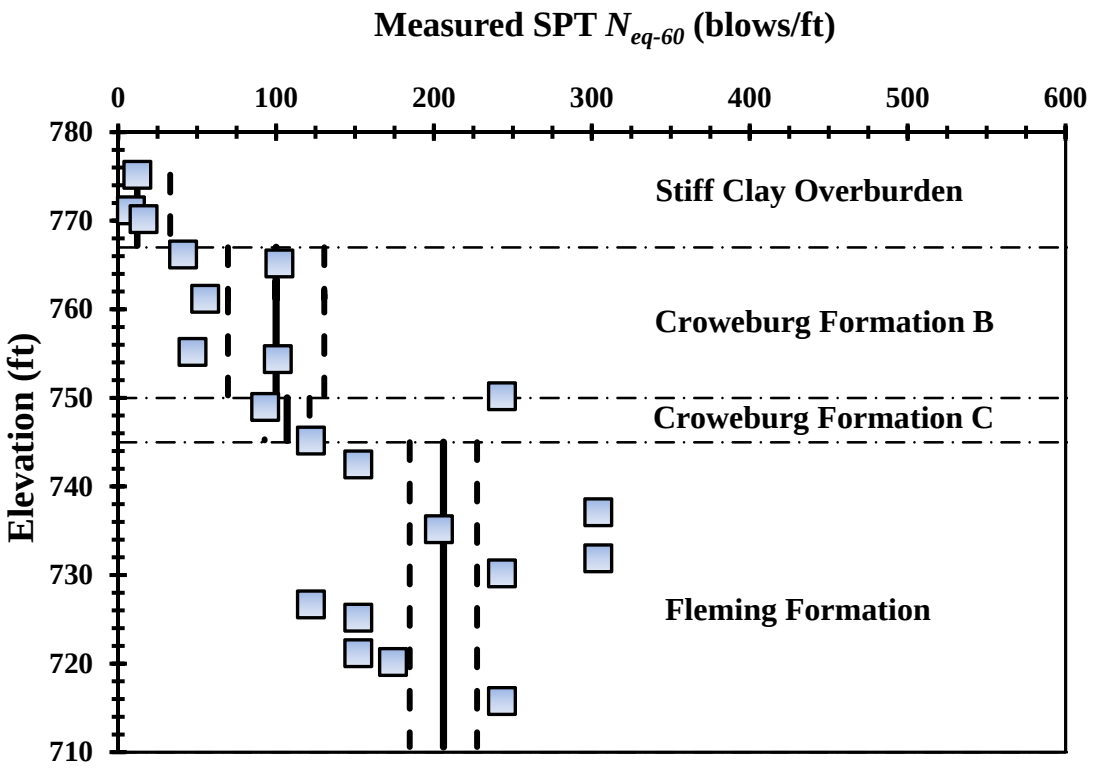

Figure 4.8- Measured N_{eq-60}-values from Warrensburg site shown with interpreted "model" values. The horizontal dash-dot lines indicate approximate boundaries between shale strata.

Mean, or "model" values for N_{eq-60} within each stratum, and corresponding values for the model standard deviation were again established using the distribution fitting tool in MATLAB®. The resulting values are shown in Figure 4.8 and tabulated in Table 4.6.

4.3.3 MTPC Measurements at Warrensburg Site

Measured *MTCP* values for the Warrensburg test site are presented in Figure 4.9 and Table 4.7. MTCP measurements ranged from 2.5 to 5.5 inches/100 blows in the

Croweburg B stratum. A single MTCP measurement was made in the Croweburg C stratum, producing a value of 7.5 in/100 blows. This measurement is indicative of the weathered zone that forms the Croweburg C stratum. MTCP measurements ranged from 1.5 to 2.5 in/100 blows in the Fleming Formation. Characteristics of the best fit probability distributions for MTCP measurements in each stratum are shown in Figure 4.10 and provided in Table 4.8.

Table 4.5- Measured SPT N_{eq-60} values for Warrensburg Site.

Elevation (ft)	**SPT Measurements**	
	Blows/6”	**N_{eq-60} (blows/ft)**
775.2	4-4-5	12
771.2	2-3-3	8
770.2	4-6-6	16
766.2	13-16-15	41
765.2	12-32-38 in 5”	102
761.2	16-19-22	55
760.2	32-88 in 2”	704
755.2	10-13-22	47
754.4	38 in 6”	101
750.2	25-38 in 3.5”	243
749.0	23-29-38 in 5.5”	93
745.2	38 in 5”	122
742.5	38 in 4”	152
740.2	38 in 1”	608
737.1	38 in 2”	304
735.2	38 in 3”	203
731.9	38 in 2”	304
730.2	38 in 2.5”	243
726.7	38 in 5”	122
725.2	38 in 4”	152
721.2	38 in 4”	152
720.2	38 in 3.5”	174
715.8	38 in 2.5”	243
710.6	38 in 1”	608

Table 4.6- Summary of characteristics for best fit probability distributions for N_{eq-60} measurements at the Warrensburg site.

Stratum	Upper Elevation Limit (ft)	Lower Elevation Limit (ft)	Number of Tests	Best Fit Distribution	Mean Value (blows/ft)	Model Standard Deviation (blows/ft)
Croweburg Stratum A	767	750	6	Lognormal	100	30.5
Croweburg Stratum B	750	745	3	Normal	107	14.2
Fleming	745	713	10	Lognormal	206	21.3

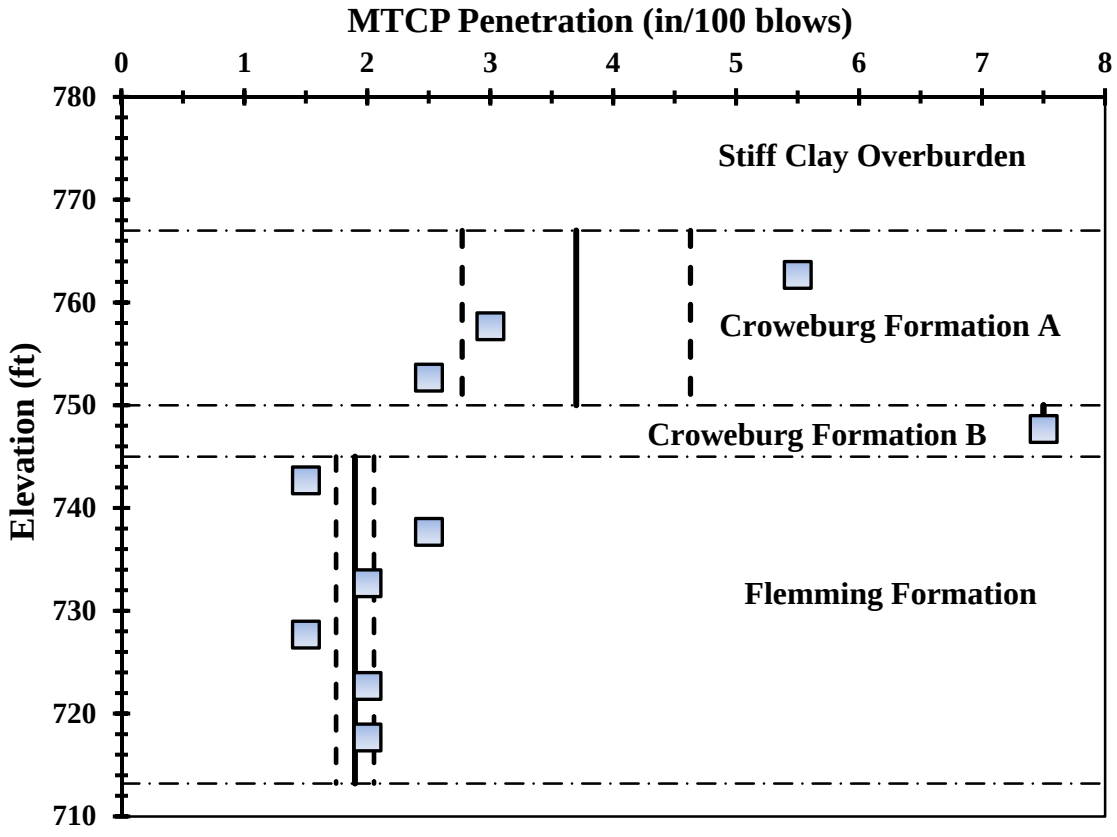

Figure 4.9- Measured MTCP values from Warrensburg site shown with interpreted "model" values. The horizontal dash-dot lines indicate approximate boundaries between shale strata.

Table 4.7- Measured MTCP values for Warrensburg Site.

Elevation (ft)	MTCP Measurements	
	Blows/6”	MTCP (in/100 blows)
762.7	50 in 4”, 50 in 1.5”	5.5
757.7	50 in 2”, 50 in 1”	3.0
752.7	50 in 2”, 50 in 0.5”	2.5
747.7	50 in 3.5”, 50 in 4”	7.5
742.7	50 in 1.25”, 50 in 0.25”	1.5
737.7	50 in 2”, 50 in 0.5”	2.5
732.7	50 in 1.5”, 50 in 0.5”	2.0
727.7	50 in 1.5”, 50 in 0”	1.5
722.7	50 in 1.5”, 50 in 0.5”	2.0
717.7	50 in 1.5”, 50 in 0.5”	2.0

Table 4.8- Summary of characteristics for best fit probability distributions for MTCP measurements at the Warrensburg site.

Stratum	Upper Elevation Limit (ft)	Lower Elevation Limit (ft)	Number of Tests	Best Fit Distribution	Mean Value (in/100 blows)	Model Standard Deviation (in/100 blows)
Croweburg Stratum B	767	750	3	Normal	3.7	0.93
Croweburg Stratum C	750	745	1	Normal	7.5	--
Fleming	745	713	6	Normal	1.9	0.15

4.4 Grandview Load Test Site

The Grandview Load Test Site is located in Grandview, Missouri within the greater Kansas City Metropolitan area. The site area is known as both the Grandview Triangle and as Three Trails Crossing due to it being the confluence of three major highways (I-435, I-470/US50, and US71) and other local routes that converge at this location (Figure 4.10).

Figure 4.10- Location of Grandview Load Test Site in the Kansas City Metropolitan area. (Google Earth, 2011f)

A full-scale test shaft was constructed and load tested at the site in 2002 during bridge construction (Miller, 2003). SPT and MTCP testing was performed several years later in 2009 so that the load test measurements could be used for development of design methods that require SPT and/or MTCP test measurements. The SPT and MTCP tests were performed at boring location GV-1 (Figure 4.11), which is located approximately 100 feet northeast of the test shaft.

4.4.1 Geology of Grandview Site

The Grandview Load Test Site consists of interbedded Pennsylvanian age shale and limestone, as is common in western Missouri. The specific formations present at the

site include, in descending order, the Chanute Shale, Cement City Limestone, Quivira Shale, Westerville Limestone, and Wea Shale.

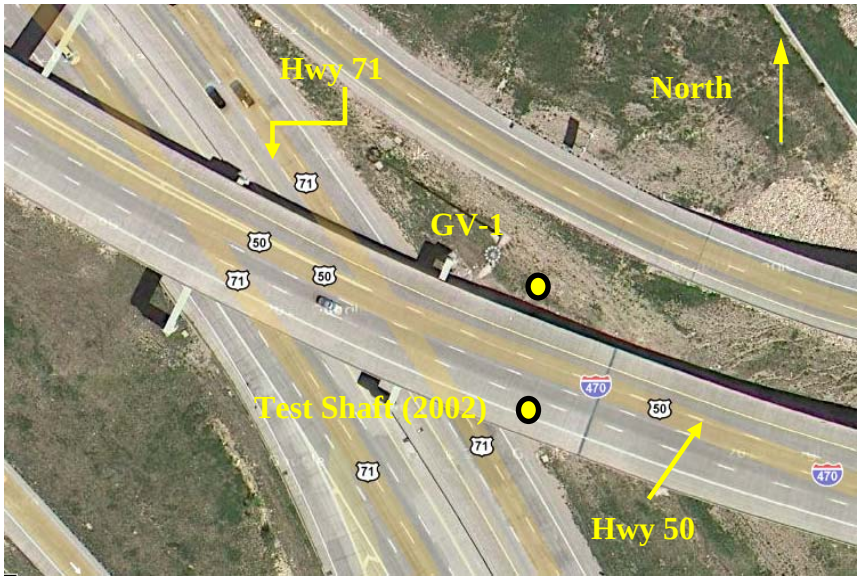

Figure 4.11- Grandview Load Test Site showing location of the SPT and MTCP test borehole and the load test performed in 2002. (Google Earth, 2011g)

The Chanute Shale formation is a silty, gray or maroon claystone overlain by a silty to sandy shale (Thompson, 1995) with UCS values ranging from 5.4 to 20.2 ksf (Miller, 2003). This formation was separated into an upper weathered stratum and a lower unweathered stratum for the purposes of this research. Beneath the Chanute Shale is the Cement City Limestone, which is a light gray, medium hard limestone. The Quivira Shale formation includes a calcareous gray shale in the middle and lower portions, and a thin clay layer in the upper portion that is overlain by a dark gray shale (Thompson, 1995). UCS values within the formation range from 22.2 to 36.4 ksf (Miller, 2003). The Westerville Limestone is a light gray medium hard limestone. Finally, the

Wea Shale is a bluish gray, silty, micaceous shale (Thompson, 1995) with UCS values ranging from 16.8 to 66.2 ksf (Miller, 2003).

4.4.2 SPT Measurements at Grandview Site

Measured N_{eq-60}-values from the Grandview site are provided in Table 4.9 and plotted in Figure 4.12. Standard Penetration Tests were performed only in the shale formations at the site. The Weathered Chanute Shale was observed from elevation 939 ft to elevation 927 ft. Measured N_{eq-60} values within this stratum ranged from 77 to 103 blows/ft. The Unweathered Chanute Shale was found between elevation 927 ft and elevation 916 ft, with measured N_{eq}-values ranging from 152 to 203 blows/ft. The Quivira Shale was encountered between elevations 911 and 905 ft. Measured N_{eq-60}values in the Quivira Shale ranged from 101 to 203 blows/foot. Finally, the Wea Shale was encountered between elevations of 898 and 864.0 ft with N_{eq-60}-values ranging from 152 to 203 blows/ft.

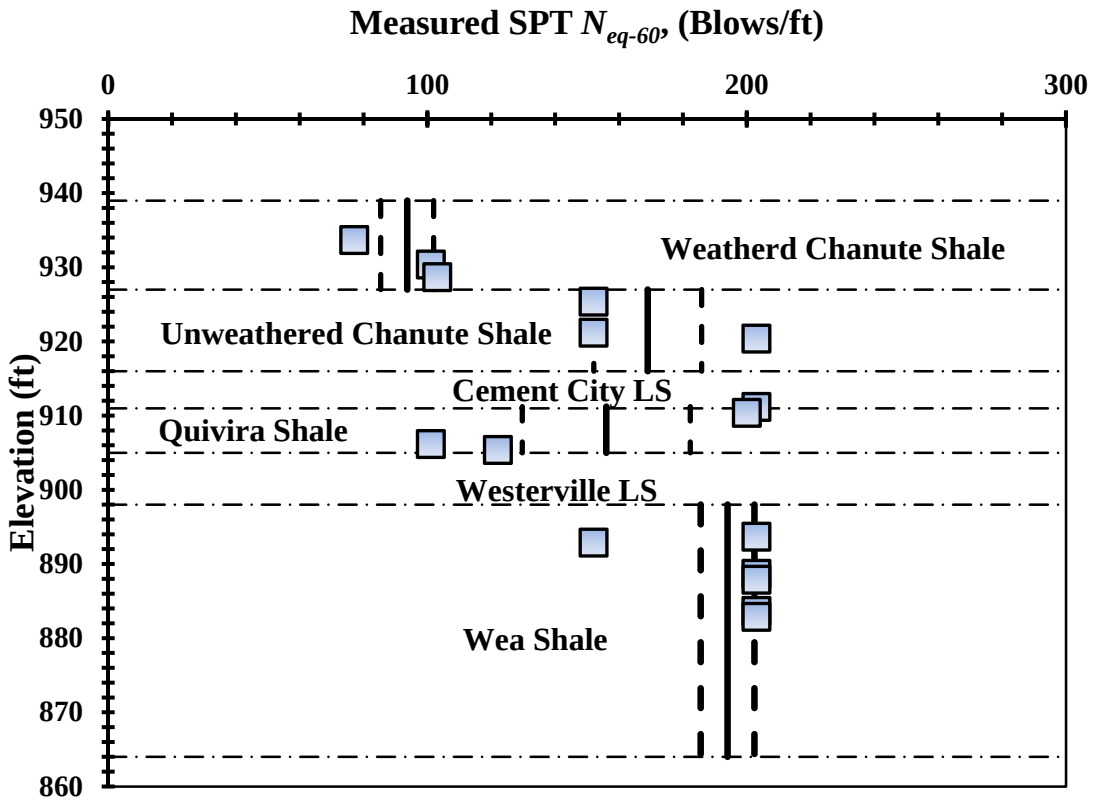

Figure 4.12- Measured N_{eq-60} values from Grandview site shown with interpreted "model" values. The horizontal dash-dot lines indicate approximate boundaries between shale and limestone strata.

As was done for the other sites, probability distributions were fit to the measured data within each stratum using the distribution fitting tool in MATLAB® to determine the mean and the standard deviation of the mean value for each stratum. The resulting values are shown in Figure 4.12. Pertinent characteristics of the best fit distributions are summarized in Table 4.10. Mean values for N_{eq-60} were 94 and 169 blows per foot for the weathered and unweathered Chanute Shale, respectively, 156 blows per foot for the Quivira Shale, and 194 blows per foot for the Wea Shale.

Table 4.9- Measured N_{eq-60} values for the Grandview Site.

Elevation (ft)	SPT Measurements	
	Blows/6”	N_{eq-60} (blows/ft)
933.7	15-18-40	77
930.4	38 in 6”	101
928.7	27-33-38 in 5”	103
925.4	35-38 in 4”	152
921.2	30-38 in 4”	152
920.4	35-38 in 3”	203
911.2	38 in 3”	203
910.4	50 in 4”	200
906.2	38 in 6”	101
905.4	38 in 5”	122
893.7	38 in 3”	203
892.9	38 in 4”	152
888.7	38 in 3”	203
887.9	38 in 3”	203
883.7	38 in 3”	203
882.9	38 in 3”	203

Table 4.10- Summary of characteristics for best fit probability distributions for N_{eq-60} measurements at the Grandview site.

Stratum	Upper Elevation Limit (ft)	Lower Elevation Limit (ft)	Number of Tests	Best Fit Distribution	Mean Value (blows/ft)	Model Standard Deviation (blows/ft)
Weathered Chanute	939	927	3	Normal	94	8.3
Unweathered Chanute	927	916	3	Normal	169	16.9
Quivira	911	905	4	Normal	156	26.3
Wea	898	864	6	Normal	194	8.4

4.4.3 MTCP Measurements at Grandview Site

Measured $MTCP$ values for the Grandview site are provided in Table 4.11 and plotted in Figure 4.13 according to the same stratigraphy used for the SPT measurements.

$MTCP$ values for the weathered Chanute Shale ranged from 1.5 to 5 in/100 blows while $MTCP$ measurements in the unweathered Chanute ranged from 6 to 9 in/100 blows. $MTCP$ values in the Quivira Shale ranged from 1 to 3.5 in/100 blows. Measurements in the Wea Shale ranged from 0.5 to 2 in/100 blows. Mean or "model" values for $MTCP$ and the standard deviation of these mean values determined from best fit probability distributions to the measured data are provided in Table 4.12 and shown in Figure 4.13.

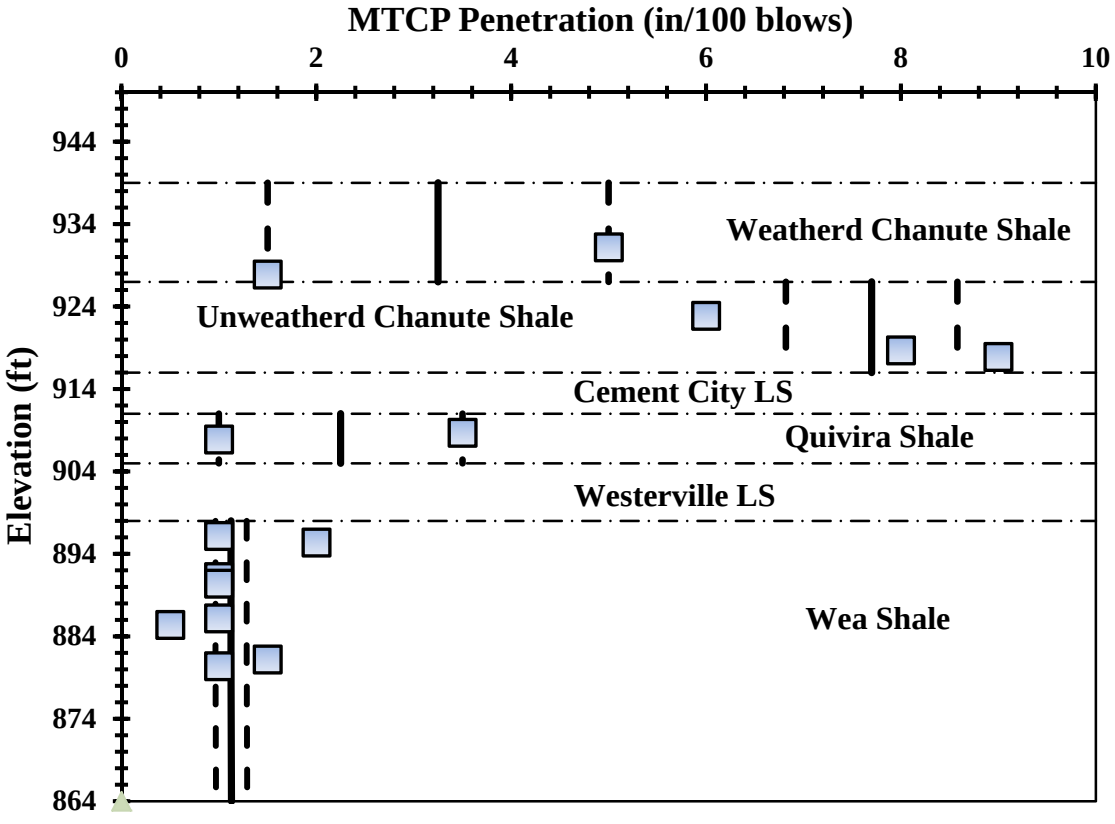

Figure 4.13- Measured $MTCP$ values from the Grandview site shown with interpreted "model" values. The horizontal dash-dot lines indicate approximate boundaries between shale and limestone strata.

Table 4.11- Measured $MTCP$ values for Grandview site.

Elevation (ft)	MTCP Measurements	
	Blows/6”	MTCP (in/100 blows)
931.2	40, 60 in 5”	5.0
927.9	50 in 1”, 50 in 0.5”	1.5
922.9	50 in 3”, 50 in 3”	6.0
918.7	50 in 4”, 50 in 4”	8.0
917.9	50 in 4”, 50 in 5”	9.0
908.7	50 in 2”, 50 in 1.5”	3.5
907.9	50 in 1”, 50 in 0”	1.0
896.2	50 in 1”, 50 in 0”	1.0
895.4	50 in 1”, 50 in 1”	2.0
891.2	50 in 0.5”, 50 in 0.5”	1.0
890.4	50 in 0.5”, 50 in 0.5”	1.0
886.2	50 in 1”, 50 in 0”	1.0
885.4	50 in 0”, 50 in 0.5”	0.5
881.2	50 in 1”, 50 in 0.5”	1.5
880.4	50 in 1”, 50 in 0”	1.0

Table 4.12- Summary of characteristics for best fit probability distributions for $MTCP$ measurements at the Grandview site.

Stratum	Upper Elevation Limit (ft)	Lower Elevation Limit (ft)	Number of Tests	Best Fit Distribution	Mean Value (in/100 blows)	Model Standard Deviation (in/100 blows)
Weathered Chanute	939	927	2	Normal	3.3	1.75
Unweathered Chanute	927	916	3	Normal	7.7	0.88
Quivira	911	905	2	Normal	2.3	1.25
Wea	898	864	8	Normal	1.1	0.16

4.5 Lexington Load Test Site

The Lexington Load Test Site is located northeast of Lexington, Missouri near the Missouri Highway 13 Bridge over the Missouri River (Figure 4.14). Approximate borehole locations for SPT and MTCP measurements are shown in Figure 4.15 along with the locations of the test shafts. SPT and MTCP measurements were performed on the north side of the river at the location denoted LEX-1 in 2009. Additional SPT measurements were also performed in 1996-1998 at the locations noted as B-3, B-9, and B-11, prior to construction of the new Highway 13 bridge. The two test shafts shown in Figure 4.16 were constructed and load tested in 1998 (Miller, 2003).

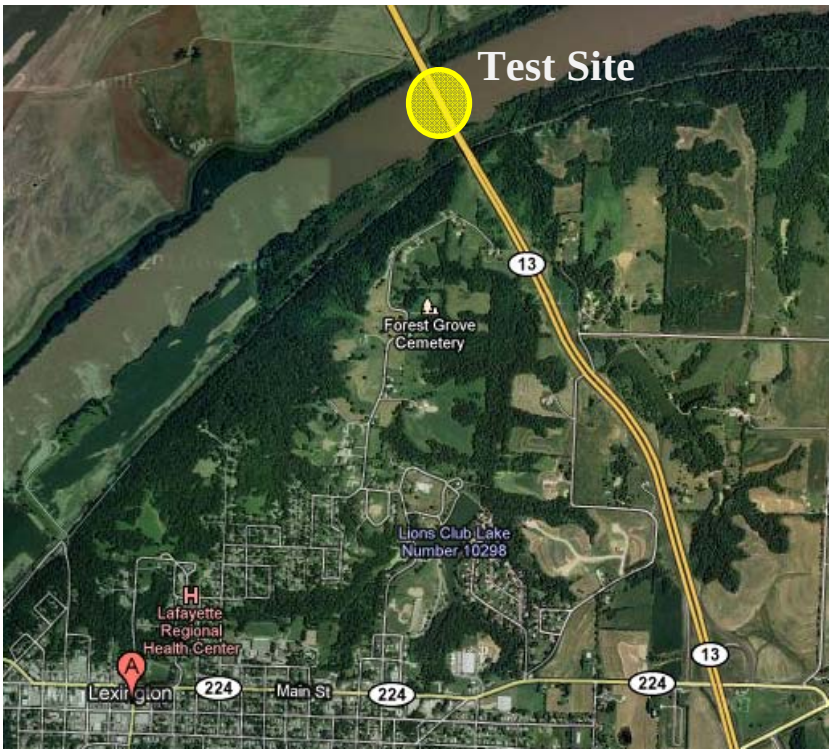

Figure 4.14- Location of Lexington Load Test Site on Missouri Highway 13 at the Missouri River Bridge near Lexington, Missouri. (Google Earth, 2011h)

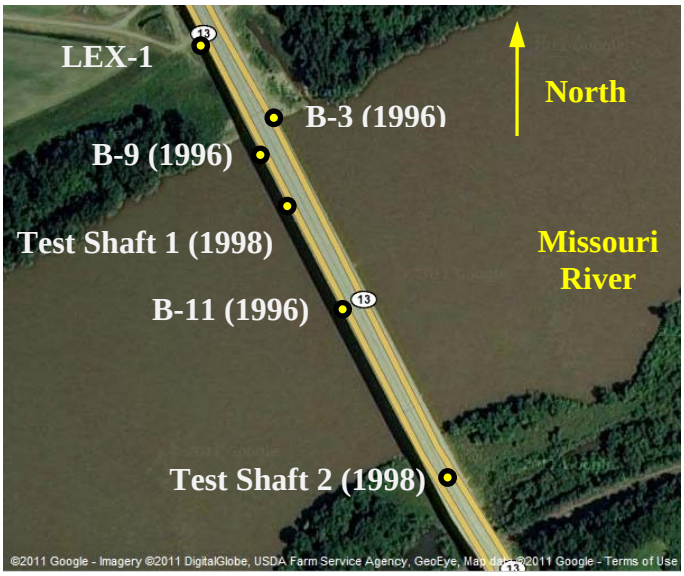

Figure 4.15- Lexington Load Test Site showing locations of boreholes where SPT and MTCP tests were conducted and locations of two test shafts (Miller, 2003). (Google Earth, 2011i)

4.5.1 Geology of Lexington Site

The Lexington Load Test Site is composed of Pennsylvanian age formations that include the Lagonda, Bevier, Verdigris, Croweburg and Fleming formations. The Lagonda formation consists of shale and siltstone or sandstone with UCS values ranging from 2.9 to 157 ksf (Miller, 2003). The Bevier Formation consists of (from top to bottom) the Bevier coal bed, a clay shale, a micaceous silt shale to siltstone, and a gray clay shale (Thompson, 1995) with UCS values ranging from 6.5 to 169.4 ksf (Miller, 2003). The Verdigris Formation consists of (from top to bottom) the Wheeler coal bed, a poorly laminated gray clay shale, a gray-green clay shale to mudstone, a black fissile shale, and a gray thick bedded shaly limestone (Thompson, 1995). UCS values within the Verdigris formation range from 4.5 to 93.7 ksf (Miller, 2003). The Croweburg formation

consists of (from top to bottom) the Fleming coal bed, underclay, a gray-green calcareous clay shale, and a fossiliferous limestone (Thompson, 1995) with UCS values ranging from 5.3 to 116.8 ksf (Miller, 2003). Finally, the Fleming Formation consists of (from top to bottom) the Fleming Coal Bed, underclay, a siltstone, lenses of fine grained sandstone and siltstone, a dark gray to black fissile shale, and a thin dark-gray fossilferous limestone (Thompson, 1995). UCS values within the Fleming Formation range from 3.1 to 25.9 ksf (Miller, 2003).

4.5.2 SPT Measurements at Lexington Site

Two separate "models" were developed to represent the conditions present at each respective test shaft location. Measured values for N_{eq-60} from borings near each test shaft are plotted versus elevation in Figures 4.16 and 4.17 to reflect the conditions present at Test Shaft 1 and Test Shaft 2, respectively. Numeric values for these measurements are also provided in Tables 4.13 and 4.15. The measured values used in Figure 4.16 and provided in Table 4.13 were taken from measurements made in historical borings B3, B9, B10, B11 and B12 as well as from boring LEX-1B that was conducted several years after conducting the load tests. Values used in Figure 4.17 and provided in Table 4.15 were taken from historical borings B4, B13, B14, B15, F45 and F50 that were conducted prior to the load tests. Tables 4.14 and 4.16 provide characteristics of the best fit probability distributions determined for N_{eq-60} in each stratum.

At the location of both shafts, the Lagonda Formation was encountered between elevations 649 to 611 ft. The Bevier Formation was encountered between elevations 611

– 574 ft. The Verdigris Formation was encountered from elevation 574 ft to elevation 564 ft. The Croweburg Formation was encountered between elevations 564 to 555 ft. Finally, the Fleming Formation was encountered between elevations 555 and 545 ft. Test Shaft 1 extended from elevation 577 ft to elevation 549 ft and thus predominantly transferred load in side resistance within the Verdigris and Croweburg Formations and in tip resistance in the Fleming Formation. Test Shaft 2 extended from elevation 605 ft to elevation 573 ft and, thus, transferred load in side resistance entirely within the Bevier Formation and transferred load in tip resistance in the Verdigris Formation.

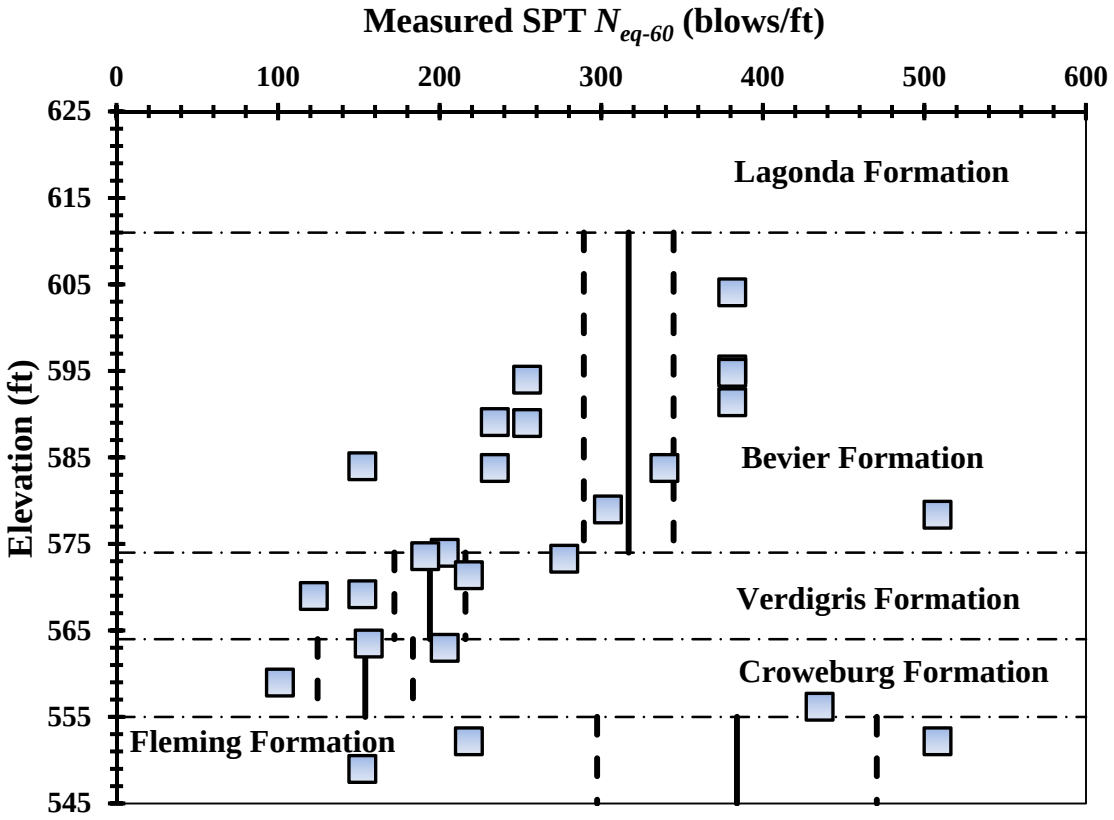

Figure 4.16- Measured SPT N_{eq-60} values from the Lexington site for Test Shaft 1 shown with interpreted "model" values. The horizontal dash-dot lines indicate approximate boundaries between different strata.

Table 4.13- Measured SPT N_{eq-60} values for Test Shaft 1 at Lexington Site.

Elevation (ft)	SPT Measurements	
	Blows/6”	N_{eq-60} (blows/ft)
604.1	31-50 in 1.5”	381
595.2	100 in 3”	381
594.8	50 in 1.5”	381
594.0	50 in 2.5”	254
591.4	100 in 3”	381
589.1	100 in 5”	234
589.0	50 in 2.5”	254
584.0	16-38 in 4”	152
583.8	100 in 5”	234
583.8	100 in 3.5”	339
579.0	38 in 2”	304
578.4	100 in 2.5”	508
574.0	38 in 3”	203
573.6	50 in 3”	191
573.3	100 in 4.5”	277
571.4	100 in 5.5”	218
569.2	50 in 4”	152
569.0	38 in 5”	122
563.5	47-60-94	156
563.0	36-100 in 6”	203
559.0	38 in 6”	101
556.2	89-11 in 0.5”	435
554.0	38 in 1”	608
552.2	100 in 2.5”	508
552.2	50 in 3”	218
549.0	38 in 3”	152

Table 4.14- Summary of characteristics for best fit probability distributions for N_{eq-60} measurements near Test Shaft 1 at the Lexington site.

Stratum	Upper Elevation Limit (ft)	Lower Elevation Limit (ft)	Number of Tests	Best Fit Distribution	Mean Value (blows/ft)	Model Standard Deviation (blows/ft)
Bevier	611	574	12	Normal	317	27.8
Verdigris	574	564	6	Normal	194	22.0
Croweburg	564	555	3	Normal	154	29.5
Fleming	555	545	5	Normal	384	86.5

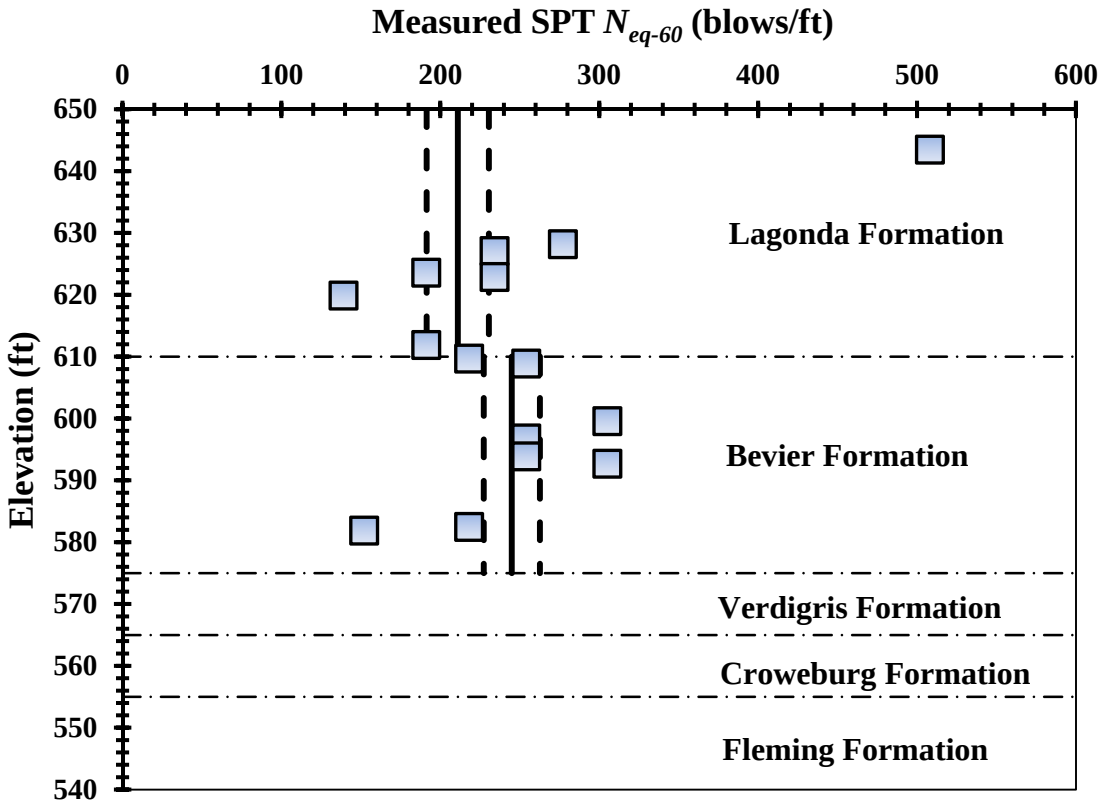

Figure 4.17- Measured SPT N_{eq-60} values from the Lexington site for Test Shaft 2 shown with interpreted "model" values. The horizontal dash-dot lines indicate approximate boundaries between different strata.

Table 4.15- Measured SPT N_{eq-60} values for borings near Test Shaft 2 at Lexington Site.

	SPT Measurements	
Elevation (ft)	**Blows/6"**	**N_{eq-60} (blows/ft)**
643.5	50-50 in 1"	508
628.2	100 in 4.5"	277
627.1	100 in 5"	234
623.6	50 in 3"	191
622.9	100 in 5"	234
619.9	50 in 4.5"	139
611.9	50 in 3"	191
609.7	50 in 2.75"	218
608.9	50 in 2.5"	254
599.6	50 in 2"	305
596.8	50 in 2.5"	254
593.9	50 in 2.5"	254
592.7	100 in 4"	305
582.5	100 in 5.5"	218
581.9	50 in 4"	152

Table 4.16- Summary of characteristics for best fit probability distributions for N_{eq-60} measurements near Test Shaft 2 at the Lexington site.

Stratum	Upper Elevation Limit (ft)	Lower Elevation Limit (ft)	Number of Tests	Best Fit Distribution	Mean Value (blows/ft)	Model Standard Deviation (blows/ft)
Lagonda	650	610	6	Normal	211	19.6
Bevier	610	575	8	Normal	245	17.7

4.5.3 MTCP Measurements at Lexington Site

$MTCP$ measurements for the Lexington site are presented in Table 4.17 and plotted in Figure 4.18. Since $MTCP$ testing was only performed in one borehole, LEX-1, a single $MTCP$ profile was created to reflect conditions at both test shafts. $MTCP$ values for the Bevier Formation ranged from 2 to 7.5 in/100 blows. One $MTCP$ measurement was performed in each of the Verdigris and Croweburg Formations resulting in an MTCP value of 1 in/100 blows in each formation. $MTCP$ values in the Fleming Formation ranged from 3.5 to 5.5 in/100 blows. Mean or "model" values for $MTCP$ and the standard deviation of these mean values determined from best fit probability distributions to the measured data are provided in Table 4.18 and also shown in Figure 4.18.

Table 4.17- Measured $MTCP$ values at Lexington Site.

Elevation (ft)	Measurements	
	Blows/6"	MTCP (in/100 blows)
581.5	42, 50 in 1"	7.5
576.5	50 in 2", 50 in 0"	2.0
571.5	50 in 1", 50 in 0"	1.0
561.5	50 in 1", 50 in 0"	1.0
556.5	50 in 2", 50 in 1.5"	3.5
551.5	50 in 3.5", 50 in 2"†	5.5

† possible sand fall-in

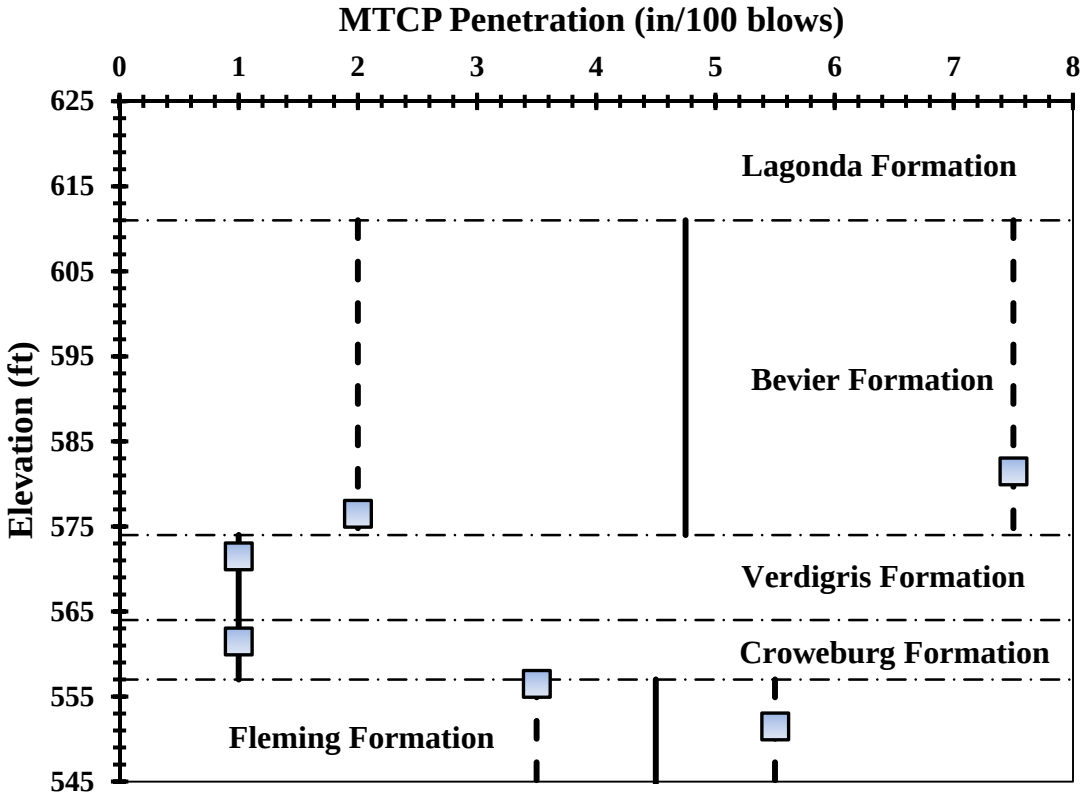

Figure 4.18- Measured MTCP values from the Lexington site, shown with interpreted "model" values. The horizontal dash-dot lines indicate approximate boundaries between shale and limestone strata.

Table 4.18- Summary of characteristics for best fit probability distribution for MTCP measurements at Lexington Site.

Stratum	Upper Elevation Limit (ft)	Lower Elevation Limit (ft)	Number of Tests	Best Fit Distribution	Mean Value (in/100 blows)	Model Standard Deviation (in/100 blows)
Bevier	611	574	2	Normal	4.75	2.75
Verdigris	574	564	1	Normal	1.0	--
Croweburg	564	557	1	Normal	1.0	--
Fleming	557	530	2	Normal	4.5	1.00

4.6 kcICON Load Test Site

The kcICON Load Test Site is located northeast of Kansas City on I29/I35/US71 (Figure 4.19). Approximate test shaft and borehole locations are shown in Figure 4.20. Standard Penetration testing was performed in 2006 in borings B-6 and B-8. In-situ testing and load testing were performed in 2008 for the construction of the kcICON bridge at locations B174+36 LT and B169+65 LT. Modified Texas Cone Penetration Testing and additional SPT measurements were also conducted in 2009 southwest of the new bridge at boring KC-1 in Figure 4.20.

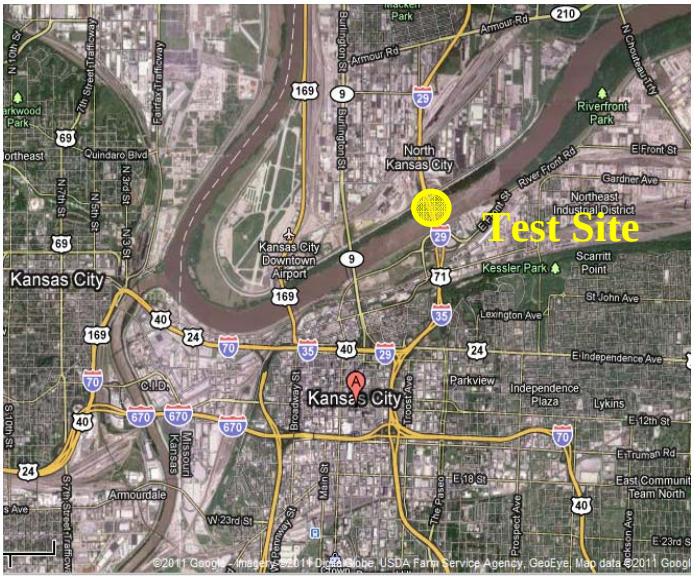

Figure 4.19- Location of kcICON Load Test Site in the Kansas City Metropolitan area. (Google Earth, 2011j)

4.6.1 Geology of kcICON Site

The geology of the kcICON test site includes (from top to bottom) a weathered shale, unweathered shale, and a soft shale stratum underlain by a compentent limestone.

The weathered and unweathered shale is a gray colored shale ranging from soft to hard, laminated in some areas with soft clay layers of less than one inch thick. UCS values ranged from 115 to 540 ksf in the unweathered zone. The shale was underlain by limestone which consisted of a pale gray and dark gray color with shale lenses.

Figure 4.20- kcICON Load Test Site showing locations of the SPT and MTCP test boreholes and the load test performed in 2008. Due to a large number of boreholes, not all SPT/MTCP boreholes are labeled. (Google Earth, 2011k)

4.6.2 SPT Measurements at kcICON Site

Measured N_{eq-60} -values from the kcICON site are provided in Table 4.19 and plotted in Figure 4.21. Standard Penetration Tests were performed only in the shale formations at the site. The weathered shale stratum was encountered from elevation 700 to 655 ft. Measured N_{eq-60}-values ranged from 120 to 398 blows/ft. The unweathered shale layer is divided in two formations kcICON A and kcICON B. kcICON A was

observed from elevation 655 to 612 ft with N_{eq-60} values ranging from 200 to 398 blows/ft. kcICON B was observed from elevations 612 to 590 ft with N_{eq-60} values ranging from 104 to 599 blows/ft. .

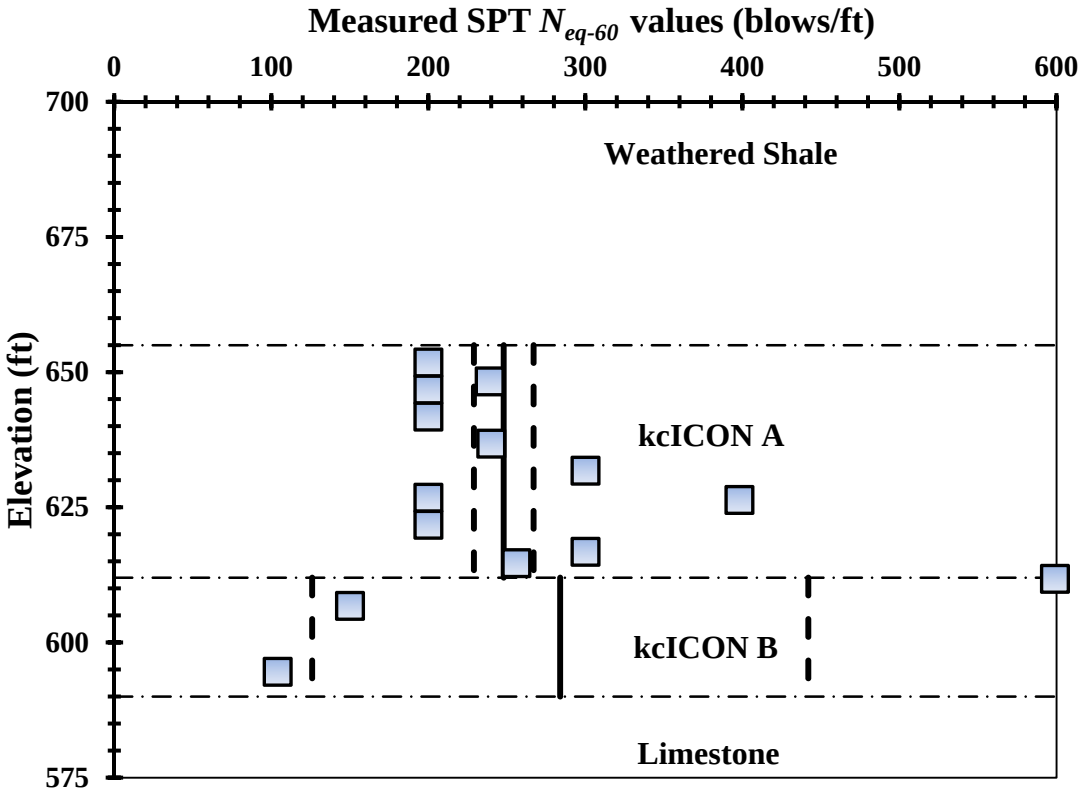

Figure 4.21- Measured N_{eq-60} values from the kcICON site shown with interpreted "model" values. The horizontal dash-dot lines indicate approximate boundaries between shale and limestone strata.

As was done for the other sites, probability distributions were fit to the measured data within each stratum using the distribution fitting tool in MATLAB® to determine the mean and the standard deviation of the mean value for each stratum. The resulting values are shown in Figure 4.21. Pertinent characteristics of the best fit distributions are summarized in Table 4.20.

Table 4.19- Measured N_{eq-60} values for the kcICON Site.

Elevation (ft)	SPT Measurements	
	Blows/6”	N_{eq-60} (blows/ft)
651.8	37 in 3”	200
648.3	72 in 5”	239
646.8	37 in 3”	200
641.8	37 in 3”	200
636.8	37 in 2.5”	240
631.8	37 in 2”	300
626.8	37 in 3”	200
626.4	72 in 3”	398
621.8	37 in 3”	200
616.8	37 in 2”	300
614.7	54 in 3”	256
611.8	37 in 1”	599
606.8	37 in 4”	150
594.6	44 in 6”	104

Table 4.20- Summary of characteristics for best fit probability distribution for SPT measurements at kcICON Site.

Stratum	Upper Elevation Limit (ft)	Lower Elevation Limit (ft)	Number of Tests	Best Fit Distribution	Mean Value (blows/ft)	Model Standard Deviation (blows/ft)
kcICON A	655	612	11	Normal	248	19.0
kcICON B	612	590	3	Normal	284	158.0

4.6.3 MTPC Measurements at kcICON Site

Measured $MTCP$ values for the kcICON site are provided in Table 4.21 and plotted in Figure 4.22 according to the same stratigraphy used for the SPT measurements. $MTCP$ values for the kcICON A stratum ranged from 0.5 to 2.5 in/100 blows while $MTCP$ measurements in the kcICON B stratum ranged from 1.0 to 2.5 in/100 blows.

Mean or "model" values for $MTCP$ and the standard deviation of these mean values determined from best fit probability distributions to the measured data are provided in Table 4.22 and also shown in Figure 4.22.

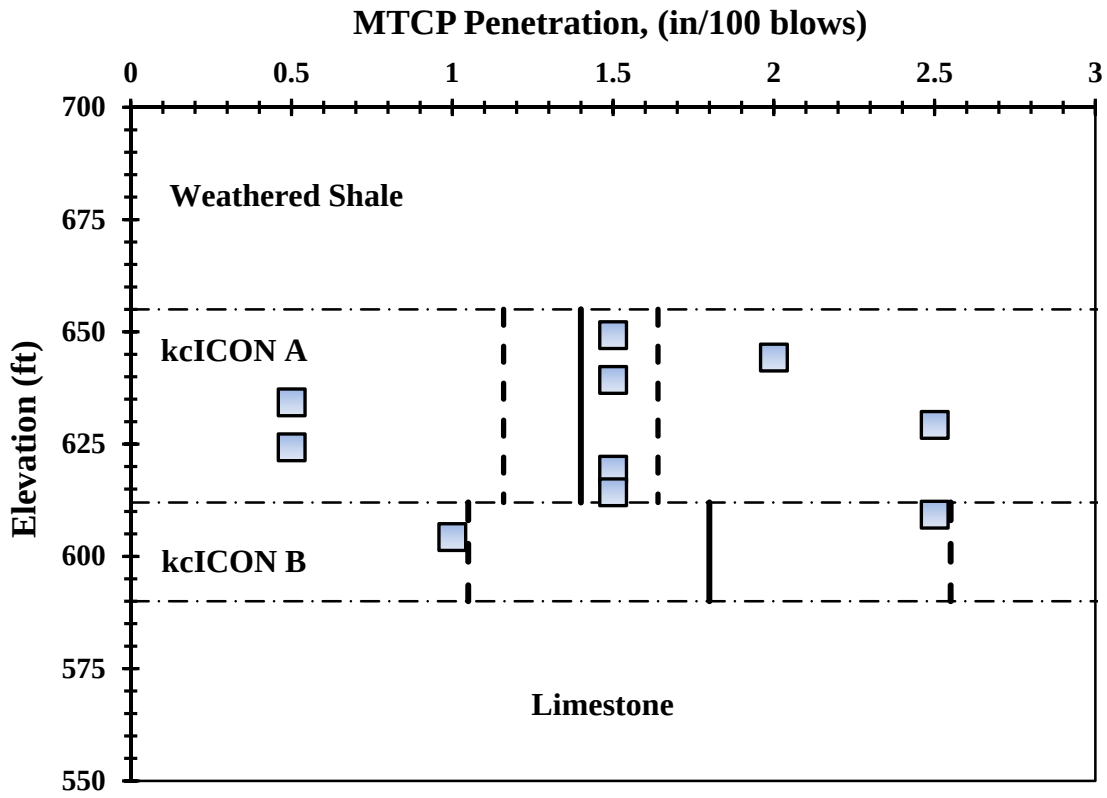

Figure 4.22- Measured MTCP values from the kcICON site shown with interpreted "model" values. The horizontal dash-dot lines indicate approximate boundaries between shale and limestone strata.

Table 4.21- Measured $MTCP$ values for the kcICON site.

Elevation (ft)	Measurements	
	Blows/6”	MTCP (in/100 blows)
649.3	50 in 1.5”, 50 in 0”	1.5
644.3	50 in 2”, 50 in 0”	2.0
639.3	50 in 1”, 50 in 0.5”	1.5
634.3	50 in 0.5”, 50 in 0”	0.5
629.3	50 in 2.5”, 50 in 0”	2.5
624.3	50 in 0.5”, 50 in 0”	0.5
619.3	50 in 1”, 50 in 0.5”	1.5
614.3	50 in 1”, 50 in 0.5”	1.5
609.3	50 in 2”, 50 in 0.5”	2.5
604.3	50 in 1”, 50 in 0”	1.0

Table 4.22- Summary of characteristics for best fit probability distribution for MTCP measurements at kcICON Site.

Stratum	Upper Elevation Limit (ft)	Lower Elevation Limit (ft)	Number of Tests	Best Fit Distribution	Mean Value (in/100 blows)	Model Standard Deviation (in/100 blows)
kcICON A	655	612	8	Normal	1.4	0.24
kcICON B	612	590	2	Normal	1.8	0.75

4.7 Waverly Load Test Site

The Waverly Load Test Site is located northeast of Waverly Missouri on U.S. Highway 65 over the Missouri River as shown in Figure 4.23. Standard Penetration Tests and load testing were performed in 2000 and 2002, respectively, for the Route 65 bridge realignment (Miller, 2003). MTCP testing was not performed at the Waverly site. SPT measurements were conducted as part of the original site investigation for design and

construction of the bridge. Only SPT measurements taken in borings near to the location of the test shaft (borings for Piers 9 through 12) were considered in this study.

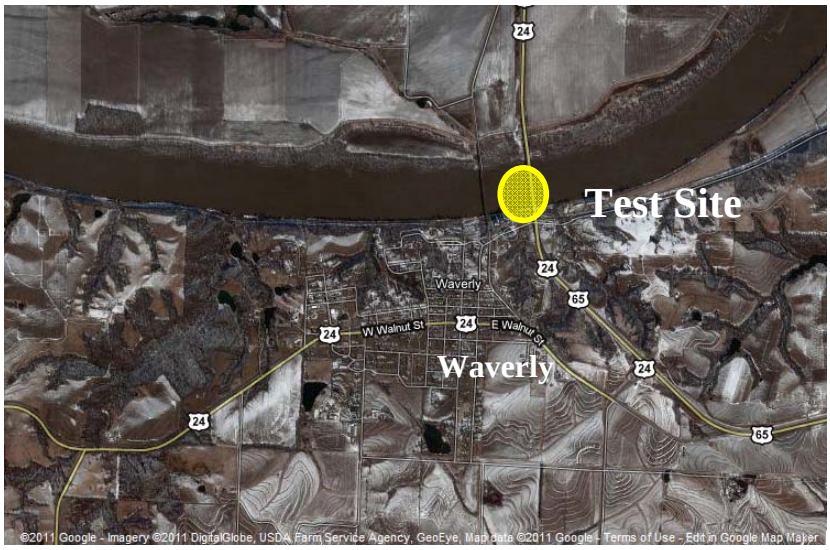

Figure 4.23 - Location of Waverly Load Test Site. (Google Earth, 2011l).

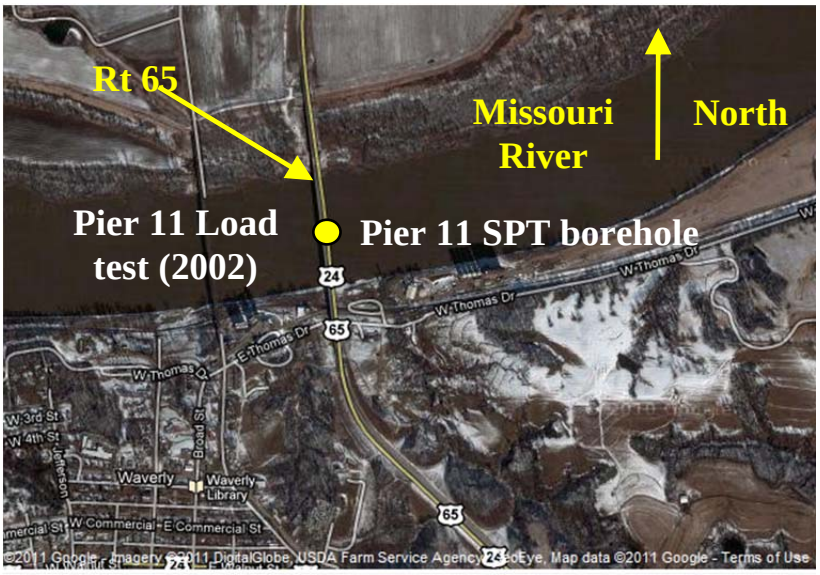

Figure 4.24 - Waverly Load Test Site showing location of the load test shaft. (Google Earth, 2011m)

4.7.1 Geology of Waverly Site

The Waverly site consists of variable thicknesses of generally sandy overburden soils overlying Pennsylvanian age bedrock from the Weir Formation. The test shaft was constructed entirely within the Weir Formation , which generally includes (from top to bottom) the Weir Pittsburg Coal bed, underclay, micaceous siltshale, limestone, shale, the Waverly coal beds, black carbonaceous shale, irregular bedded limestone, coarse grained sandstone and shale (Miller, 2003). For this work, the Weir formation was subdivided into three strata. Stratum A extends from approximate elevation 610 feet to elevation 582 feet and includes a gray to purple claystone and greenish-gray clay shale (Miller, 2003) with UCS values ranging from 1.4 to 27.8 ksf. Shale samples from this stratum were observed to be slickensided. Weir Stratum B extends from elevation 582 feet to elevation 564 feet and includes (from top to bottom) two separate coal layers, a gray claystone (underclay), gray micaceous siltshale, and gray clay shale (Miller, 2003) with UCS values ranging from 4.2 to 76.2 ksf. Weir Stratum C extends below elevation 564 feet and consists of limestone and sandstone.

4.7.2 SPT Measurements at Waverly Site

Measured N_{eq-60} -values from the Waverly site are provided in Table 4.23 and plotted in Figure 4.25. Measured N_{eq-60} -values from Weir Stratum A ranged from 156 to 600 blows per foot. Measurements from Weir Stratum B ranged from 240 to 600 blows/ft while measurements from Weir Stratum C ranged from 240 to 400 blows/ft.

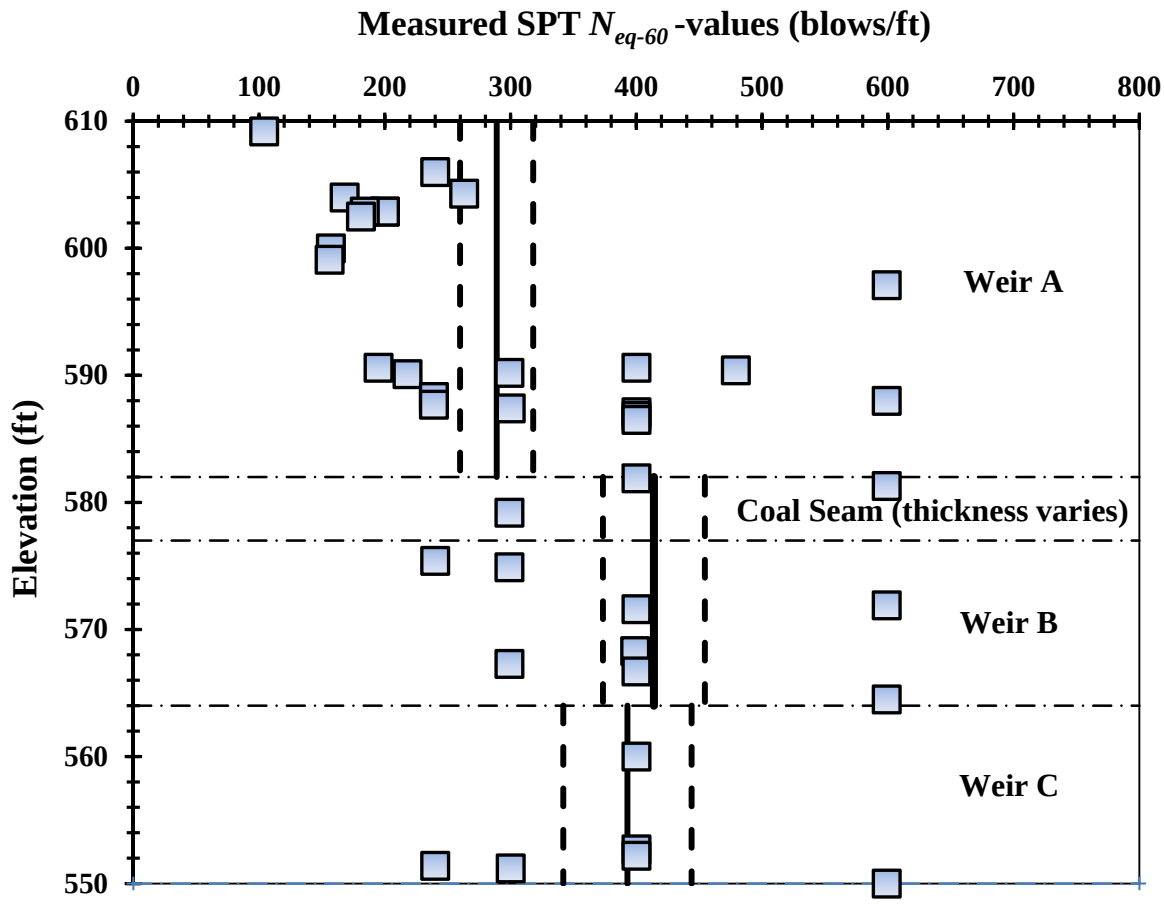

Figure 4.25- Measured SPT N_{60}-values from the Waverly site shown with interpreted model values. The horizontal dash-dot lines indicate approximate boundaries between shale.

As was done for the other sites, probability distributions were fit to the measured data within each stratum using the distribution fitting tool in MATLAB® to determine the mean and the standard deviation of the mean value for each stratum. The resulting values are shown in Figure 4.25. Pertinent characteristics of the best fit distributions are summarized in Table 4.24. Mean values for N_{eq-60} are 289 blows per foot for Weir Stratum A, 414 blows per foot for Weir Stratum B, and 393 blows per foot for Weir Stratum C.

Table 4.23- Measured N_{eq-60} values for the Waverly Site.

Elevation (ft)	SPT Measurements	
	Blows/6”	N_{eq-60} (blows/ft)
609.2	27, 29, 43 in 5.5”	104
606.0	74 in 5”	240
604.3	46, 36 in 2”	263
604.0	36, 46 in 4”	168
602.9	74 in 6”	200
602.9	74 in 6”	200
602.9	40, 34 in 3”	184
602.5	18, 56 in 5”	181
600.0	39, 43 in 4”	157
599.1	50, 32 in 3”	156
597.1	74 in 2”	599
590.6	62, 20 in 1.5”	195
590.6	74 in 3”	400
590.4	82 in 2.5”	479
590.2	82 in 4”	299
590.1	82 in 5.5”	218
588.3	82 in 5”	239
588.0	82 in 2”	599
587.7	82 in 5”	239
587.4	74 in 4”	300
587.1	74 in 3”	400
586.8	74 in 3”	400
586.5	74 in 3”	400
581.9	74 in 3”	400
581.3	74 in 2”	599
579.2	82 in 4”	299
575.4	74 in 5”	240
574.9	82 in 4”	299
571.9	74 in 2”	599
571.6	74 in 3”	400
568.3	82 in 3”	399
567.3	82 in 4”	299
566.7	74 in 3”	400
564.5	82 in 2”	599
560.0	74 in 3”	400
552.7	74 in 3”	400
552.2	74 in 3”	400
551.4	74 in 5”	240
551.2	74 in 4”	300
550.0	74 in 2”	599

Table 4.24- Summary of characteristics for best fit probability distribution for SPT measurements at Waverly Site.

Stratum	Upper Elevation Limit (ft)	Lower Elevation Limit (ft)	Number of Tests	Best Fit Distribution	Mean Value (blows/ft)	Model Standard Deviation (blows/ft)
Weir A	610	582	23	Lognormal	289	29.1
Weir B	582	564	11	Lognormal	414	40.5
Weir C	564	550	6	Lognormal	393	51.0

4.8 Dearborn Load Test Site

The Dearborn Load Test Site is located northeast of Dearborn, Missouri on State Route 116 where it crosses the Platte River (Figure 4.26). Approximate test shaft and borehole locations are shown in Figure 4.27.

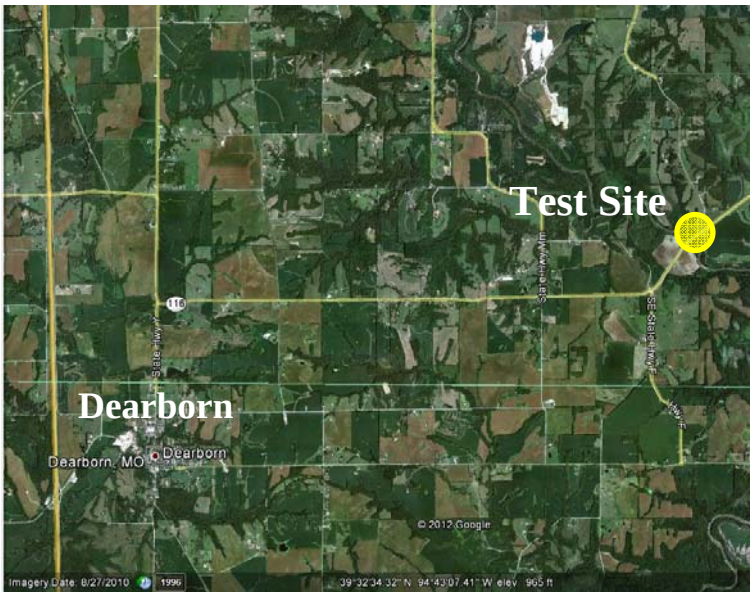

Figure 4.26 - Location of Dearborn Load Test Site. (Google Earth, 2011n).

Figure 4.27 - Dearborn Load Test Site showing locations of the SPT boreholes and the load test performed. (Google Earth, 2011o).

4.8.1 Geology at Dearborn Site

The Dearborn test site consists of approximately 38 feet of overburden underlain by a gray, moderately weathered shale and slightly weathered shale. Uniaxial compressive strengths in the shale range from 3.4 to 68.0 ksf. For this work, the shale was separated into two different strata: Shale A, which extends from elevation 780 feet to elevation 765 feet, and Shale B, which extends from elevation 765 feet to elevation 740 feet.

4.8.2 SPT Measurements at Dearborn Site

SPT measurements were made in the shale as part of the original site investigation program for the bridge in 2002 and again just prior to performing the load test in 2004. Only measurements made in borings within a distance of approximately 200 feet from the load test shaft were considered in this work. Measured N_{eq-60} -values from the Dearborn site are provided in Table 4.25 and plotted in Figure 4.28. Tests in the Stratum A material produced N_{eq-60}-values ranging from 133 to 200 blows per foot with a mean of 161 blows/ft. Tests in Stratum B produced N_{eq-60}-values ranging from 266 to 800 blows/ft with a mean of 414 blows/ft.

Table 4.25- Measured N_{eq-60}values for the Dearborn Site.

	SPT Measurements	
Elevation (ft)	**Blows/6”**	**N_{eq-60} (blows/ft)**
774.5	50 in 6”	133
774.1	50 in 6”	133
773.3	73 in 6”	178
769.1	50 in 4”	200
764.5	50 in 2”	400
764.1	50 in 2”	400
762.8	73 in 4”	266
759.5	50 in 2”	400
759.1	50 in 2”	400
754.5	50 in 2”	400
754.1	50 in 2”	400
752.5	73 in 3”	355
749.5	50 in 2”	400
749.1	50 in 2”	400
744.5	50 in 1”	800
744.1	50 in 2”	400
742.3	73 in 3”	355

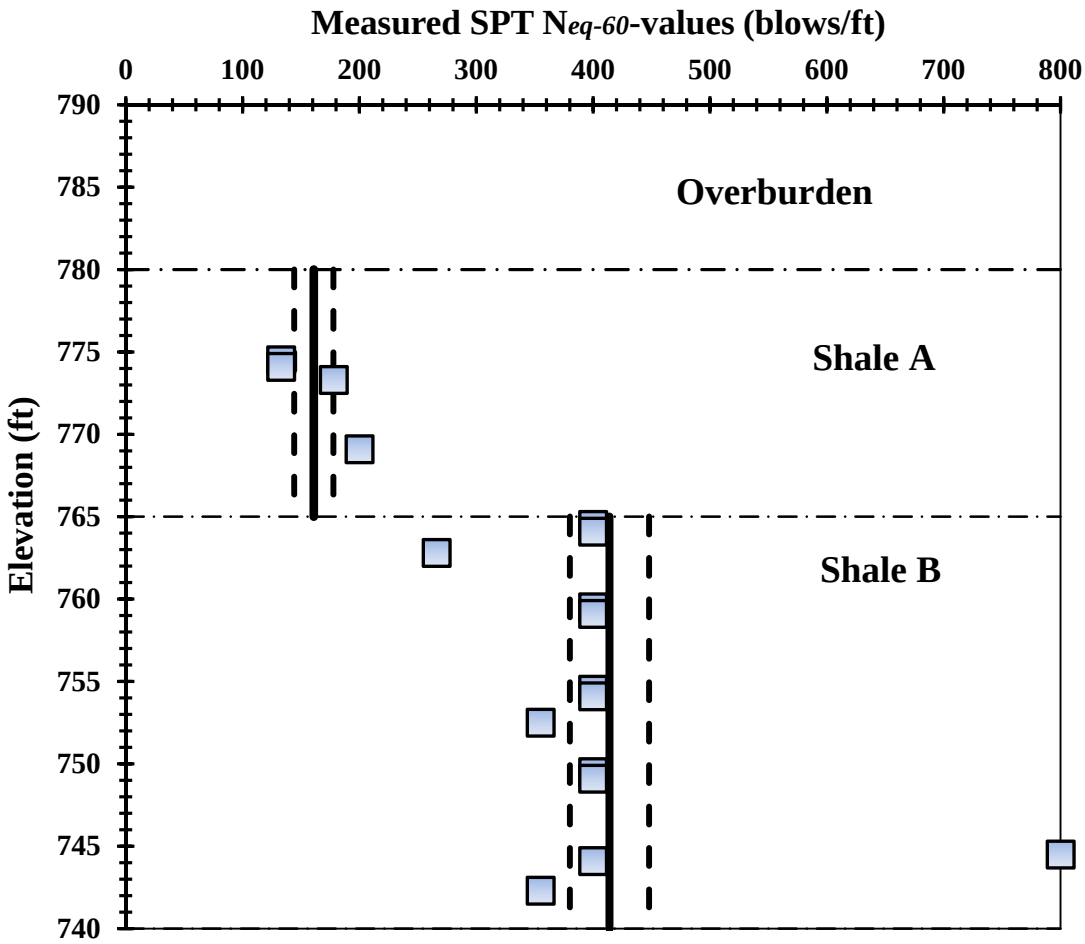

Figure 4.28- Measured SPT N_{eq-60} values from the Dearborn site shown with interpreted model values. The horizontal dash-dot lines indicate approximate boundaries between shale.

Table 4.26- Summary of characteristics for best fit probability distribution for SPT measurements at Dearborn Site.

Stratum	Upper Elevation Limit (ft)	Lower Elevation Limit (ft)	Number of Tests	Best Fit Distribution	Mean Value (blows/ft)	Model Standard Deviation (blows/ft)
Shale A	780	765	4	Normal	161	16.8
Shale B	765	740	13	Normal	414	33.9

4.9 Summary

SPT and MTCP measurements for two new load test sites, at Frankford and Warrensburg, and five historical load test sites were presented in this chapter. The geological stratigraphy and in-situ measurements completed at each site were presented. The measurements were divided into respective geological strata and mean or model N_{eq-60}or $MTCP$ values were calculated to represent the in situ measurements in each stratum. These data were subsequently used to develop predictive relationships that relate in-situ test measurements to tip and side resistance for drilled shafts in Missouri shales as described in subsequent chapters.

Chapter 5 - Development of Relations to Predict Shaft Capacity from SPT and MTCP Measurements

5.1 Introduction

Design of drilled shafts requires prediction of unit side and tip resistance values for the soil and/or rock present at a site and subsequent calculation of the total shaft capacity for shafts of different sizes using these unit values. Unit side and tip resistance values are commonly predicted using empirical relations that relate unit side or tip resistance to various soil or rock characteristics, including in situ test measurements. In this chapter, the development of empirical relations for predicting unit side and tip resistance from SPT and MTCP measurements in shale is described. Measurements of ultimate unit side and tip resistance from a number of field test sites are first summarized along with corresponding in-situ test measurements established in Chapter 4. The methods used to establish design relations from these measurements are then described. Finally, predictive relations established from analysis of the field load test and in situ test measurements are presented and compared to relations established previously by others.

5.2 Summary of Data Used to Develop Predictive Relations

Design relations were developed based on ultimate unit side and tip resistance values determined from field load tests and corresponding N_{eq-60} and $MTCP$ values established in Chapter 4. These values are summarized in Tables 5.1 through 5.6. Tables

5.1 and 5.2 summarize unit tip resistance measurements obtained from tests performed at the Warrensburg and Frankford sites, respectively, while Table 5.3 summarizes similar measurements taken from several historical load test sites. Similarly, Tables 5.4 and 5.5 respectively summarize unit side resistance measurements from the Warrensburg and Frankford load test sites and Table 5.6 provides results from several historical load tests.

Table 5.1- Summary of maximum measured unit tip resistance and corresponding mean N_{eq-60} and *MTCP* values from the Warrensburg Load Test Site.

Test Shaft	**Tip Elevation (ft)**	**Maximum Unit Tip Resistance (ksf)**	**Ultimate Value? (yes/no)**	**Mean N_{eq-60} (blows/ft)**	**Mean *MTCP* (in/100 blows)**
W1	750.4	41.8	No	107	7.5
W2	749.7	63.1	No	107	7.5
W3	735.5	175.0	No	206	1.9
W4	733.5	134.0	No	206	1.9
W5	756.4	100.3	Yes	100	3.7
W6	749.7	58.7	No	107	7.5
W7	749.1	188.6	Yes	107	7.5
W8	735.1	251.6	No	206	1.9
W9	735.2	158.9	No	206	1.9
W10	746.2	32.1	Yes	107	7.5
W11	745.9	57.9	No	107	7.5
W12	749.3	53.7	Yes	107	7.5
W13	749.9	44.1	No	107	7.5
W14	750.1	45.1	No	107	7.5
W15	749.6	66.9	No	107	7.5

Unit side and tip resistance values provided in the tables are the maximum values observed during the respective tests. These values were established from strain gauge measurements and the load applied by the O-cell™. Since failure was not always observed for all shafts, the tables indicate whether an "ultimate value" was achieved during the test (i.e. whether ultimate failure was actually observed) for the respective shaft tip or shaft segment. Decisions regarding whether failure had occurred were made

by inspection of the unit side resistance versus deflection or unit tip resistance versus deflection curves for the respective shaft tip or shaft segment. Cases where the resistance versus deflection curves had "flattened out", with little or no increase in resistance occurring with additional displacement, were deemed to have failed and to reflect ultimate values. Conversely, cases where additional resistance was being mobilized when the test was completed were deemed to not have reached an ultimate condition.

Table 5.2- Summary of maximum measured unit tip resistance and corresponding mean N_{eq-60} and *MTCP* values from the Frankford Load Test Site.

Test Shaft	Tip Elevation (ft)	Maximum Unit Tip Resistance (ksf)	Ultimate Value? (yes/no)	Mean N_{eq-60} (blows/ft)	Mean *MTCP* (in/100 blows)
F1	643.2	78.1	No	229	1.7
F2	640.9	121.1	No	229	1.7
F3	638.5	134.3	No	229	1.7
F4	637.6	271.4	Yes	229	1.7
F5	630.1	190.2	No	229	1.7
F6	636.6	297.5	Yes	229	1.7
F7	629.3	211.4	Yes	229	1.7
F8	640.4	84.7	No	229	1.7
F9	647.0	29.4	No	74	3.5
F10	645.2	44.5	No	74	3.5

Table 5.3- Summary of maximum measured unit tip resistance and corresponding mean N_{eq-60} and *MTCP* values from several historical load tests.

Test Site	Test Shaft	Tip Elevation (ft)	Maximum Unit Tip Resistance (ksf)	Ultimate Value? (yes/no)	Mean N_{eq-60} (blows/ft)	Mean *MTCP* (in/100 blows)
Lexington	LEX1	548.8	160.6	No	384	4.5
Lexington	LEX2	573.0	144.0	Yes	194	--
Kansas City	KC1	611.4	280.0	No	284	1.8
Dearborn	D1	763.3	133.8	No	414	--
Waverly	WAV1	558.0	110.0	No	393	--

Table 5.4- Summary of maximum measured unit side resistance and corresponding mean N_{eq-60} and MTCP values from the Warrensburg Load Test Site.

Test Shaft	Interval		Maximum Unit Side Resistance (ksf)	Ultimate Value? (yes/no)	Mean N_{eq-60} (blows/ft)	Mean *MTCP* (in/100 blows)
	Lower Elev. (ft)	Upper Elev. (ft)				
W1	761.4	765.5	2.1	Yes	100	3.7
	752.5	761.4	3.3	Yes	100	3.7
W2	760.6	764.8	6.3	Yes	100	3.7
	751.8	760.6	2.6	Yes	100	3.7
W3	760.4	765.4	6.5	Yes	100	3.7
	753.3	760.4	4.6	Yes	100	3.7
	745.3	753.3	5.8	Yes	105	6.1
	738.4	745.3	4.6	Yes	206	1.9
W4	760.9	767.0	5.6	Yes	100	3.7
	753.8	760.9	2.3	Yes	100	3.7
	745.8	753.8	5.3	Yes	105	6.1
	738.9	745.8	5.3	Yes	206	1.9
W5	762.1	765.0	1.5	No	100	3.7
	757.0	762.1	1.8	No	100	3.7
W6	760.6	764.6	4.7	No	100	3.7
	756.6	760.6	3.8	Yes	100	3.7
	751.7	756.6	5.2	Yes	100	3.7
W7	756.3	764.3	2.4	No	100	3.7
	749.2	756.3	2.9	No	100	3.7
W8	756.3	762.3	3.2	Yes	100	3.7
	750.3	756.3	5.9	Yes	100	3.7
	744.3	750.3	5.3	Yes	107	7.5
	735.6	744.3	16.1	Yes	206	1.9
W9	756.7	762.6	3.7	Yes	100	3.7
	744.6	756.7	3.7	Yes	103	5.3
	735.6	744.6	4.0	No	206	1.9
W10	762.3	767.3	1.2	No	100	3.7
	752.3	762.3	2.1	No	100	3.7
	747.0	752.3	3.3	Yes	100	3.7
W11	762.7	767.7	1.8	No	100	3.7
	757.7	762.7	2.8	No	100	3.7
	752.7	757.7	1.4	No	100	3.7
	747.3	752.7	3.7	No	104	5.6
W12	760.6	764.5	1.0	Yes	100	3.7
	756.5	760.6	3.8	Yes	100	3.7
	751.4	756.5	8.8	Yes	100	3.7
W13	761.5	765.0	2.3	Yes	100	3.7
	756.9	761.5	1.9	Yes	100	3.7
	752.0	756.9	7.4	Yes	100	3.7
W14	761.4	765.6	2.5	Yes	100	3.7
	757.3	761.4	2.4	Yes	100	3.7
	752.5	757.3	5.0	Yes	100	3.7
W15	760.8	764.9	3.0	Yes	100	3.7
	756.8	760.8	4.5	Yes	100	3.7
	751.8	756.8	6.2	Yes	100	3.7

Table 5.5 - Summary of maximum measured unit side resistance and corresponding mean N_{eq-60} and *MTCP* values from the Frankford Load Test Site.

Test Shaft	Interval		Maximum Unit Side Resistance (ksf)	Ultimate Value? (yes/no)	Mean N_{eq-60} (blows/ft)	Mean *MTCP* (in/100 blows)
	Lower Elev. (ft)	Upper Elev. (ft)				
F1	654.9	657.3	0.7	Yes	29	--
	652.4	654.9	1.9	Yes	74	3.5
	649.9	652.4	8.4	Yes	74	3.5
	647.5	649.9	6.1	Yes	74	3.5
	644.4	647.5	21.4	Yes	229	1.7
F2	653.2	656.2	0.9	Yes	56	--
	650.2	653.2	6.1	No	74	3.5
	647.2	650.2	3.7	No	74	3.5
	641.8	647.2	12.5	No	229	1.7
F3	653.7	657.7	0.6	Yes	29	--
	649.7	653.7	6.7	Yes	74	3.5
	645.2	649.7	6.2	Yes	74	3.5
	643.1	645.2	10.6	Yes	140	2.7
	639.1	643.1	42.9	Yes	229	1.7
F4	655.1	658.1	0.6	Yes	29	--
	652.1	655.1	2.4	Yes	43	--
	649.1	652.1	10.9	Yes	74	3.5
	646.1	649.1	8.4	Yes	74	3.5
	643.1	646.1	23.9	Yes	229	1.7
	638.1	643.1	27.5	Yes	229	1.7
F5	650.7	655.2	4.2	Yes	74	3.5
	646.2	650.7	5.2	Yes	74	3.5
	642.2	646.2	12.2	Yes	152	2.6
	638.2	642.2	19.2	Yes	229	1.7
	632.6	638.2	37.3	Yes	229	1.7
F6	654.0	657.0	1.3	Yes	44	--
	651.0	654.0	9.2	No	74	3.5
	648.0	651.0	5.0	No	74	3.5
	645.0	648.0	6.7	Yes	74	3.5
	642.0	645.0	18.6	No	229	1.7
	637.0	642.0	34.3	No	229	1.7
F7	650.1	654.5	8.9	Yes	74	3.5
	644.5	650.1	5.8	Yes	74	3.5
	641.1	644.5	20.7	Yes	229	1.7
	637.5	641.1	32.3	Yes	229	1.7
	634.0	637.5	36.8	Yes	229	1.7
F8	653.1	656.2	1.7	Yes	42	--
	650.1	653.1	8.4	No	74	3.5
	647.2	650.1	1.6	Yes	74	3.5
	644.2	647.2	5.2	No	229	1.7
	641.3	644.2	9.3	No	229	1.7
F9	653.8	656.8	1.0	Yes	29	--
	650.8	653.8	8.5	Yes	74	3.5
	647.7	650.8	9.8	Yes	74	3.5
F10	656.0	657.8	0.9	Yes	29	--
	654.0	656.0	1.1	Yes	29	--
	651.8	654.0	6.2	Yes	74	3.5
	649.8	651.8	9.1	Yes	74	3.5
	645.8	649.8	9.0	Yes	74	3.5

Table 5.6- Summary of maximum measured unit side resistance and corresponding mean N_{eq-60} and *MTCP* values from historical load test sites.

Test Site	Test Shaft	Interval		Maximum Unit Side Resistance (ksf)	Ultimate Value? (yes/no)	Mean N_{eq-60} (blows/ft)	Mean *MTCP* (in/100 blows)
		Lower Elev. (ft)	Upper Elev. (ft)				
Lexington	LEX1	572.5	577.2	7.7	No	194	4.8
		567.6	572.5	19.2	No	194	1.0
		564.3	567.6	39.3	No	194	1.0
		560.5	564.3	18.4	Yes	153	1.0
		556.3	559.4	18.3	Yes	153	1.0
Lexington	LEX2	599.3	605.0	4.9	No	245	--
		596.0	599.3	14.5	No	245	--
		591.1	596.0	34.5	No	245	--
		578.0	582.9	15.2	Yes	245	--
Grandview	G1	927.0	934.0	6.3	Yes	94	3.3
		921.0	927.0	6.2	Yes	169	7.7
		915.5	921.0	7.7	Yes	169	7.7
		905.0	915.5	23.8	Yes	157	2.3
		898.0	905.0	47.9	No	--	--
		893.4	898.0	12.3	Yes	195	1.1
Waverly	WV1	599.6	607.6	1.7	No	289	--
		584.6	599.6	2.1	No	289	--
		574.6	584.6	6.5	No	414	--
		563.3	574.6	12.4	No	414	--
		560.6	563.6	59.0	No	393	--
Dearborn	D1	765.3	773.3	15.3	No	161	--
Kansas City	KC1	636.2	641.8	11.6	Yes	249	1.4
		630.2	636.2	16.2	Yes	249	1.4
		624.2	630.2	16.3	Yes	249	1.4
		618.2	624.2	16.4	Yes	249	1.4
		613.3	618.2	15.7	Yes	249	1.4

The mean values for in-situ test measurements provided in Tables 5.1 through 5.6 were established from the "model profiles" established in Chapter 4. The N_{eq-60} and $MTCP$ values provided for tip resistance correspond to values appropriate for the depth range within a distance of two diameters below the tip of the respective shaft. Values provided for side resistance correspond to values appropriate for the depth range of the respective shaft segment.

In cases where a shaft segment extends across multiple strata (established in Chapter 4), a weighted average of the N_{eq-60} or $MTCP$ values was taken as

$$X_{avg} = \frac{[(X_1)*(L_1)]+[(X_2)*(L_2)]}{L_1+L_2} \quad (5.1)$$

where X_{avg} is the weighted average mean value of the in-situ test measurement, X_1 is the mean in-situ test measurement in stratum 1, L_1 is the length of the shaft segment within stratum 1, X_2 is the mean in-situ test measurement in stratum 2, and L_2 is the length of the shaft segment within stratum 2.

As an example, if a shaft segment extends 2 feet in one stratum with $N_{eq-60} = 178$ and 1.5 feet in a second stratum with $N_{eq-60} = 288$, the weighted average value of N_{eq-60} would be calculated as

$$N_{eq-60-avg} = \frac{[(178)*(2)]+[(288)*(1.5)]}{2+1.5} = 225\,\frac{blows}{ft} \quad (5.2)$$

5.3 Methods for Developing Predictive Relations

Empirical design relations were generally developed by fitting curves to the empirical data summarized in Section 5.2 using ordinary or weighted least squares regression techniques. A total of four different predictive relations were developed:

- a relation to predict ultimate unit tip resistance from N_{eq-60}-values,
- a relation to predict ultimate unit side resistance from N_{eq-60}-values,
- a relation to predict ultimate unit tip resistance from $MTCP$-values, and
- a relation to predict ultimate unit side resistance from $MTCP$ -values.

Specific details of the regression analyses performed to develop these relations are described in subsequent sections. For all analyses, only the data corresponding to failure in side or tip resistance (i.e. those data indicated as being "ultimate" values in Tables 5.1 through 5.6) were used in the least squares regression analyses so the resulting relations reflect the ultimate unit resistance.

5.4 Relations between SPT N_{eq-60} and Shaft Capacity

Two new design relations were developed to respectively relate the ultimate unit side resistance and ultimate unit tip resistance from the various load tests to the SPT N_{eq-60}-values established for the respective test sites. Linear relations with zero intercepts were used for the predictive relations, expressed as:

$$E(y|x) = \beta x \tag{5.3}$$

where $E(y|x)$ is the expected value of y for a given x, and β is the least squares best fit coefficient (Ang and Tang, 1975). In this instance, y corresponds to the predicted ultimate unit side or tip resistance and x corresponds to the mean SPT N_{eq-60}-value for the appropriate shale stratum.

5.4.1 Relation between SPT N_{eq-60} and Ultimate Unit Tip Resistance

Maximum measured unit tip resistance values are plotted versus the corresponding mean SPT N_{eq-60}-values for all load tests in Figure 5.1. In the figure, the

circled data points reflect measurements from tests where the ultimate condition was reached while uncircled data points reflect the maximum measured unit tip resistance achieved for tests where the ultimate condition was not reached.

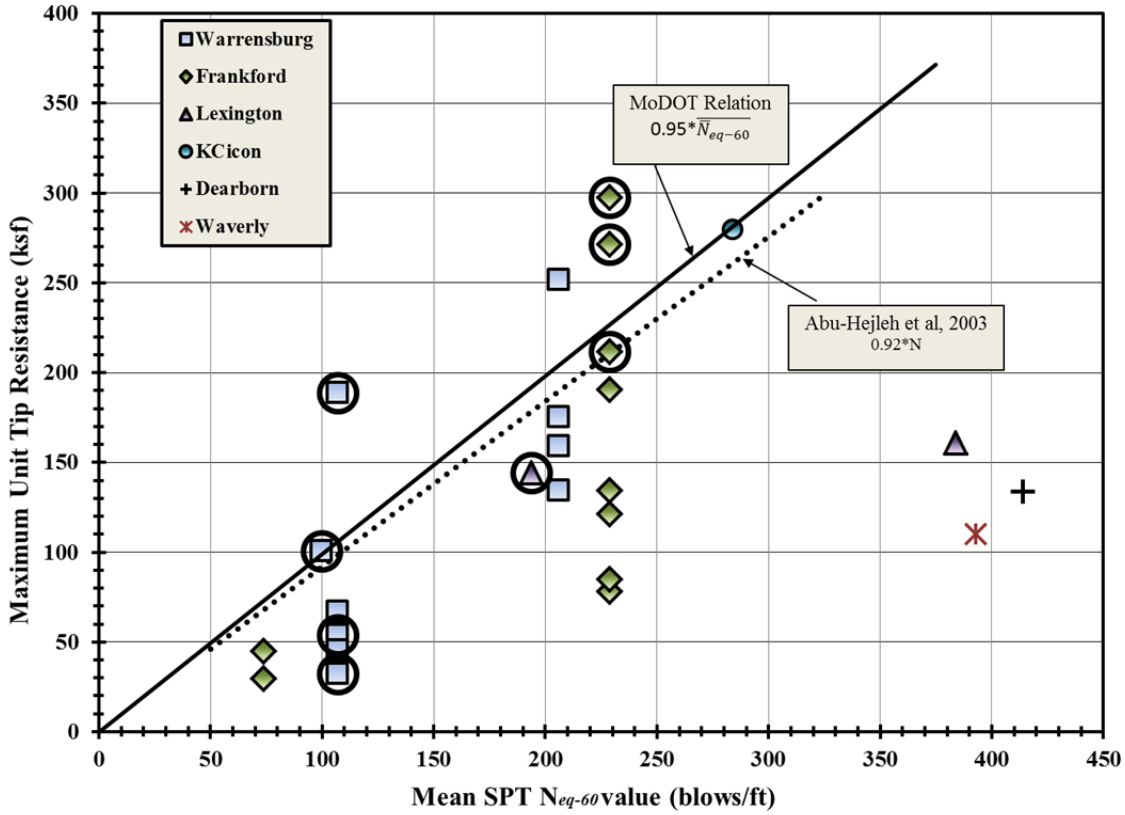

Figure 5.1 - Maximum measured unit tip resistance values from field load tests plotted versus the mean value of N_{eq-60} for the stratum below the shaft tip.

The least squares best fit trend line established to reflect the relation between ultimate unit tip resistance and the mean value of N_{eq-60} is also shown in Figure 5.1. The best fit relation can be expressed as:

$$q_p = 0.95 * \overline{N_{eq-60}} \qquad (5.4)$$

where q_p is the predicted ultimate unit tip resistance (in ksf), and $\overline{N_{eq-60}}$ is the mean value of N_{eq-60} for the rock below the shaft tip (in blows/ft). The predictive relation for the UCSB design method (Abu-Hejleh et al., 2003) is also shown in Figure 5.1. The UCSB relation predicts tip resistance values that are slightly lower than those predicted using Equation 5.4.

5.4.2 Relation between SPT N_{eq-60} and Ultimate Unit Side Resistance

Maximum measured unit side resistance values are plotted versus the corresponding mean SPT N_{eq-60}-values for all load tests in Figure 5.2. Also shown in the figure is the least squares best fit trend line taken to reflect the relation between ultimate (circled data) unit side resistance and the mean value of N_{eq-60}. This best fit relation can be expressed as:

$$q_s = \frac{\overline{N_{eq-60}}}{15} \tag{5.5}$$

where q_s is the predicted ultimate unit side resistance (in ksf), and $\overline{N_{eq-60}}$ is the mean N_{eq-60}-value for the shale along the shaft segment (in blows/ft).

The relation for the UCSB design method described in Chapter 2 (Abu-Hejleh, et al. 2003) is also shown in Figure 5.2. The UCSB method predicts side resistance values that are approximately 10 percent greater than those predicted using Equation 5.5. These alternative relations are practically identical as such small differences are easily explained by minor differences in the empirical measurements used to establish the alternative relations.

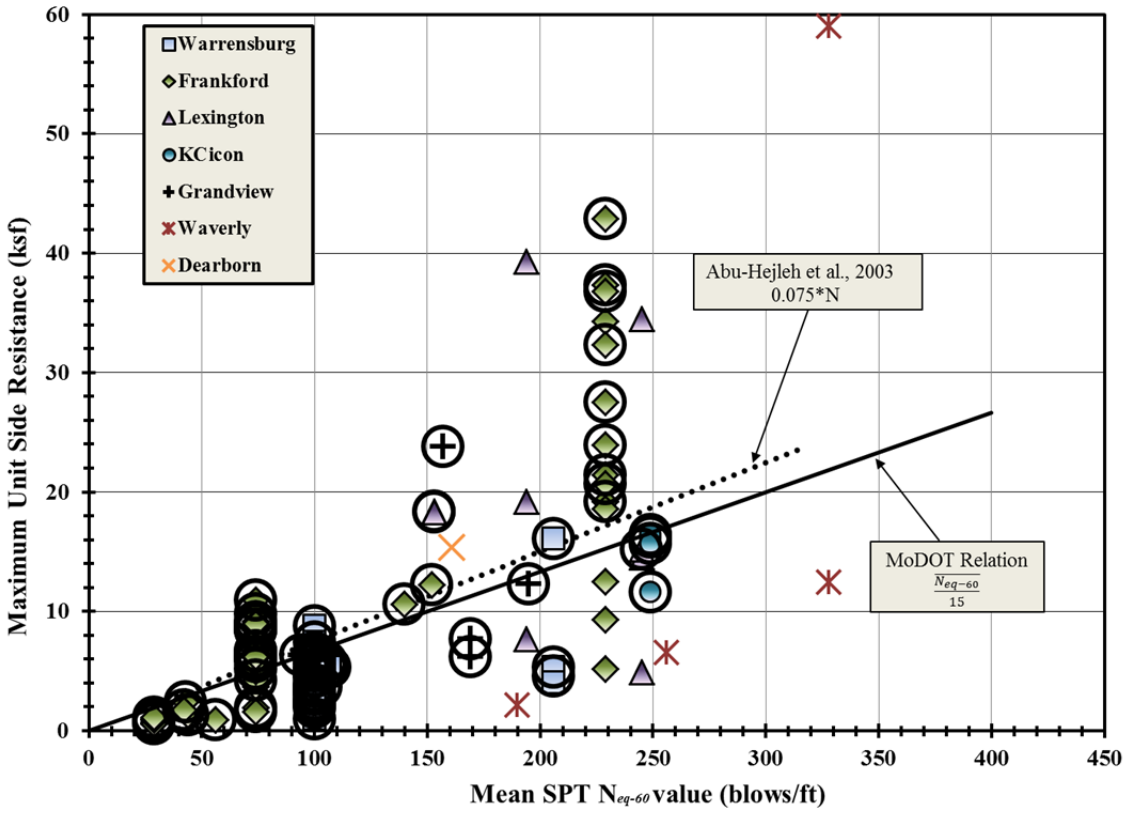

Figure 5.2 - Maximum measured unit side resistance values from field load tests plotted versus the mean value of N_{eq-60} for the shaft segment.

5.5 Relations between $MTCP$ and Shaft Capacity

Two new design relations were also developed to respectively relate the ultimate unit side resistance and ultimate unit tip resistance from the various load tests to the $MTCP$-values established for the respective test sites. Load test measurements from two of the load test sites, the Dearborn and Waverly sites, were not included in the analyses since MTCP tests were not performed at these sites.

Unlike the SPT relations presented in Section 5.4, the relationships between ultimate unit side and tip resistance and $MTCP$ are nonlinear. The nonlinear best fit

relations among $MTCP$-values and ultimate unit side and ultimate unit tip resistance were established by "linearizing" the regression as (Ang and Tang, 1975):

$$E(y|x) = \alpha + \beta g(x) \tag{5.6}$$

where $E(y|x)$ is the expected value of y for a given x, α and β are the least squares best fit coefficients, and $g(x)$ is a predetermined nonlinear function of x. The function $g(x)$ can be taken as any nonlinear function of x that produces a reasonable fit to the data. The specific nonlinear function used for fitting the empirical data for this work was a power function of the form

$$g(x) = ax^b \tag{5.7}$$

where a and b are the coefficient and exponent of the power relation, respectively. This functional form is consistent with prior relations developed by Nam and Vipulanandan (2010).

5.5.1 Relation between $MTCP$ and Ultimate Unit Tip Resistance

Maximum measured unit tip resistance values are plotted versus the corresponding mean $MTCP$-values for all load tests in Figure 5.3. Also shown in the figure is the nonlinear best fit trend line established to relate unit tip resistance with the mean value of $MTCP$. This best fit relation can be expressed as:

$$q_p = 500 \cdot \overline{MTCP}^{-1.22} \tag{5.8}$$

where q_p is the predicted ultimate unit tip resistance (in ksf), and $\overline{MTCP}$ is the mean value of $MTCP$ for the rock beneath the shaft tip (in in/100 blows).

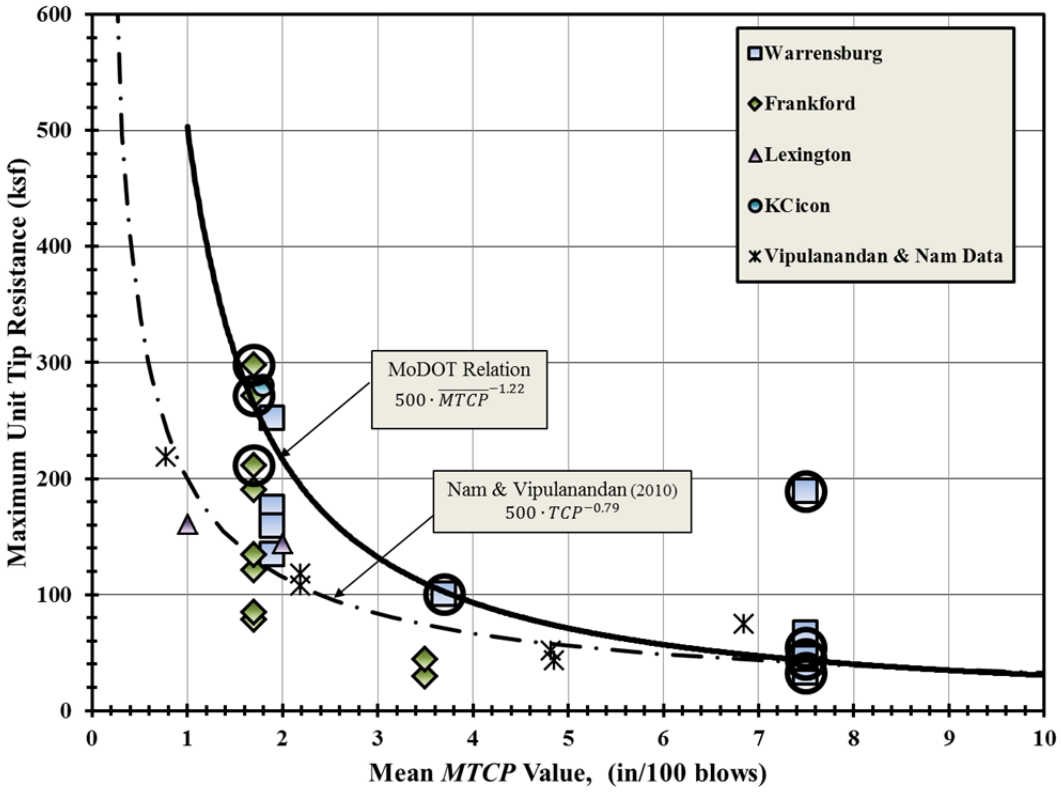

Figure 5.3 - Maximum measured unit tip resistance values from field load tests plotted versus the mean value of $MTCP$ for the shale below the shaft tip.

The design relation proposed by Nam and Vipulanandan (2010) is also shown in Figure 5.3. As shown in the figure, the Nam and Vipulanandan relation predicts ultimate unit tip resistance values that are substantially lower than those predicted using Equation 5.8 for penetration values less than 6 in/100 blows. The observed differences may be attributed to the different geological conditions or construction methods, considering that the Nam and Vipulanandan relation was developed based on results of three load tests performed in Texas while Equation 5.8 is based on results of twenty eight load tests conducted in Missouri. Also, one of the tests used to develop the Nam and Vipulanandan

relation did not reach the ultimate condition; rather, the ultimate values for this test were established from finite element analyses (Nam and Vipulanandan, 2010).

5.5.2 Relation between $MTCP$ and Ultimate Unit Side Resistance

Measured maximum unit side resistance values are plotted versus the corresponding mean $MTCP$-values for all load tests in Figure 5.4 along with the nonlinear best fit trend line that was fit to the values deemed to be ultimate values. The best fit relation can be expressed as:

$$q_s = 29 \cdot \overline{MTCP}^{-1.14} \tag{5.9}$$

where q_s is the predicted ultimate unit side resistance (in ksf), and $\overline{MTCP}$ is the mean value of $MTCP$ for the rock beneath the shaft tip (in in/100 blows).

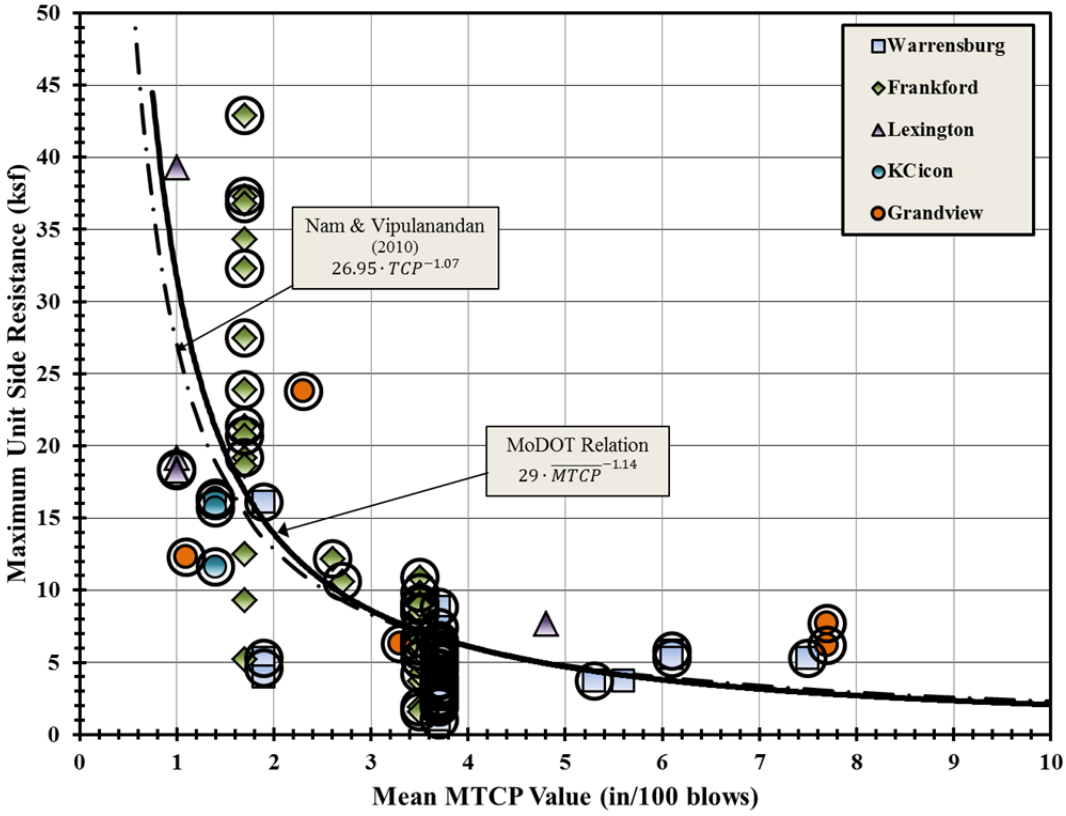

Figure 5.4- Measured unit side resistance values from field load tests plotted versus the mean value of $MTCP$ for the shaft segment.

The relation of Equation 5.9 produces similar ultimate unit side resistance values to the relation proposed by Nam and Vipulanandan (2010), which is also shown in Figure 5.4. Such small differences can easily be explained by differences in the empirical data sets, differences in the geologic materials for these data sets, and potentially different construction practices.

5.6 Summary

In this chapter, results from load tests performed on thirty one full-scale drilled shafts were presented with the corresponding values for $MTCP$ and SPT N_{eq-60}. Design relations for predicting ultimate unit side and ultimate unit tip resistance for drilled shafts from SPT and MTCP measurements were then proposed based on least squares regression analyses of the empirical data sets. The proposed design relations for predicting ultimate unit side resistance are generally similar to relations previously proposed by others. The proposed design relation for predicting ultimate unit tip resistance from N_{eq-60} is also similar to previously proposed relations. However, the proposed design relation for predicting ultimate unit tip resistance from $MTCP$ produces predictions that substantially exceed those predicted using the relation proposed by Nam and Vipulanandan (2010) for mean $MTCP$-values less than 6 in/100 blows.

Chapter 6 – Characterization of Variability and Uncertainty in Predictive Relations for Shaft Capacity

6.1 Introduction

Design of drilled shafts using load and resistance factor design (LRFD) methods preferably accounts for the variability and uncertainty in the capacity of drilled shafts. Variability and uncertainty in shaft capacity arises from variability and uncertainty in the input parameters to the design relations (e.g. SPT N_{eq-60}-values and $MTCP$-values for the relations presented in Chapter 5) and variability and uncertainty in the empirical design relations themselves. The variability and uncertainty of the input parameters from the field test sites were described in Chapter 4. In Chapter 5, best fit design relationships that relate shaft capacity to SPT and MTCP measurements were presented. These design relations have variability and uncertainty that arises from the precision of the load test measurements, from differences in construction techniques used for the various test shafts, and other sources. Regardless of the source of the variability and uncertainty in the design relations, it must be accounted for and addressed for appropriate calibration of resistance factors for LRFD.

This chapter first describes how variability and uncertainty in the predictive relations are represented. The approach taken for quantifying this variability and uncertainty and judging how it relates to the design relation is then described. Finally, the quantitative variability and uncertainty established for the predictive relations from Chapter 5 are presented.

6.2 Representation of Variability and Uncertainty in Predictive Relations

The predictive design relations presented in Chapter 5 among unit side and tip resistance and in-situ test measurements are provided as deterministic relationships in that a specific value of unit side or tip resistance will be produced for a given mean value of the input variable. This is appropriate for design equations. However, in reality there is significant variability and uncertainty in the design relations, as illustrated by the scatter present in the empirical data shown in Figures 5.1 through 5.4. The variability and uncertainty arises from a number of sources including the precision of the load test measurements, differences in construction methods used for individual test shafts, and simple random variability of the measurements.

In order to account for the variability and uncertainty in the design relations, a probabilistic variable, M, is introduced to represent the variability and uncertainty in the design relations in a normalized manner. The design relations, including the variability and uncertainty about the relations, are therefore represented as

$$q(x) = f(x) \cdot M(x) \tag{6.1}$$

where $q(x)$ is the probabilistic design relation including the variability and uncertainty present in the relation, x is the mean value of the input parameter for the design relation, $f(x)$ is the best fit, deterministic function established for the design relation (a deterministic relation), and $M(x)$ is a dimensionless (normalized) multiplicative variable or function that accounts for the variability and uncertainty in the design relation (Baecher & Christian, 2003). Note that $M(x)$ may or may not be established to be a function of the input parameter, x (i.e. M may be chosen to be independent of x).

If the predictive relation is a "best fit" relation that is taken to reflect the mean of the empirical data, the variable M can be taken to have a mean value of 1.0 (because there is no bias in the relation so it is normalized by itself). The standard deviation of M is established by normalizing the distribution reflecting the actual variability of measurements about the best fit relation by the mean value as

$$\sigma_M(x) = \frac{\sigma_{f(x)|x}(x)}{f(x)} \tag{6.2}$$

where $\sigma_M(x)$ is the standard deviation of M, which may be a function of x, $\sigma_{f(x)|x}(x)$ is the conditional standard deviation of the predicted value for a given x, and $f(x)$ is the predicted value for the same x, which is taken to be the mean. Methods used to establish the conditional standard deviation for the different predictive relations from Chapter 5 are described subsequently.

6.3 Calculation of Conditional Standard Deviation for Predictive Relations

The conditional standard deviation used in Equation 6.2 should reflect the variability and uncertainty in the established relation between the predicted variable (e.g. unit side resistance or unit tip resistance) and the input parameter (e.g. SPT N_{eq-60}-value or $MTCP$-value). This is illustrated in Figure 6.1, which shows a conditional distribution of the unit side resistance for a given value of $N_{eq-60} = 200$ blows/ft for the data and design relation shown previously in Figure 5.2.

There are several issues that must be considered when quantifying the conditional standard deviation associated with the empirical relationship. There are, in fact, several

different standard deviations that can be calculated to reflect different aspects of uncertainty and variability. Each of these could be appropriate depending on the intended use. The conditional standard deviation also depends on whether constant or non-constant variance is assumed in the fitting procedure. Each of these issues is described in more detail in this section.

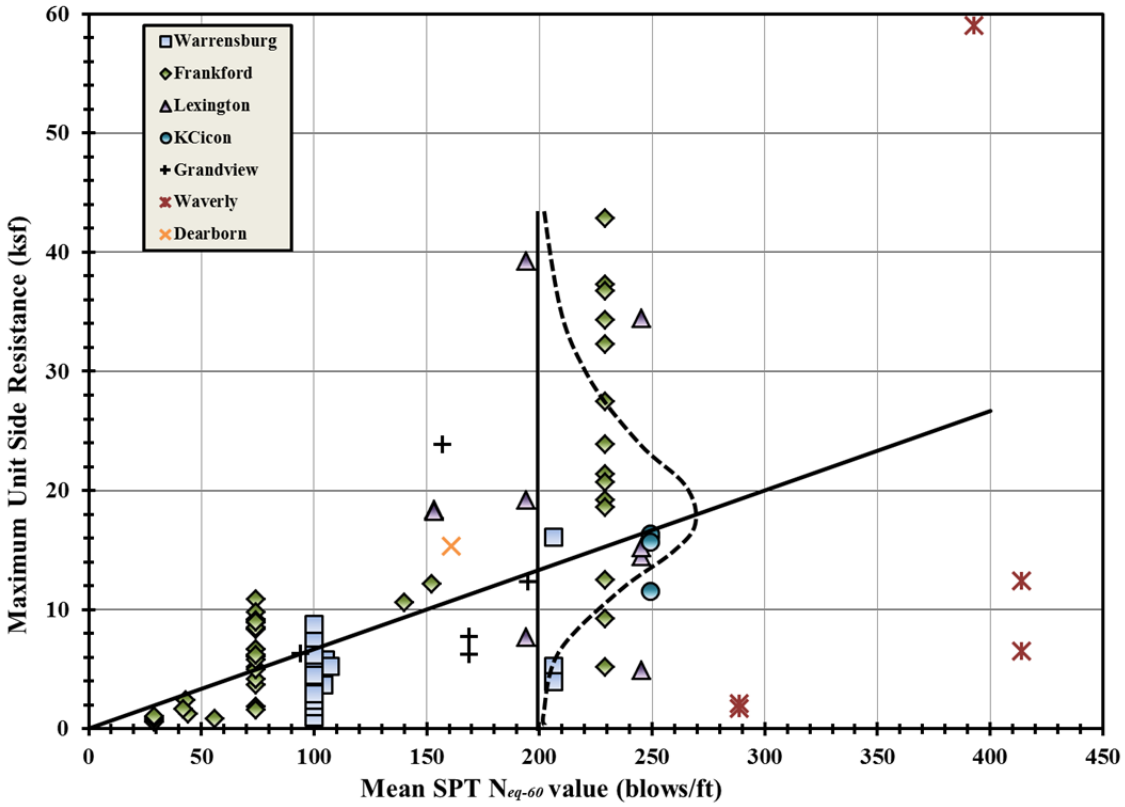

Figure 6.1- Illustration of conditional distribution of ultimate unit side resistance at $N_{eq-60} = 200$ blows/ft.

6.3.1 Selection of Appropriate Conditional Standard Deviation

Three different conditional standard deviations can be calculated to represent different aspects of variability and uncertainty in the predictive relations. The three

alternatives include calculating the conditional standard deviation to reflect random or measurement variability, to reflect model uncertainty, or to reflect the so-called total variability, which combines both the random or measurement variability and model uncertainty.

The total standard deviation, σ_{total}, which reflects the total variability, is calculated as:

$$\sigma_{total} = \sqrt{\sigma_{model}^2 + \sigma_{random}^2} \quad (6.3)$$

where σ_{model} is a "model" standard deviation that reflects the uncertainty of the "model" fit (i.e. the uncertainty in the best fit trend line given the empirical data) and σ_{random} is a random or measurement standard deviation that reflects random scatter in the empirical data.

For a linear regression through observed data, σ_{random} can be calculated as (Ang and Tang, 1975)

$$\sigma_{random} = \sqrt{\frac{\sum_{i=1}^{n}(\hat{y}_i - \bar{y})}{n-2}} \quad (6.4)$$

where $\hat{y}_i$ is a measured value of the predicted variable (e.g. unit side resistance), $\bar{y}$ is the predicted value of the same variable for the same input values, and n is the number of measured values. σ_{random} is the conditional standard deviation of the empirical data about the best fit relation (also referred to as the standard error of the estimate).

The model standard deviation, σ_{model}, is calculated from the standard deviations of the best fit parameters. For a general linear regression, σ_{model} is calculated as

$$\sigma_{model} = \sqrt{\sigma_{slope}^2 \cdot x^2 + \sigma_{intercept}^2 + 2 \cdot x \cdot \sigma_{slope} \cdot \sigma_{intercept} \cdot \rho} \quad (6.5)$$

where σ_{slope} and $\sigma_{intercept}$ are the standard deviations (standard errors) of the slope and intercept of the regression, x is the input value for the regression, and ρ is the correlation coefficient between the slope and intercept. For a linear regression that is forced to have a zero intercept, the model standard deviation can be simplified to become:

$$\sigma_{model} = \sqrt{\sigma_{slope}^2 \cdot x^2} \tag{6.6}$$

Values for use in Equations 6.5 and 6.6 are generally output from least squares regression analyses (e.g. the *LINEST* function in MS Excel© or the *regstats* function in Matlab©).

Note that the value of σ_{model} generally varies with the value of the input parameter x. Values for σ_{random} may or may not vary with the value of the input parameters depending on whether constant or non-constant variance is assumed for the regression, as described in the subsequent section. Values for σ_{total} also generally vary with x since σ_{total} is a function of both σ_{model} and σ_{random}.

The random or measurement variability, as represented by σ_{random}, reflects the conditional variability of the empirical data about the best fit trend line and is the standard deviation that most people think about when analyzing data. The model standard deviation, σ_{model}, reflects the uncertainty in the best fit "model" and how well the model actually reflects the true relationship since there is a limited amount of data. σ_{model} will tend to be smaller when there is substantial data and larger when there is little data. In fact, for a given set of data, σ_{model} will tend to be smaller in regions where there is substantial data (e.g. near the middle of the "fit") and larger in regions where there is less data (e.g. near the "ends" of the "fit"). The total variability, as represented by σ_{total}, reflects the combined variability and uncertainty due to both random variability and

model uncertainty, and is generally appropriate for representing the variability and uncertainty in a new measurement of some relevant parameter.

Since the objective of foundation design is to predict the capacity for new foundations, the total standard deviation is generally appropriate to represent the variability and uncertainty present in a new prediction of foundation capacity. Equation 6.3 was, therefore, used for establishing the standard deviation for the parameter M in Equation 6.1.

6.3.2 Assumption of Constant or Non-constant Variance for σ_{random}

Common linear regression analyses, such as those performed using the MS Excel© *LINEST* function, are generally conducted under the assumption of constant variance. This assumption means that the conditional standard deviation, σ_{random}, is taken to be constant and independent of the value of the input parameter (recall that the variance is the square of the standard deviation). This result is illustrated in Figure 6.2, which shows empirical measurements of unit side resistance plotted as a function of N_{eq-60}, along with the least squares best fit regression line (solid line) established under the assumption of constant variance and lines representing the regression plus or minus one standard deviation (dashed lines). As shown in the figure, the distance between the regression line and the lines representing plus or minus one standard deviation is constant and independent of the value of N_{eq-60}. This is a result of the assumption of constant variance. Least squares regression analyses performed with the assumption of constant variance are generally referred to as "ordinary" least squares analyses.

While the assumption of constant variance is common and some data sets do largely satisfy this assumption, it is not universally appropriate for all data sets. In cases where the data do not conform to the assumption of constant variance, it is possible to perform weighted regression analyses that allow the standard deviation (or variance) to vary with the value of the input parameter (Ang and Tang, 1975).

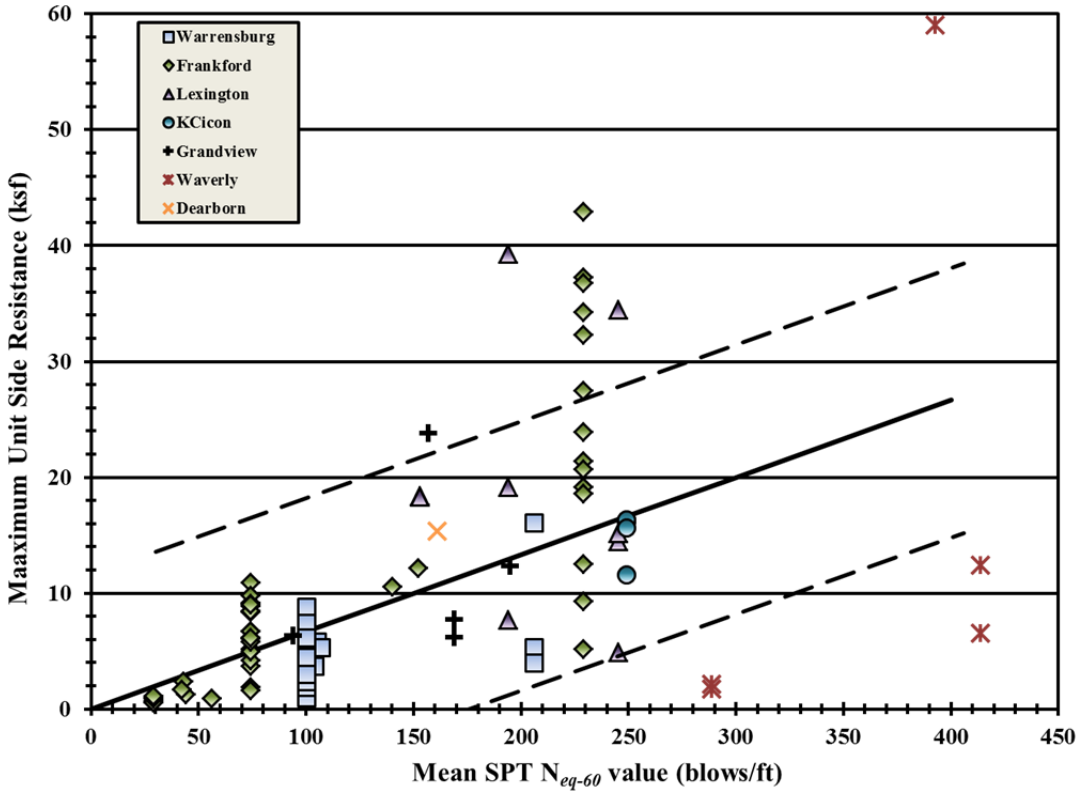

Figure 6.2- Illustration of assumption of constant variance for least squares regression of unit side resistance versus N_{eq-60}. Solid line depicts best fit regression relationship, while the dashed lines depict the regression relation plus or minus one standard deviation.

In general, weighted regression should be performed using weighting factors selected so that the resulting variance reasonably reflects the scatter in the empirical data.

For the current work, however, two alternatives were considered: unweighted least squares regression (i.e. ordinary least squares) and weighted least squares regression with the weights selected to be the inverse of the value of the regression equation. The first alternative corresponds to the common least squares method under the assumption of constant variance, as illustrated in Figure 6.2. The second alternative produces the result of having a constant coefficient of variation (recall the coefficient of variation is equal to the standard deviation divided by the mean). This alternative is illustrated in Figure 6.3, which shows the same data set plotted in Figure 6.2 but with the regression relation and lines depicting the regression plus or minus one standard deviation being established under the assumption of having a constant coefficient of variation. As shown in the figure, the distance between the regression line and the lines depicting plus or minus one standard deviation increases in proportion to the value of the input variable (N_{eq-60}). In this case, the standard deviation increases in proportion to the value of the regression equation.

It is noteworthy that the best fit regression relations determined using least squares under the assumption of constant standard deviation and under the assumption of constant coefficient of variation are different. For the work described in this thesis, both types of regression analyses were performed for each of the different predictive relations established in Chapter 5. The resulting regression relations and lines reflecting the regression plus or minus one standard deviation were then plotted (e.g. Figures 6.2 and 6.3) and judgment was used to select the form of regression that best represented the empirical data. The regression equations presented in Chapter 5 correspond to the type of regression that produced the best fit with the empirical data, including consideration of

the scatter about the regression relation. For this research, the constant coefficient of variation assumption (i.e. weighted regression with weights selected to be inversely proportional to the regression value) was found to better represent the variability of the data about the regression lines for all four empirical relations described in Chapter 5. Specific characterization of the variability and uncertainty present in each of these relations, as determined from least squares regression analyses assuming a constant coefficient of variation, is provided in the following section.

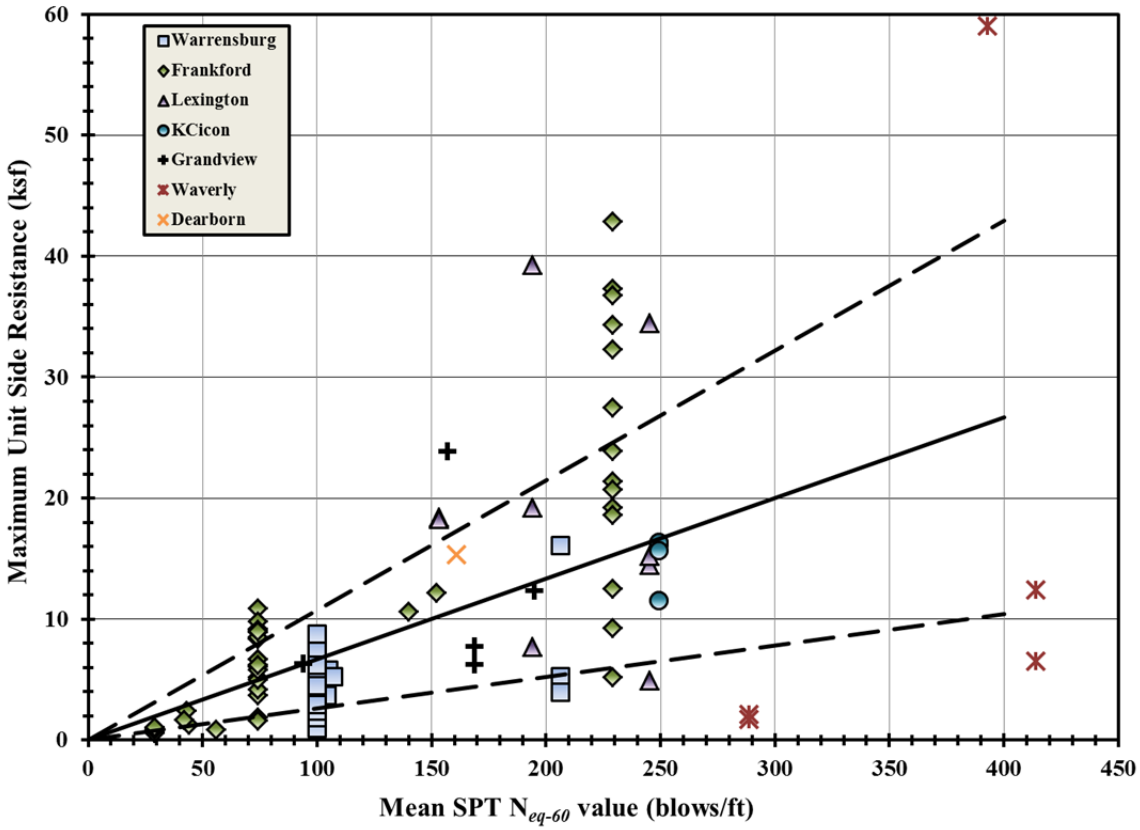

Figure 6.3- Illustration of assumption of non-constant variance from weighted least squares regression of unit side resistance versus N_{eq-60} with the regression weights chosen to produce a constant coefficient of variation. Solid line depicts best fit regression relationship, while the dashed lines depict the regression relation plus or minus one standard deviation.

6.4 Characterization of Variability and Uncertainty for Design Relations

As described in Section 6.2, the variability and uncertainty in the design relations is quantified in the parameter M, which is a dimensionless, probabilistic, multiplicative factor that is multiplied by the deterministic design relation to produce probabilistic estimates of the predicted variable (i.e. unit side or tip resistance). Tables 6.1 through 6.4 summarize measures of variability and uncertainty determined from the weighted least squares regression analyses for the design relationships presented in Chapter 5. Tables 6.1 and 6.2 show the measures for the design relations that respectively predict ultimate unit side resistance and ultimate unit tip resistance from SPT measurements (i.e. for Equations 5.5 and 5.4, respectively). Similarly, Tables 6.3 and 6.4 show results from the regression analyses for the relations that respectively predict ultimate unit side and ultimate unit tip resistance from MTCP measurements (i.e. for Equations 5.9 and 5.8, respectively). In each table, values are provided for a range in values for the input variables (N_{eq-60} and $MTCP$) since the probabilistic measures generally depend on the value of the input variables.

In the Tables 6.1 through 6.4, the model standard deviation, σ_{model}, was computed using Equation 6.5 and the total standard deviation, σ_{total}, was computed using Equation 6.3. Values for $\overline{q_s}$ and $\overline{q_p}$ were computed using the best fit regression relations presented in Chapter 5. The mean values for the parameter M, μ_M, are all 1.0 since they reflect the normalized value for $\overline{q_s}$ or $\overline{q_p}$ (i.e. $\overline{q_s}$ or $\overline{q_p}$ normalized by itself). Finally, values for σ_M were calculated from Equation 6.2, which is simply σ_{total} divided by $\overline{q_s}$ or $\overline{q_p}$.

Table 6.1- Summary of measures of variability and uncertainty for design relation relating ultimate unit side resistance to N_{eq-60} (Equation 5.5).

SPT N_{eq-60}	**Variability Measure**				
	σ_{model}	σ_{total}	$\overline{q_s}$	μ_M	σ_M
1	0.00	0.04	0.1	1.0	0.612
50	0.22	2.03	3.3	1.0	0.612
100	0.44	4.06	6.6	1.0	0.612
150	0.66	6.09	10.0	1.0	0.612
200	0.88	8.12	13.3	1.0	0.612
250	1.10	10.15	16.6	1.0	0.612
300	1.32	12.18	19.9	1.0	0.612
350	1.54	14.22	23.2	1.0	0.612
400	1.76	16.25	26.6	1.0	0.612

Table 6.2- Summary of measures of variability and uncertainty for design relation relating ultimate unit tip resistance to N_{eq-60} (Equation 5.4).

SPT N_{eq-60}	**Variability Measure**				
	σ_{model}	σ_{total}	$\overline{q_p}$	μ_M	σ_M
1	0.18	0.49	1.0	1.0	0.514
50	8.79	24.75	48.2	1.0	0.514
100	17.58	49.49	96.3	1.0	0.514
150	26.38	74.24	144.5	1.0	0.514
200	35.17	98.98	192.6	1.0	0.514
250	43.96	123.73	240.8	1.0	0.514
300	52.75	148.48	289.0	1.0	0.514
350	61.54	173.22	337.2	1.0	0.514
400	70.34	197.97	385.4	1.0	0.514

As shown in the tables, the mean value for the variable M is identically 1.0 in all cases since these values reflect the predicted values normalized by itself. The other variability measures, however, generally vary with the value of the input variable. In the case of Tables 6.1 and 6.2, which provide measures for the SPT design relations, the values for σ_{model} and σ_{total} both increase in proportion to the value of $\overline{q_s}$ or $\overline{q_p}$. As a result, the values for σ_M are constant over the range of the regression. This is a result of using weighted linear regression equation with zero intercept (and, thus, one degree of

freedom). In contrast, Tables 6.3 and 6.4, which provide measures for the MTCP design relations, show that σ_M varies with the value of the input variable. This is a result of using a nonlinear regression with two degrees of freedom. Thus, σ_{model} varies with the value of the input variable, and this propagates to produce the result that both σ_{total} and σ_M also vary with the value of the input variable.

Table 6.3- Summary of measures of variability and uncertainty for design relation relating ultimate unit side resistance to $MTCP$ (Equation 5.9).

MTCP	**Variability Measure**				
	$\boldsymbol{\sigma_{model}}$	$\boldsymbol{\sigma_{total}}$	$\boldsymbol{\overline{q_s}}$	$\boldsymbol{\mu_M}$	$\boldsymbol{\sigma_M}$
1	5.02	17.41	28.7	1.0	0.608
2	1.17	7.68	13.0	1.0	0.589
3	0.56	4.82	8.2	1.0	0.586
4	0.49	3.49	5.9	1.0	0.588
5	0.48	2.73	4.6	1.0	0.591
6	0.47	2.23	3.7	1.0	0.595
7	0.46	1.89	3.1	1.0	0.600
8	0.44	1.63	2.7	1.0	0.604
9	0.43	1.44	2.4	1.0	0.609
10	0.41	1.29	2.1	1.0	0.613

Table 6.4- Summary of measures of variability and uncertainty for design relation relating ultimate unit tip resistance to $MTCP$ (Equation 5.8).

MTCP	**Variability Measure**				
	$\boldsymbol{\sigma_{model}}$	$\boldsymbol{\sigma_{total}}$	$\boldsymbol{\overline{q_p}}$	$\boldsymbol{\mu_M}$	$\boldsymbol{\sigma_M}$
1	99.00	145.4	495.0	1.0	0.294
2	25.96	52.70	213.3	1.0	0.247
3	13.09	30.94	130.3	1.0	0.237
4	9.73	22.03	91.9	1.0	0.240
5	8.48	17.30	70.7	1.0	0.247
6	7.77	14.36	56.2	1.0	0.256
7	7.23	12.35	46.6	1.0	0.265
8	6.77	10.88	39.6	1.0	0.275
9	6.37	9.75	34.3	1.0	0.284
10	6.01	8.85	30.2	1.0	0.293

The values shown for σ_M in Tables 6.1 through 6.4 for the respective design relations provide an indication of relative variability and uncertainty in the design relations. Values for σ_M are essentially coefficients of variation (standard deviation divided by the mean value) since they are normalized by the mean values. Comparisons of the specific values for the different relations indicate the following:

- The design relations for predicting the ultimate unit side resistance and ultimate unit tip resistance from SPT measurements both have relatively large variability and uncertainty, with standard deviations on the order of 50 to 60 percent of the mean or predicted value.
- Similarly, the design relation for predicting ultimate unit side resistance from MTCP measurements also has relatively large variability and uncertainty, with a standard deviation on the order of 60 percent of the mean or predicted value.
- In contrast, the design relation for predicting ultimate unit tip resistance from MTCP measurements has less variability and uncertainty, with a standard deviation on the order of 25 to 30 percent of the mean or predicted value.

Thus, the results presented in this chapter suggest that the relation for predicting unit tip resistance from MTCP measurements is substantially more reliable than the other proposed design relations.

6.5 Summary

Variability and uncertainty in the predictive relations must be quantified in order to probabilistically calibrate resistance factors for design using LRFD. In this chapter,

variability and uncertainty for the four proposed design relationships presented in Chapter 5were represented using a dimensionless, probabilistic variable M to reflect the normalized, conditional total standard deviation. Regression analyses were performed for each of these four relations using the available empirical data presented in Chapter 5 to quantify the variability and uncertainty in each relation. Results of these regression analyses show that the total variability and uncertainty for three of the four design relations is generally consistent, with the standard deviation being approximately 50 to 60 percent of the predicted value for unit side or tip resistance. The design relation for predicting unit tip resistance from MTCP measurements was the exception to this finding. The standard deviation for this design relation was found to be approximately 25 to 30 percent of the predicted value for unit tip resistance. The results presented in this chapter were subsequently used to develop resistance factors that account for the variability and uncertainty in each relation, as described in Chapter 7.

Chapter 7 – Calibration of Resistance Factors for Design Using SPT and MTCP Measurements

7.1 Introduction

Resistance factors developed for design of drilled shafts in shale based on Standard Penetration Test (SPT) and modified Texas Cone Penetration (MTCP) test measurements are presented in this chapter. A general overview of the calibration methods is first provided along with descriptions of the probabilistic analyses used to calibrate the resistance factors. Recommended resistance factors for design of shafts using SPT and MTCP measurements are then presented.

7.2 General Calibration Method

In Load and Resistance Factor Design (LRFD), load factors and resistance factors are respectively applied to nominal load values and nominal resistance values to account for variability and uncertainty in the load and resistance. This is generally accomplished using a design requirement expressed as an inequality of the form:

$$q_s \cdot A_s \cdot \phi_s + q_p \cdot A_p \cdot \phi_p \geq \gamma_{LL} \cdot LL + \gamma_{DL} \cdot DL \quad (7.1)$$

where q_s is the nominal unit side resistance determined from a selected predictive relation (e.g. the relations presented in Chapter 5), A_s is the perimeter surface area for the interface where side resistance is mobilized, ϕ_s is the resistance factor applied to side resistance, q_p is the nominal unit tip resistance determined from a selected predictive

relation, A_p is the area of the drilled shaft tip, ϕ_p is the resistance factor applied to tip resistance, γ_{LL} is the load factor applied to the live load, LL is the nominal live load, γ_{DL} is the load factor applied to dead load, and DL is the nominal dead load.

Equation 7.1 establishes a design requirement that must be satisfied for an acceptable design to be produced. This requirement states that the factored resistance (the left hand side of the inequality) must be greater than or equal to the factored load (the right hand side of the inequality). The design requirement provided in Equation 7.1 is generally satisfied by varying the dimensions of the foundation, and hence A_s and A_p, until the requirement is just satisfied.

Load and resistance factors can be established in a number of ways, ranging from simple judgment to more formal probabilistic calibrations. The objective of probabilistic calibration of load and/or resistance factors is to establish factors that will produce designs that have some target probability of failure (or target reliability[1]) if the design requirement is just satisfied. The focus of the present work is probabilistic calibration of the resistance factors ϕ_s and ϕ_p in Equation 7.1 for design of drilled shafts using SPT and MTCP measurements.

In applying Equation 7.1, the nominal values for unit side and tip resistance (q_s and q_p, respectively) are established using predictive relations like those presented in Chapter 5 that have variability and uncertainty, and described in Chapter 6. The resistance factors, ϕ_s and ϕ_p, therefore preferably account for this variability and uncertainty in addition to other significant sources of variability and uncertainty. For the

[1] Note that the probability of failure is the complement of reliability: $p_f = 1 - r$ where p_f is the probability of failure and r is the reliability.

present work, the variability of the input parameters (N_{eq-60} or $MTCP$ values), the variability and uncertainty in the predictive relations (from Chapter 6), and the variability of live and dead loads were considered in calibrating the resistance factors.

The first step to probabilistically establish resistance factors is perform probabilistic analyses to identify a representative design problem that has design parameters that produce some target reliability. In the case of drilled shafts to be designed from SPT or MTCP measurements, the design problem must include definition of stratigraphy, values for DL and LL, dimensions for the drilled shaft, values for the mean or nominal N_{eq-60} or $MTCP$ for each stratum, as well as values reflecting the variability and uncertainty in the mean N_{eq-60} or $MTCP$-values for each stratum. Establishing a problem that has a specific target reliability typically requires some iteration on these parameters, or the variability of these parameters, until the target probability of failure is achieved. The approach used in this work was to vary the dimensions of the drilled shaft until the target probability of failure was achieved, since the dimensions are considered to be deterministic and, thus, have only a first order effect on the resulting probability of failure.

Once some combination of design parameters that produces the target reliability is established, the value(s) for the resistance factor(s) that will produce the target reliability when applied to the nominal values for the parameters can be back-calculated from Equation 7.1. That is, for the combination of parameters that satisfies the design relation with the target reliability, the resistance factor(s) are determined such that they just satisfy the design relation when applied to the nominal parameter values. If the selected problem is truly representative, the resistance factor(s) determined in this way will

subsequently produce the target reliability when applied to different problems if the input parameters have variability and uncertainty that is consistent with that used in the example problem.

This concept is generally implemented using a "performance function", g, that expresses the strength limit state in the form of an inequality that is satisfied when the performance function is greater than or equal to zero. From Equation 7.1, the performance function is:

$$g = q_s \cdot A_s \cdot \phi_s + q_p \cdot A_p \cdot \phi_p - \gamma_{LL} \cdot LL - \gamma_{DL} \cdot DL \geq 0 \qquad (7.2)$$

In this form, an example problem is established such that the probability of the function g being greater than or equal to zero is equal to the target reliability when all load (γ) and resistance (ϕ) factors are set to equal 1.0. Once such an example problem is established, the resistance factor(s) can be back-calculated by setting $g = 0$, substituting nominal (usually mean) values for the input parameters (q_s, A_s, q_p, A_p, LL, and DL) and appropriate load factors for the limit state being considered into Equation 7.2, and solving for the resistance factors ϕ.

A problem arises when multiple resistance factors are being determined because the performance function involves two unknowns (ϕ_s and ϕ_p) but only one equation. This problem can be resolved by separately considering example problems that involve only side or tip resistance, thereby eliminating one of the resistance factors from the performance function and allowing the other to be back-calculated. Thus, when considering a problem where tip resistance is neglected, the resistance factor for side resistance can be calculated as:

$$\phi_s = \frac{\gamma_{LL} \cdot LL - \gamma_{DL} \cdot DL}{q_s \cdot A_s} \qquad (7.3)$$

Similarly, when considering a problem where side resistance is neglected, the resistance factor for tip resistance can be calculated as:

$$\phi_p = \frac{\gamma_{LL} \cdot LL - \gamma_{DL} \cdot DL}{q_p \cdot A_p} \quad (7.4)$$

Once resistance factors for side and tip resistance are established in this manner, the assumption can be made that these same resistance factors can be applied when considering problems involving both side and tip resistance. Using resistance factors established in this manner is inherently conservative for cases involving both side and tip resistance because the sum of side and tip resistance will necessarily be more reliable than the reliability of side resistance or tip resistance considered individually. Some might argue that it is overly conservative since drilled shafts often derive some resistance from side resistance and some from tip resistance. However, it is important to remember that the resistance factors should also be appropriate for cases where one may have only side resistance (e.g. in karstic conditions) or only tip resistance (e.g. for shafts that are "tipped" in strong rock). In such cases, the resistance factors will accurately reflect the reliability. In cases where both side and tip resistance are substantial, the resistance factors established in this way will produce foundations that are more reliable than the target reliability, with the magnitude of the difference being a function of the correlation between side and tip resistance.

7.3 Probabilistic Analysis Method

For the present work, probabilistic analyses used to develop representative design problems that produce the target reliability were performed using the Monte Carlo

simulation method. The Monte Carlo method (Baecher and Christian, 2003) is generally a straightforward way to determine the reliability (or probability of failure) for problems involving several different sources of variability and uncertainty without restrictions on the specific distributions of the input variables. For this research, a computer program was written to perform Monte Carlo simulations using the software MATLAB©. This program calculates values for the performance function, g, of Equation 7.2 based on probabilistic distributions for each of the input parameters (N_{eq-60} and $MTCP$), the model uncertainty variable, M, described in Chapter 6, and the live and dead loads. A typical result from the Monte Carlo simulations is shown in Figure 7.1. The result of the simulations is a histogram of performance function values that can be used to establish the probability of g being greater than or equal to zero.

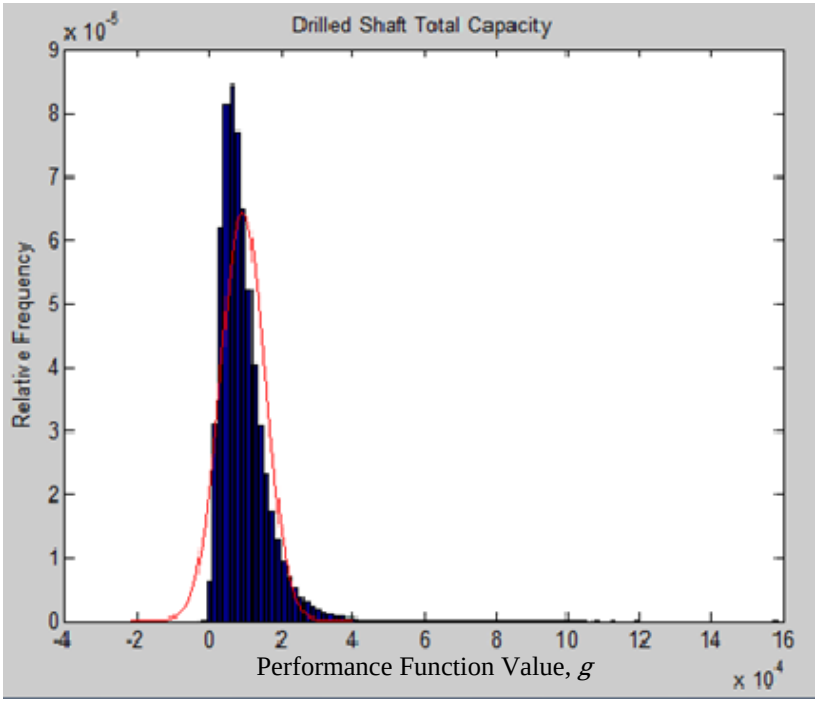

Figure 7.1- Typical distribution of the performance function, g, from Monte Carlo simulations.

7.4 Target Probabilities of Failure

Establishing target reliabilities, or target probabilities of failure, is a complex policy decision that involves consideration of the consequences of failure and the costs involved with increasing reliability. Target values of the probability of failure adopted for this work were established by the Missouri Department of Transportation (MoDOT) based on the work of Huaco et al. (2012) and are presented in Table 7.1. The target probabilities of failure vary for different bridge classifications because the consequences of failure vary with bridge classification. For this work, different resistance factors were established for each of the different target probabilities of failure so that design can be performed to achieve the appropriate target probability of failure for the roadway and structure involved. Calibrated resistance factors for each of these target probabilities of failure are provided in the following sections.

7.5 Resistance Factors for Design Based on N_{eq-60}

Resistance factors were established for calculation of factored tip and side resistance from N_{eq-60} following the procedures described previously in this chapter. In this section, the representative design problems used for calibration of resistance factors are documented. The specific performance functions used for the probabilistic analyses are also presented along with values and distributions used for the relevant input parameters. Finally, the resistance factors determined from the probabilistic calibrations for both side and tip resistance are presented. In all cases, resistance factors were

established to be a function of the variability and uncertainty present in N_{eq-60}, as represented by the coefficient of variation (COV) of the mean value of N_{eq-60}.

Table 7.1- Target probabilities of failure for Strength Limit States for different MoDOT bridge classifications. (from Huaco et al., 2012)

Classification	Target Probability of Failure
Major Bridges (>$100M)	1 in 10,000
Major Bridges (<$100M)	1 in 5,000
Bridges on Major Roads	1 in 1,500
Bridges on Minor Roads	1 in 300

7.5.1 Resistance Factors for Tip Resistance from N_{eq-60}

The performance function used for probabilistic analysis of tip resistance determined from N_{eq-60} is:

$$g_p = 0.95 \cdot N_{eq-60} \cdot A_p \cdot M_p \cdot \phi_p - \gamma_{LL} \cdot LL - \gamma_{DL} \cdot DL \qquad (7.5)$$

where g_p is the probabilistic performance function for tip resistance determined from N_{eq-60}, N_{eq-60} is the probabilistic mean SPT N-value for the material at the shaft tip, A_p is the deterministic area of the shaft tip, M_p is the probabilistic model uncertainty variable reflecting the variability and uncertainty in the predictive relation (from Chapter 6), ϕ_p is the resistance factor for tip resistance, LL is the probabilistic value for live load, and DL is the probabilistic value for dead load. Note that the term $0.95 \cdot N_{eq-60}$ in Equation 7.5 represents the nominal unit tip resistance from Equation 5.4.

The respective values and probability distributions used for each of the parameters in the calibration analyses are summarized in Table 7.2. Values for A_p were varied for each specific analysis in order to achieve the desired target probability of failure. The mean value and standard deviation of the model uncertainty variable, M_p, were taken from analysis of the variability and uncertainty in the predictive relation as described in Chapter 6. Mean values for dead and live load were selected to reflect typical values for dead and live load and to maintain a dead load to live load ratio of 2:1. The coefficients of variation for dead load and live load were taken from Kulicki et al. (2007).

Table 7.2- Summary of input parameters used for probabilistic analyses to calibrate resistance factors for tip resistance determined from N_{eq-60}.

Variable	**Distribution**	**Mean**	**Standard Deviation**	**COV**
N_{eq-60} (blows/ft)	Lognormal	50 200 400	varies	0.0 – 1.0
A_p	Deterministic	varied to produce target p_f	--	--
M_p	Lognormal	1.0	0.514	0.514
γ_{LL}	Deterministic	1.75	--	--
LL (kips)	Lognormal	500	42	0.12
γ_{DL}	Deterministic	1.25	--	--
DL (kips)	Lognormal	1000	70	0.10

Calibrated resistance factors for each of the established target probabilities of failure (from Table 7.1) are plotted versus the coefficient of variation of the mean value for N_{eq-60} in Figure 7.2. The computed resistance factor values are also provided in Tables A.1 through A.4 in the Appendix. As shown in Figure 7.2, the magnitude of the

resistance factor needed to achieve the target probability of failure depends on the magnitude of the coefficient of variation (COV) for N_{eq-60} (which reflects the variability and uncertainty in the mean of N_{eq-60}). Calibrations were therefore performed for COV equal to 0.0, 0.1, 0.3, 0.5, 0.7, 0.9, and 1.0 to reflect the range in values that might be encountered in practice. Calibrations were also performed for several mean values of N_{eq-60} covering the range over which the predictive relation is valid ($N_{eq-60} \leq 400\ blows/ft$) to evaluate the potential effect of the specific value used for N_{eq-60}. Differences in the computed resistance factors were found to be negligible so average values for the resistance factors determined for different values of N_{eq-60} are reported and recommended for practical use.

As expected, resistance factors determined for roadway classifications with greater target probabilities of failure are greater than those determined for roadway classifications with lesser probabilities of failure. The resistance factors also decrease with increasing COV to account for the additional variability and uncertainty introduced when N_{eq-60} is less reliably defined. The computed resistance factors range from a maximum of 0.34 for design of "Bridges on Minor Roads" when N_{eq-60} is perfectly established (i.e. $COV = 0.0$) to a low of 0.025 for design of "Major Bridges (>$100M)" when N_{eq-60} is very poorly defined (i.e. $COV = 1.0$). These resistance factors are generally lower than those needed for design methods that are based on use of uniaxial compressive strength measurements on shale core (Loehr et al., 2011), which indicates that design of shafts using SPT measurements involves greater variability and uncertainty than is present when using uniaxial compressive strength measurements.

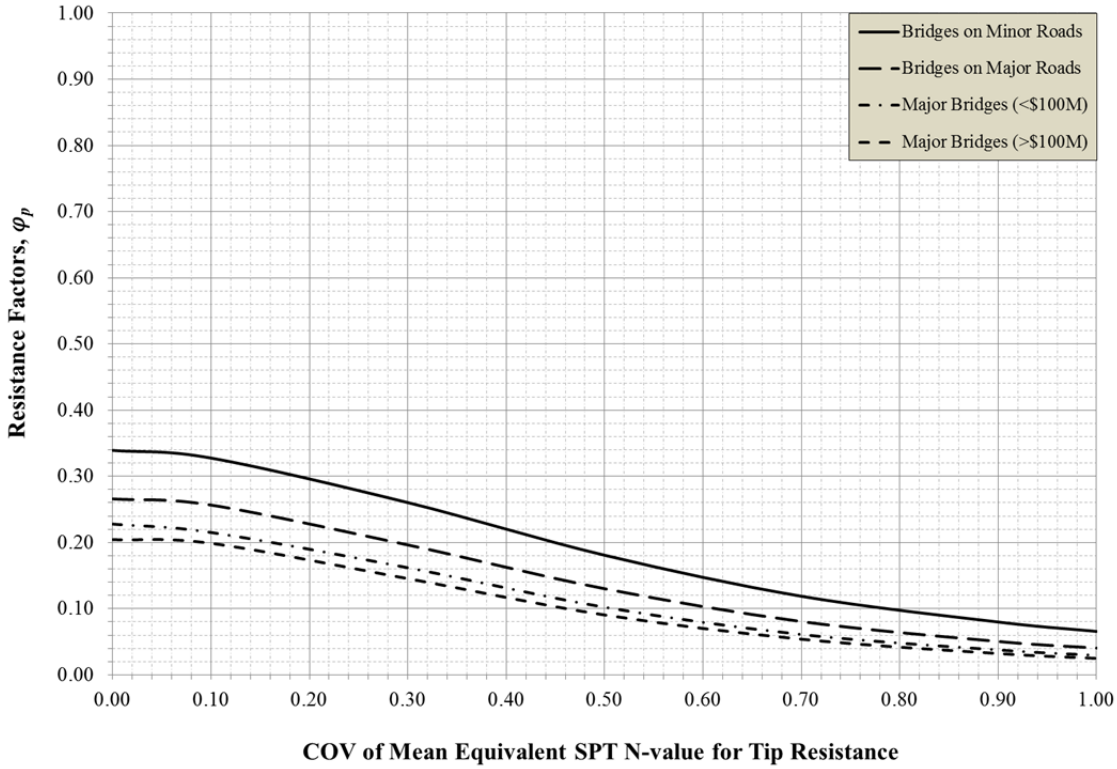

Figure 7.2- Resistance factors for establishing the factored unit tip resistance for drilled shafts in shale based on SPT N_{eq-60} measurements.

7.5.2 Resistance Factors for Side Resistance from N_{eq-60}

The performance function used for probabilistic analysis of side resistance determined from N_{eq-60} is:

$$g_s = \frac{N_{eq-60}}{15} \cdot A_s \cdot M_s \cdot \phi_s \ - \gamma_{LL} \cdot LL - \gamma_{DL} \cdot DL \qquad (7.6)$$

where g_s is the probabilistic performance function for side resistance determined from N_{eq-60}, N_{eq-60} is the probabilistic mean SPT N-value for the material along the shaft perimeter, A_s is the deterministic surface area of the shaft perimeter, M_s is the probabilistic model uncertainty variable reflecting the variability and uncertainty in the predictive relation (from Chapter 6), ϕ_s is the resistance factor for side resistance, LL is

the probabilistic value for live load, and DL is the probabilistic value for dead load. Note that the term $N_{eq-60}/15$ in Equation 7.6 represents the nominal unit side resistance from Equation 5.5.

The respective values and probability distributions used for the parameters in the calibration analyses are summarized in Table 7.3. Values for A_s were varied for each analysis to produce the desired target probability of failure. The mean value and standard deviation of the model uncertainty variable, M_s, were taken from analysis of the variability and uncertainty in the predictive relation as described in Chapter 6. Mean values for dead and live load were established to reflect generally typical values for dead and live load and to maintain a 2:1 dead load to live load ratio. The coefficients of variation for dead load and live load were taken from Kulicki et al. (2007).

Table 7.3- Summary of input parameters used for probabilistic analyses to calibrate resistance factors for side resistance determined from N_{eq-60}.

Variable	**Distribution**	**Mean**	**Standard Deviation**	**COV**
N_{eq-60} (blows/ft)	Lognormal	50 200 400	varies	0.0 – 1.0
A_s	Deterministic	varied to produce target p_f	--	--
M_s	Lognormal	1.0	0.612	0.612
γ_{LL}	Deterministic	1.75	--	--
LL (kips)	Lognormal	500	42	0.12
γ_{DL}	Deterministic	1.25	--	--
DL (kips)	Lognormal	1000	70	0.10

Calibrated resistance factors for each of the established target probabilities of failure are plotted versus the coefficient of variation of the mean value for N_{eq-60} in

Figure 7.3. The resistance factors are also provided in Tables A.1 – A.4 in the Appendix. The resistance factors provided again reflect average values of resistance factors computed for N_{eq-60} equal to 50, 200 and 400 blows/ft. Resistance factors for side resistance are lower than those presented previously for tip resistance because predictions of side resistance from SPT measurements are more variable and uncertain than predictions of tip resistance. Resistance factors range from a high of 0.26 for "Bridges on Minor Roads" when N_{eq-60} is perfectly established to a low of 0.02 for "Major Bridges (>$100 million)" when N_{eq-60} is poorly defined.

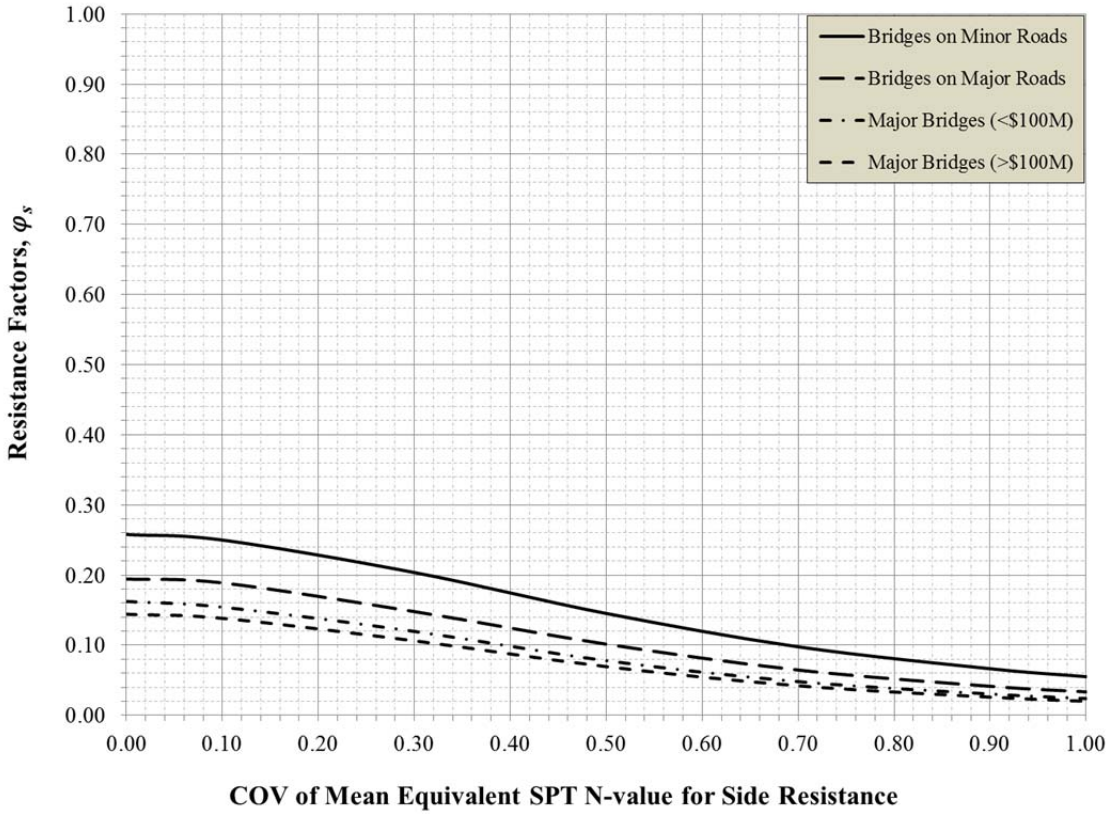

Figure 7.3- Resistance factors for establishing the factored unit side resistance for drilled shafts in shale based on SPT N_{eq-60} measurements.

7.6 Resistance Factors for Design Based on $MTCP$

Resistance factors for calculation of factored tip and side resistance from MTCP measurements were established using the procedures described previously in this chapter. In this section, the representative design problems used for calibration of resistance factors are described. The specific performance functions used for the probabilistic analyses are also presented along with the values for the relevant parameters and the distributions used for probabilistic parameters. Finally, the resistance factors determined from the probabilistic calibrations for both side and tip resistance are presented. All resistance factors were established to be a function of the variability and uncertainty in $MTCP$, as represented by the coefficient of variation (COV) of the mean value of $MTCP$.

7.6.1 Resistance Factors for Tip Resistance from $MTCP$

The performance function used for probabilistic analysis of tip resistance determined from $MTCP$ values is:

$$g_p = 500 \cdot MTCP^{-1.22} \cdot A_p \cdot M_p \cdot \phi_p - \gamma_{LL} \cdot LL - \gamma_{DL} \cdot DL \qquad (7.7)$$

where g_p is the probabilistic performance function for tip resistance determined from $MTCP$, $MTCP$ is the probabilistic mean value of $MTCP$ for the material at the shaft tip, A_p is the deterministic area of the shaft tip, M_p is the probabilistic model uncertainty that reflects the variability and uncertainty in the predictive relation (from Chapter 6), γ_{LL} is the deterministic load factor for live load, LL is the probabilistic value for live load, γ_{DL} is the deterministic load factor for dead load, and DL is the probabilistic value for dead

load. The term $500 \cdot MTCP^{-1.22}$ in Equation 7.7 represents the nominal unit tip resistance from Equation 5.8.

Values and probability distributions used for each of parameters for the calibration analyses are summarized in Table 7.4. The mean and standard deviation of the model uncertainty variable, M_p, were taken from analysis of the variability and uncertainty in the predictive relation as described in Chapter 6. For design from $MTCP$ values, the model uncertainty varies slightly with the value of $MTCP$. Thus, appropriate values for the model uncertainty were used based on the value of $MTCP$ being considered (within the range shown in Table 7.4). Mean values for dead and live load were established to reflect generally typical values for dead and live load and to maintain a 2:1 dead load to live load ratio. The coefficients of variation for dead load and live load were taken from Kulicki et al. (2007). Shaft dimensions were varied to produce the target reliability and the values for A_p were calculated based on the shaft size being considered.

Table 7.4- Summary of input parameters used for probabilistic analyses to calibrate resistance factors for tip resistance determined from $MTCP$.

Variable	Distribution	Mean	Standard Deviation	COV
$MTCP$ (in/100 blows)	Lognormal	1 4 8	varies	0.0 – 1.0
A_p	Deterministic	varied to produce target p_f	--	--
M_p	Lognormal	1.0	0.240-0.294	0.240-0.294
γ_{LL}	Deterministic	1.75	--	--
LL (kips)	Lognormal	500	42	0.12
γ_{DL}	Deterministic	1.25	--	--
DL (kips)	Lognormal	1000	70	0.10

Calibrations were performed for mean $MTCP$ values of 1, 4, and 8 in/100 blows, which span the range over which the predictive relation (Equation 5.8) is valid. As a result, resistance factors were initially developed for each $MTCP$ value, as shown in Figure 7.4 for the target probability of failure for "Bridges on Minor Roads". Differences in the resistance factors developed for $MTCP$ values of 1, 4 and 8 in/100blows were generally small so an average value was used to establish representative resistance factors to avoid having resistance factors that also depend on the mean value. The final recommended resistance factors are plotted in Figure 7.5 and provided in Tables A.5 – A.8 in the Appendix.

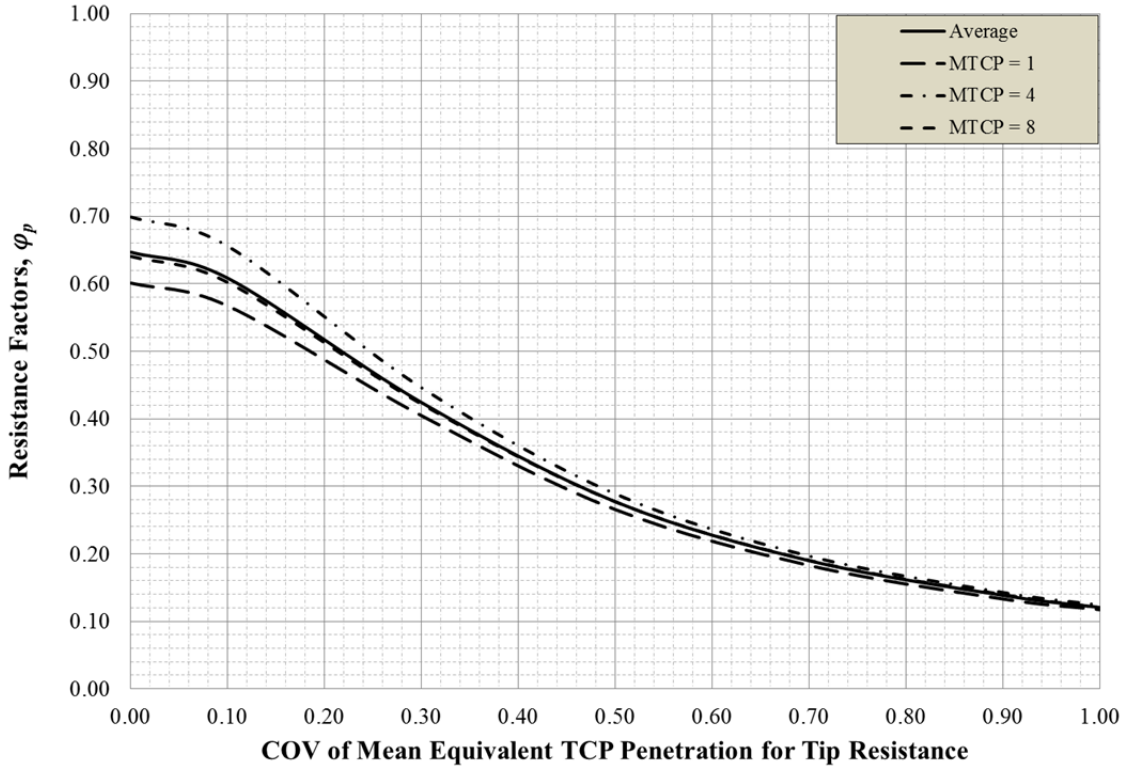

Figure 7.4- Computed resistance factors for unit tip resistance for drilled shafts in shale for $MTCP$=1,4, and 8 in/100 blows and average resistance factors for "Bridges on Minor Roads" classification.

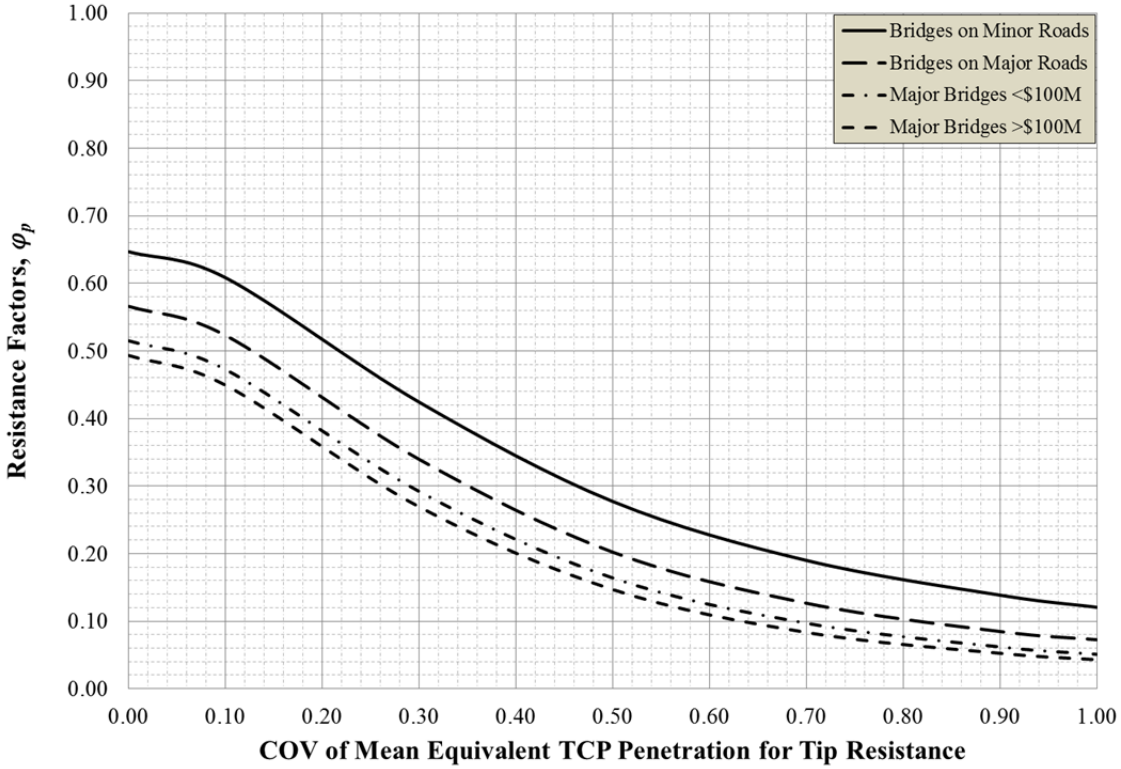

Figure 7.5- Resistance factors for establishing the factored unit tip resistance for drilled shafts in shale based on MTCP measurements.

As shown in Figure 7.5, resistance factors for low values of COV for MTCP measurements are substantially greater than those for similar values of COV for N_{eq-60} (Figure 7.2). This suggests that MTCP measurements are generally a better predictor of unit tip resistance in shales than SPT measurements; i.e. when reliable estimates of $MTCP$ are available, the reliability of the predicted unit tip resistance is relatively high. However, it is also noteworthy that resistance factors for tip resistance from MTCP measurements are more sensitive to the COV of the mean value of $MTCP$. Thus, when designing from SPT measurements, performing additional SPT tests to reduce the COV of the mean value of N_{eq-60} provides for only marginal improvements in the resistance factor that can be used (because the predictive relation is not very reliable). However,

when designing from MTCP measurements, performing additional tests to reduce the COV is likely to have a substantial effect on the resistance factor that can be used.

7.6.2 Resistance Factors for Side Resistance from MTCP

The performance function used for probabilistic analysis of side resistance determined from $MTCP$ values is:

$$g_s = 29 \cdot MTCP^{-1.14} \cdot A_s \cdot M_s \cdot \phi_s - \gamma_{LL} \cdot LL_{dist} - \gamma_{DL} \cdot DL_{dist} \qquad (7.8)$$

where g_s is the probabilistic performance function for side resistance determined from $MTCP$, $MTCP$ is the probabilistic mean value of MTCP measurements for the material along the shaft perimeter, A_s is the deterministic surface area of the shaft perimeter, M_s is the probabilistic model uncertainty reflecting variability and uncertainty in the predictive relation (from Chapter 6), ϕ_s is the resistance factor for side resistance, LL and DL are probabilistic values for live and dead load, respectively, and γ_{LL} and γ_{DL} are deterministic load factors for live load and dead load, respectively. Note that the term $29 \cdot MTCP^{-1.14}$ represents the nominal unit side resistance from Equation 5.9.

Values and probability distributions used for each parameter in the calibration analyses are summarized in Table 7.5. As described in the previous section, calibration analyses were performed for several values of $MTCP$ because the model uncertainty was determined to depend on the magnitude of $MTCP$. Differences in resistance factors established for different values of $MTCP$ were again found to be small so average values determined for $MTCP$ equal to 1, 4 and 8 were used for the final recommended values, shown in Figure 7.6 and provided in Tables A.9 – A.12 in the Appendix.

Table 7.5- Summary of input parameters used for probabilistic analyses to calibrate resistance factors for side resistance determined from $MTCP$.

Variable	Distribution	Mean	Standard Deviation	COV
$MTCP$ (in/100 blows)	Lognormal	1 4 8	varies	0.0 – 1.0
A_s	Deterministic	varied to produce target p_f	--	--
M_s	Lognormal	1.0	0.593-0.618	0.593-0.618
γ_{LL}	Deterministic	1.75	--	--
LL (kips)	Lognormal	500	42	0.12
γ_{DL}	Deterministic	1.25	--	--
DL (kips)	Lognormal	1000	70	0.10

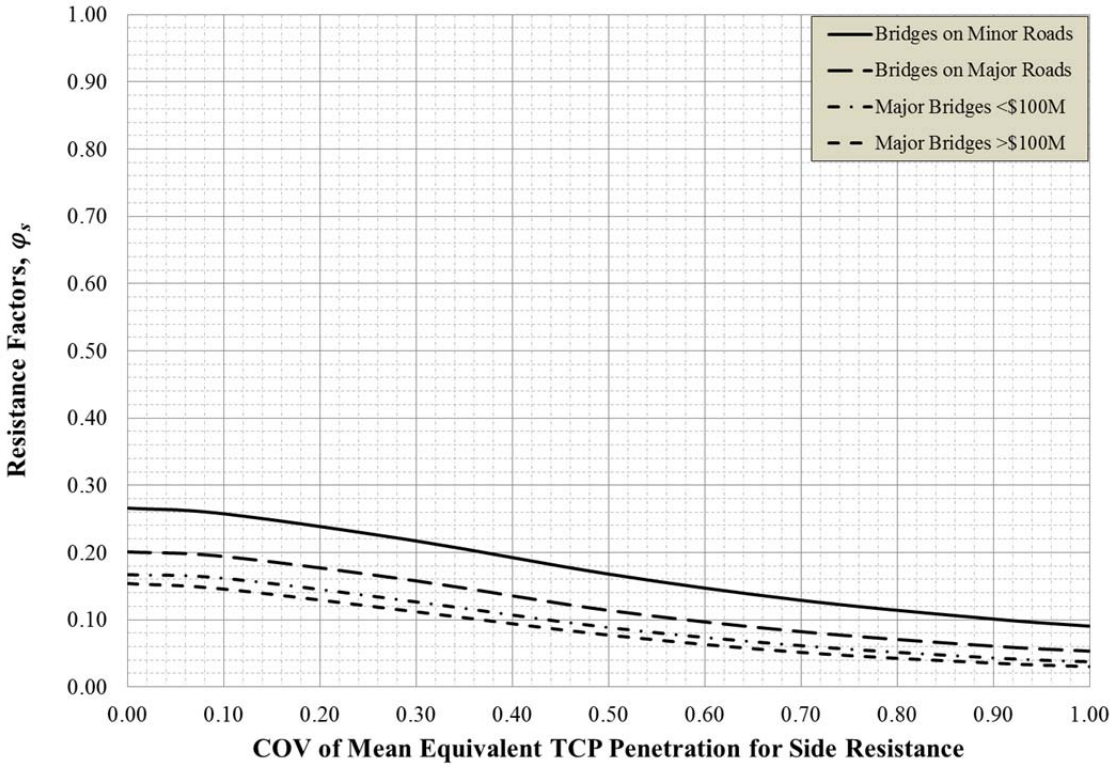

Figure 7.6- Resistance factors for establishing the factored unit side resistance for drilled shafts in shale based on MTCP measurements.

Figure 7.6 shows that resistance factors for establishing side resistance from MTCP measurements are substantially less than those determined for establishing tip resistance from MTCP measurement (Figure 7.5). Values range from 0.26 for "Bridges on Minor Roads" with highly reliable estimates of $MTCP$ to 0.03 for "Major Bridges (>$100M)" with poorly defined values for $MTCP$.

7.7 Summary

In this chapter, methods used for calibration of resistance factors for estimation of factored tip and side resistance for design using SPT and MTCP measurements were described and recommended resistance factors were presented. The resistance factors for design using SPT measurements were found to be relatively low for both tip and side resistance, which reflects the relatively high uncertainty associated with predicting side and tip resistance from SPT measurements in shale. Resistance factors for estimation of factored side resistance from MTCP measurements were also relatively low for similar reasons. However, resistance factors for estimation of factored tip resistance from MTCP measurements were substantially higher, which is an indication that MTCP measurements serve as a relatively good predictor of unit tip resistance for drilled shafts in shale.

Chapter 8 - Comparison of Design Methods

The purpose of this chapter is to present comparisons among the proposed SPT- and TCP-based design methods and several existing design methods through a practical design example. The design example was formulated based on SPT and MTCP measurements from the Frankford test site. Drilled shafts were designed using the proposed SPT- and TCP-based design methods described in previous chapters as well as the Updated Colorado SPT-based design method (Abu-Hejleh et atl. 2003), the TCP method proposed by Nam and Vipulanandan (2010), and MoDOT's previous design method based on uniaxial compression tests on intact rock cores (MoDOT, 2009). Calculations performed using each of these methods are presented in this chapter, including characterization of the relevant design parameters, establishing appropriate resistance factors or factors of safety, and finally, sizing of the drilled shafts.

8.1 Example Problem

The example problem addressed throughout this chapter was derived from in situ test and uniaxial compressive strength measurements from the Frankford load test site. The site consists of approximately 15 feet of weathered shale overlying 25 feet of unweathered shale as illustrated in Figure 8.1. The upper highly weathered shale is denoted as Stratum A, the underlying weathered shale as Stratum B, and the unweathered shale is denoted as Stratum C. Test measurements, and the standard deviations, coefficients of variation (COV), and resistance factors are denoted by the respective

strata. The resistance derived from Stratum A was neglected for all calculations based on the presumption that the overall contribution would be inconsequential.

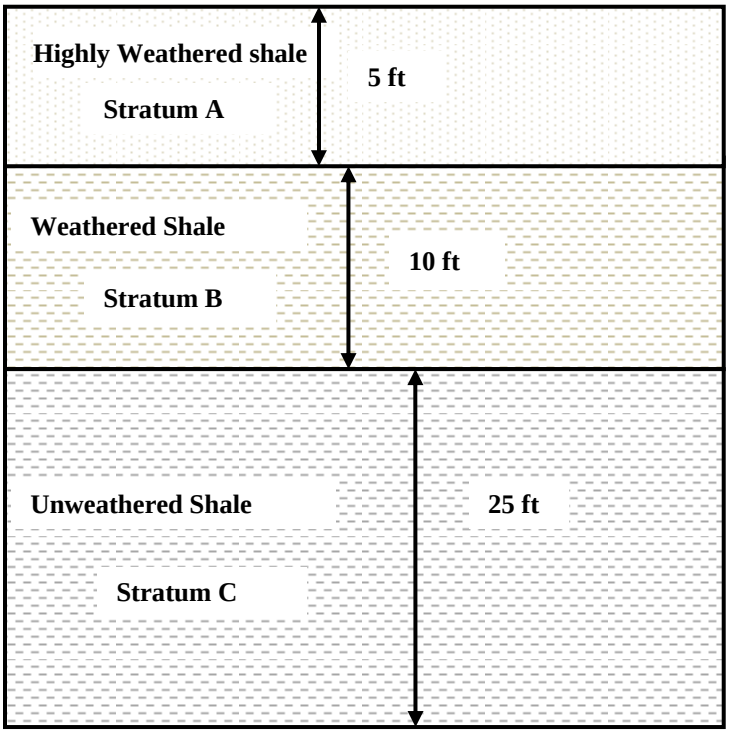

Figure 8.1- Frankford test site stratigraphy for the example problem.

The shafts are designed to support a nominal dead load (DL) of 700 kips and a nominal live load (LL) of 350 kips. The bridge to be supported is assumed to be classified as a "bridge on a major roadway" for the proposed design methods.

As described previously, design of drilled shafts using the proposed design methods depends on the coefficient of variation (COV) of the mean of the relevant design parameter (N_{eq-60} or $MTCP$). Furthermore, this COV value depends heavily on the number of measurements available for the relevant design parameter so that the resulting

shaft size, and the comparison of shaft sizes derived from alternative methods, will depend upon the number of available measurements. Two cases were therefore evaluated for each of the proposed methods to illustrate the effect of the quantity of tests and to "bound" the range of shaft sizes produced using the proposed methods. One of these cases corresponds to a situation where relatively few measurements are available while the other corresponds to a situation where a relatively large number of measurements is available. Specific measurements used for these two cases are provided subsequently.

When designing drilled shafts, there are often multiple combinations of shaft dimensions that will satisfy the design requirements. For the design calculations presented in this chapter, the preferred design alternative for each method was selected as the one having the least cost. Unit costs used for these comparisons were loosely established from historical bid prices for drilled shafts from MoDOT projects as summarized in Table 8.1.

Table 8.1- Drilled Shaft Cost per Linear Foot

Shaft Diameter (ft)	Unit Cost ($/LF)
3.0	$ 400.00
3.5	$ 500.00
4.0	$ 600.00
4.5	$ 700.00
5.0	$ 800.00
5.5	$ 900.00
6.0	$ 1,000.00
6.5	$ 1,100.00
7.0	$ 1,200.00

8.2 Design Using Standard Penetration Test Measurements

Three alternative drilled shaft designs were developed for the example problem using SPT measurements. The first was developed using the proposed SPT Design method with a relatively small number of SPT measurements. The second was developed using the proposed SPT design method, but with a larger number of measurements. Finally, the third design was developed using the UCSB design method described in Chapter 2 for comparison with the proposed methods. Specific calculations for each of these methods are presented in this section.

The design procedure followed included the following steps:

1. Establish nominal and factored values for both the dead load (DL) and live load (LL);
2. Establish mean values and coefficients of variation for the equivalent SPT N-value, N_{eq-60}, for each stratum;
3. From the mean values previously established, compute the nominal unit side resistance and/or nominal unit tip resistance for each stratum;
4. Establish appropriate resistance factors for side and tip resistance in each stratum based on the respective coefficients of variation;
5. Compute factored values for unit side and/or unit tip resistance in each stratum; and, finally,
6. Size the drilled shafts to provide a factored total resistance that equals or exceeds the total factored load.

Calculations performed to complete each of these steps are presented in this section. To simplify the notation, the "60" will be dropped from N_{eq-60}, but all provided measurements are adjusted to account for hammer efficiency.

8.2.1 Design Using Proposed Method with Small Number of Measurements

The nominal loads for the example problem are:

$DL = 700^{k}$

$LL = 350^{k}$

The associated load factors for the Strength I limit state are:

$\gamma_{DL} = 1.25$

$\gamma_{LL} = 1.75$

so that the total factored load, denoted γQ, is:

$$\gamma Q = \gamma_{DL} \cdot DL + \gamma_{LL} \cdot LL = 1.25 \cdot 700^{k} + 1.75 \cdot 350^{k} = 1{,}488^{k} \quad (8.1)$$

The factored resistance is determined from the proposed method based on the mean value of N_{eq}, denoted $\overline{N_{eq}}$; the coefficient of variation of $\overline{N_{eq}}$, denoted $COV_{\overline{Neq}}$, and the corresponding resistance factors presented in Chapter 7. Figure 8.2 shows the measured N_{eq} values used for this case and Table 8.2 provides the specific measured values.

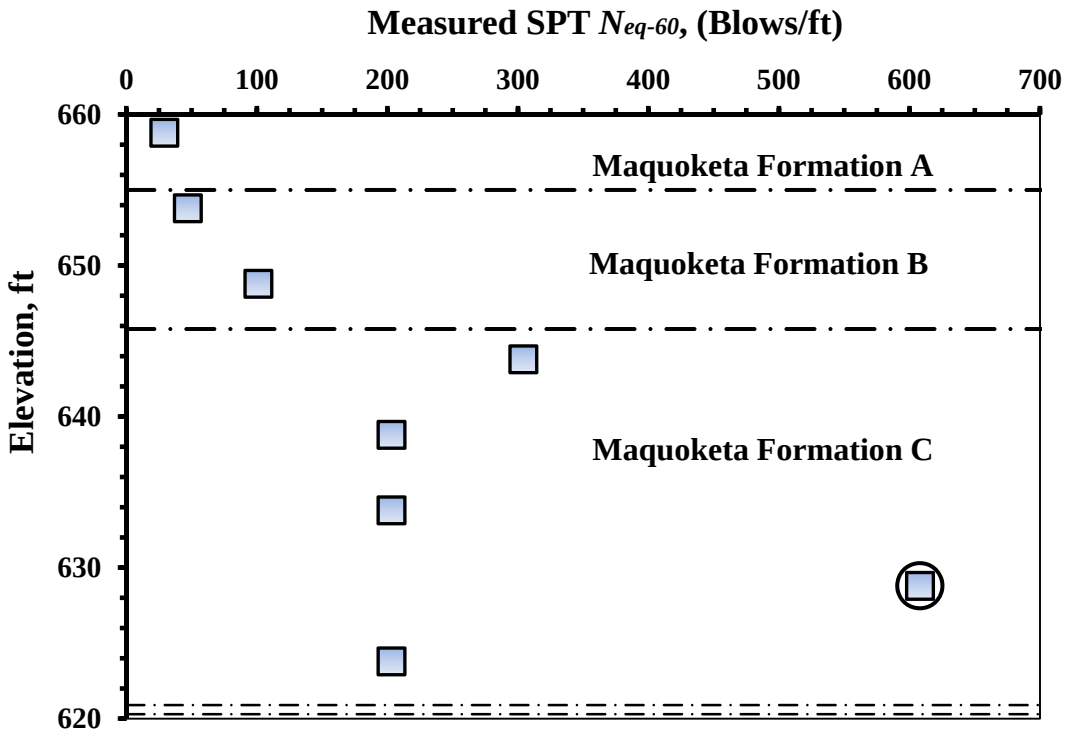

Figure 8.2- SPT measurements used for example problem.

Table 8.2- N_{eq-60} values for example problem.

Stratum	$\boldsymbol{N_{eq-60}}$ **(blows/ft)**
B	47
B	101
C	304
C	203
C	203
C	203

From this data, the mean value of N_{eq} for Stratum B and Stratum C are:

$\overline{N_{eq-B}} = 74\ blows/ft$, and

$\overline{N_{eq-C}} = 228\ blows/ft$.

To establish values for $COV_{\overline{Neq}}$, the standard deviation of the N_{eq} measurements ($\sigma_{\widehat{N_{eq}}}$) was first calculated from Equation 4.2 to be 38.2 blows/ft for Stratum B and 50.5 blows/ft for Stratum C. The standard deviation of the mean, or "model" value of $\overline{N_{eq}}$, denoted $\sigma_{\overline{N_{eq}}}$, was then computed from Equation 4.1. The resulting values for $\sigma_{\overline{N_{eq}}}$ for Stratum B and Stratum C were found to be 27 blows/ft and 25 blows/ft, respectively.

An empirical modifier is applied to the standard deviation of the mean value, $\sigma_{\overline{N_{eq}}}$, to address the potential for underestimating the standard deviation, especially when small numbers of tests are available (MoDOT, 2013). The empirical "test quantity modifier", ζ is determined as a function of the number of available measurements from Figure 8.3. For the case being considered, there are two N_{eq} measurements in Stratum B and four N_{eq} measurements in Stratum C. This results in test quantity modifiers of 2.5 and 2.15 for Stratum B and Stratum C, respectively. The coefficients of variation for both strata are, thus, calculated as:

$$COV_{\overline{N_{eq}}-B} = \frac{\zeta \cdot \sigma_{\overline{N_{eq}}-B}}{\overline{N_{eq}}-B} = \frac{2.5 \cdot 27}{74} = 0.91, \text{ and} \tag{8.2}$$

$$COV_{\overline{N_{eq}}-C} = \frac{\zeta \cdot \sigma_{\overline{N_{eq}}-C}}{\overline{N_{eq}}-C} = \frac{2.15 \cdot 25}{228} = 0.24. \tag{8.3}$$

Using these values for $COV_{\overline{N_{eq}}-B}$ and $COV_{\overline{N_{eq}}-C}$, the resistance factors are then determined from Figure 8.4 for side resistance and Figure 8.5 for tip resistance as illustrated in the figures. The resistance factor, ϕ_{s-B}, for side resistance in Stratum B is found to be 0.04 while the resistance factor, ϕ_{p-B}, for tip resistance in Stratum B is found to be 0.05. For Stratum C, the resistance factor, ϕ_{s-C}, for side resistance is 0.16 and the resistance factor, ϕ_{p-C}, for tip resistance is 0.22.

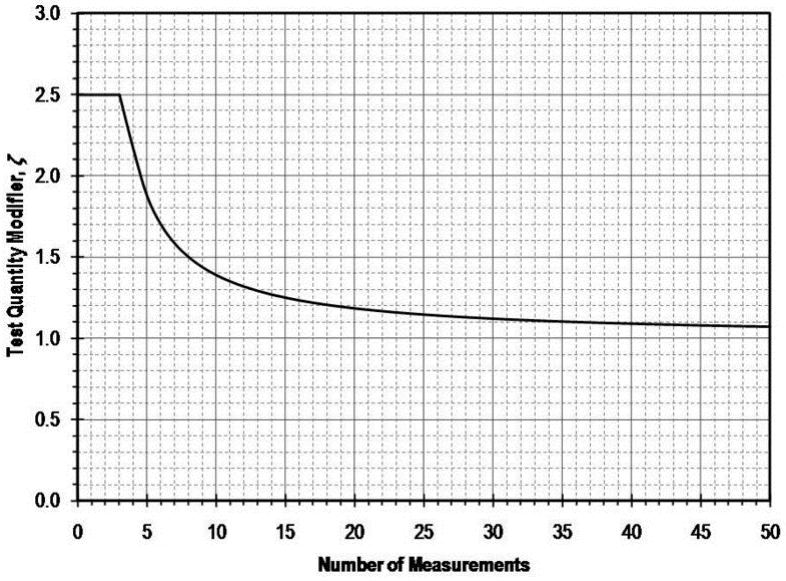

Figure 8.3- Empirical modifier that accounts for the number of measurements (MoDOT, 2013).

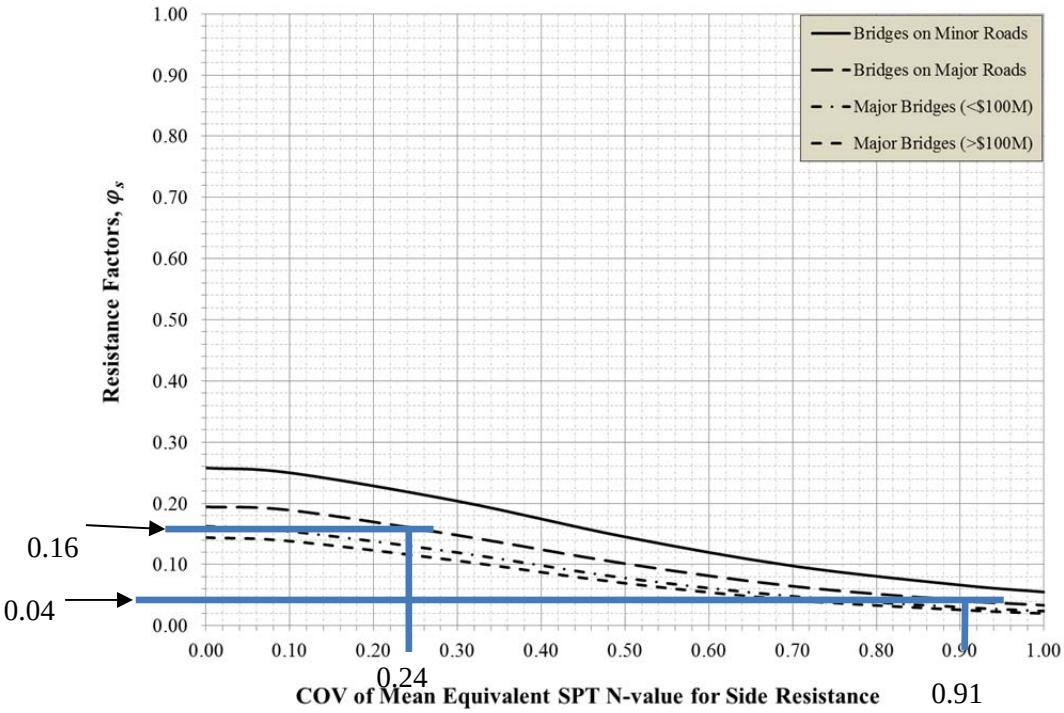

Figure 8.4- Resistance factors for side resistance for proposed SPT method using small number of measurements. Lines shown reflect specific resistance factors established for Stratum B and Stratum C for example problem.

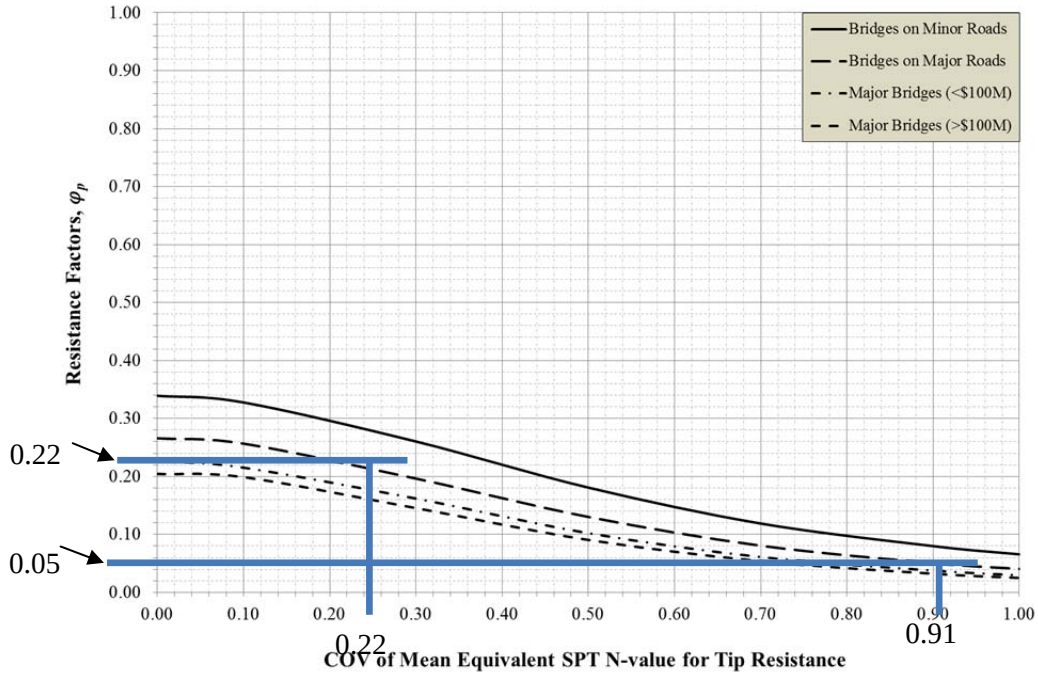

Figure 8.5- Resistance factors for tip resistance for proposed SPT method using small number of measurements. Lines shown reflect specific resistance factors established for Stratum B and Stratum C for example problem.

The nominal unit side and tip resistance for Stratum B and Stratum C are calculated as:

$$q_{s-B} = \frac{74\ blows/ft}{15} = 4.9\ ksf, \tag{8.4}$$

$$q_{s-C} = \frac{228\ blows/ft}{15} = 15.2\ ksf, \tag{8.5}$$

$$q_{p-B} = 0.95 \times 74\ blows/ft = 70\ ksf, \text{ and} \tag{8.6}$$

$$q_{p-C} = 0.95 \times 228\ blows/ft = 217\ ksf. \tag{8.7}$$

The resulting factored unit side and tip resistance are then calculated as:

$$\phi_{s-B} \cdot q_{s-B} = 0.04 \cdot 4.9\ ksf = 0.2\ ksf \tag{8.8}$$

$$\phi_{s-C} \cdot q_{s-C} = 0.16 \cdot 15.2\ ksf = 2.4\ ksf \tag{8.9}$$

$$\phi_{p-B} \cdot q_{p-B} = 0.05 \cdot 70\ ksf = 3.5\ ksf \tag{8.10}$$

$$\phi_{p-C} \cdot q_{p-C} = 0.22 \cdot 217\ ksf = 47.7\ ksf \quad (8.11)$$

Using these values for factored unit side and tip resistance, the factored total resistance was computed for shafts with diameters ranging from 5 to 7 feet, and lengths ranging from 10 to 24 feet. From these calculations, a 6.5 foot diameter and 15 feet long shaft produces a total factored resistance of 1624 kips that just exceeds the total factored load. For this shaft, the factored side resistance in Stratum B is 41 kips and the factored tip resistance from Stratum C is 1583 kips. The cost per linear foot for a 6.5 foot diameter shaft is $1,100 (Table 8.1), which leads to a total cost of $16,500 per shaft.

8.2.2 Design Using Proposed SPT Method with Large Number of Measurements

To demonstrate the influence of the number of test measurements, the example from the previous section was reanalyzed assuming that 15 additional test measurements were available in each of the relevant strata but assuming that the means and standard deviations for the test measurements remained the same. Increasing the number of tests changes the standard deviation of the mean values and decreases the test quantity modifier to 1.2 for both strata, which in turn changes the values for the coefficient of variation of the mean N_{eq} values. The new values become:

$$\sigma_{\overline{N_{eq}}-B} = \frac{38.2}{\sqrt{17}} = 9.3 \quad (8.12)$$

$$\sigma_{\overline{N_{eq}}-C} = \frac{50.5}{\sqrt{19}} = 11.6 \quad (8.13)$$

$$COV_{\overline{N_{eq}}-B} = \frac{\zeta \cdot \sigma_{\overline{N_{eq}}-B}}{\overline{N_{eq}}-B} = \frac{1.2 \cdot 9.3}{74} = 0.15, \text{ and} \quad (8.14)$$

$$COV_{\overline{N_{eq}}-C} = \frac{\zeta \cdot \sigma_{\overline{N_{eq}}-C}}{\overline{N_{eq}}-C} = \frac{1.2 \cdot 11.6}{228} = 0.06. \quad (8.15)$$

Using these new coefficients of variation, the resistance factors for side resistance become 0.18 and 0.20, as illustrated in Figure 8.6. Similarly, the new resistance factors for tip resistance become 0.24 and 0.26 as illustrated in Figure 8.7.

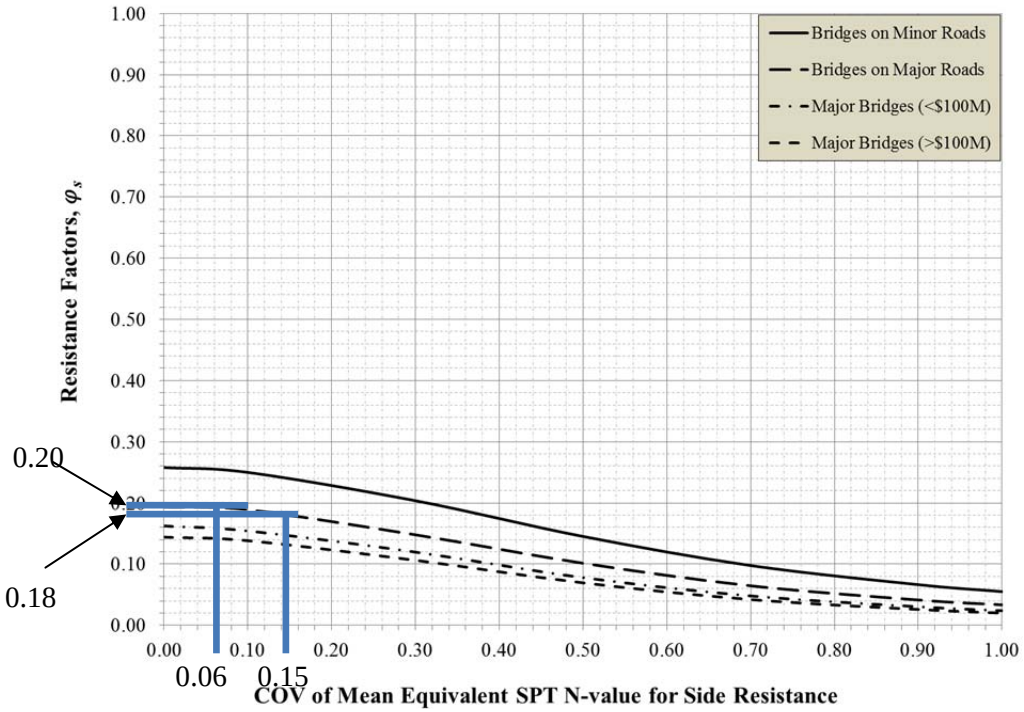

Figure 8.6- Resistance factors for side resistance for proposed SPT method using large number of measurements. Lines shown reflect specific resistance factors established for Stratum B and Stratum C for example problem.

The nominal unit side and tip resistance for Stratum B and Stratum C are again:

$$q_{s-B} = \frac{74\ blows/ft}{15} = 4.9\ ksf, \quad (8.16)$$

$$q_{s-C} = \frac{229\ blows/ft}{15} = 15.2\ ksf, \quad (8.17)$$

$$q_{p-B} = 0.95 \times 74\ blows/ft = 70\ ksf, \text{ and} \quad (8.18)$$

$$q_{p-C} = 0.95 \times 228\, blows/ft = 217\, ksf. \quad (8.19)$$

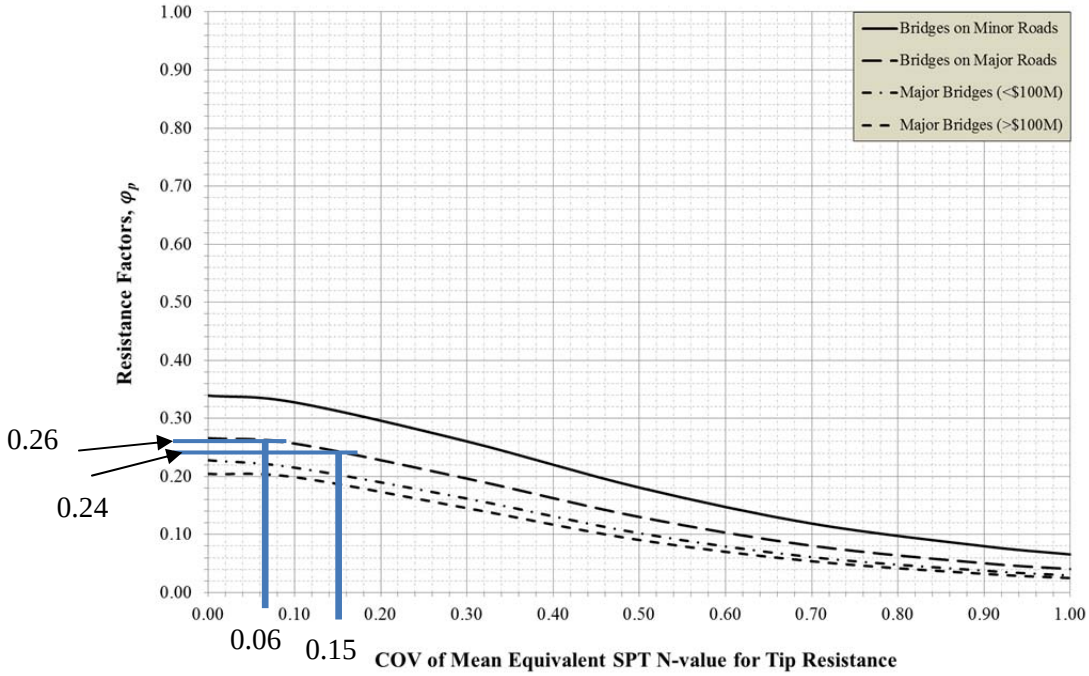

Figure 8.7- Resistance factors for tip resistance for proposed SPT method using large number of measurements. Lines shown reflect specific resistance factors established for Stratum B and Stratum C for example problem.

Applying the new resistance factors, the factored unit side and tip resistance become:

$$\phi_{s-B} \cdot q_{s-B} = 0.18 \cdot 4.9\, ksf = 0.9\, ksf \quad (8.20)$$

$$\phi_{s-C} \cdot q_{s-C} = 0.20 \cdot 15.2\, ksf = 3.0\, ksf \quad (8.21)$$

$$\phi_{p-B} \cdot q_{p-B} = 0.24 \cdot 70\, ksf = 16.8\, ksf \quad (8.22)$$

$$\phi_{p-C} \cdot q_{p-C} = 0.26 \cdot 217\, ksf = 56.4\, ksf \quad (8.23)$$

The factored total resistance was computed for shafts with diameters ranging from 4 to 7 feet, and lengths ranging from 10 to 28 feet. From these calculations, the shaft size that produced a resistance that equaled or exceeded the total factored load was 5.5 feet diameter and 15 feet in length. For this shaft, the total factored resistance was

determined to be 1496 kips. The factored side resistance in Stratum B was 156 kips. The factored tip resistance from Stratum C was 1340 kips. The cost per linear foot for 5.5 feet diameter shafts is approximately $900 (Table 8.1), which leads to a total cost per shaft of $13,500. Thus, the additional tests lead to cost savings of approximately $3,000 per shaft, even without changing the mean value or the standard deviation of the test measurements. These savings are a result of having more confidence in the mean value, and thus a lower coefficient of variation of the mean value of the design parameter.

8.2.3 Design Using UCSB Method

The UCSB design method is an allowable stress design (ASD) method, which accounts for uncertainty through use of a factor of safety rather than through use of load and/or resistance factors. As such, the method was not developed to achieve a specific target probability of failure. Direct comparison of designs developed using the proposed method and the UCSB method is therefore difficult because the alternative methods do not produce designs with the same reliability. Designs with lower reliability can be expected to result in greater costs in the future because of differences in performance. Such costs are not reflected in estimates for "construction costs" that are presented here. The estimated construction costs are nevertheless compared here to provide an indication of expected differences in construction costs using the alternative methods.

As was the case for the previous calculations, the dead load and live load are taken to be:

DL = 700 kips

LL = 350 kips

So that the total design load, Q, is:

$$Q = DL + LL = 700^k + 350^k = 1050^k \quad (8.24)$$

The allowable unit side and tip resistance for Stratum B and Stratum C are calculated from Equations 2.8 and 2.7 to be:

$$q_{s-B} = 0.037 \cdot 74 = 2.7\ ksf, \quad (8.25)$$

$$q_{s-C} = 0.037 \cdot 228 = 8.4\ ksf, \quad (8.26)$$

$$q_{p-B} = 0.46 \cdot 74 = 34.0\ ksf, \text{ and} \quad (8.27)$$

$$q_{p-C} = 0.46 \cdot 228 = 105.3\ ksf. \quad (8.28)$$

Using these values, the total allowable resistance was computed for shafts with diameters ranging from 3 to 4 feet. From these calculations, a 3.5 feet diameter shaft with a length of 15 feet produces an allowable resistance of 1310 kips, that just exceeds the total required load of 1050 kips. The estimated cost for this shaft (Table 8.1) is $500 per linear foot, which produces a total cost of $7,500 per shaft.

8.2.4 Comparison of Shafts from Different Designs

Table 8.3 provides a summary of shaft dimensions and estimated costs determined for the example problem using the proposed design method with small and large numbers of measurements and using the UCSB design method. The estimated cost for a shaft designed using the UCSB method is approximately $6,000 less than that for a shaft designed using the proposed methods with a relatively large number of SPT measurements and approximately $9,000 less than the cost for a shaft designed using the

proposed methods with relatively little testing. However, it is important to emphasize that shafts designed using the proposed methods will achieve a target reliability associated with bridges on major roads, whereas shafts designed using the UCSB method are only purported to have a factor of safety of approximately 2, which is low by most standards of practice. Thus, direct comparison of costs resulting from the UCSB and the proposed methods only serve to illustrate anticipated cost differences that would be anticipated if designing using the different methods rather than an indication of the efficiency of the different methods. Shafts designed using the UCSB method will have lesser reliability, and thus, the apparent cost savings come with the consequence of having lower reliability.

Table 8.3- Comparison of shafts produced from alternative SPT design methods for the example problem.

Shaft Characteristics	Proposed SPT Method		UCSB Method
	Small Number of Measurements	Large Number of Measurements	
Diameter (ft)	6.5	5.5	3.5
Length (ft)	15	15	15
Cost ($)	16,500	13,500	7,500

In contrast, comparison of estimated costs for shafts designed using the proposed methods with small and large numbers of measurements reflect the value of the additional SPT measurements since both designs produce shafts with approximately the same reliability. Thus, the $3,000 difference in estimated cost for each shaft between designs using small and large numbers of measurements reflects the “value” that would be achieved by making the additional measurements. This value can be compared the

estimated costs for making the additional measurements to facilitate decision making regarding whether the additional measurements are likely to be justified.

8.3 Design Using Modified Texas Cone Penetration Test Measurements

Three alternative designs were developed based on modified Texas Cone Penetration test measurements. The first was developed using the proposed MTCP-based design method utilizing the MTCP test measurements from the Frankford test site. The second was also developed using the proposed MTCP-based design method, but considering a hypothetical case with identical mean $MTCP$ values but substantially greater uncertainty in $MTCP$ values. The final design was developed using the method proposed by Nam and Vipulanandan (2010). For each of these designs, the shafts is designed to support the same dead load and live load and considering the same stratigraphy considered previously for design bases on SPT measurements. Figure 8.8 shows the measured $MTCP$ values used for this example and Table 8.4 provides the specific measured values.

Table 8.4- $MTCP$ values for example problem.

Stratum	***MTCP*** **(in/100 blows)**
B	3.5
B	3.5
C	1.75
C	1.75
C	2.0
C	1.25
C	1.50

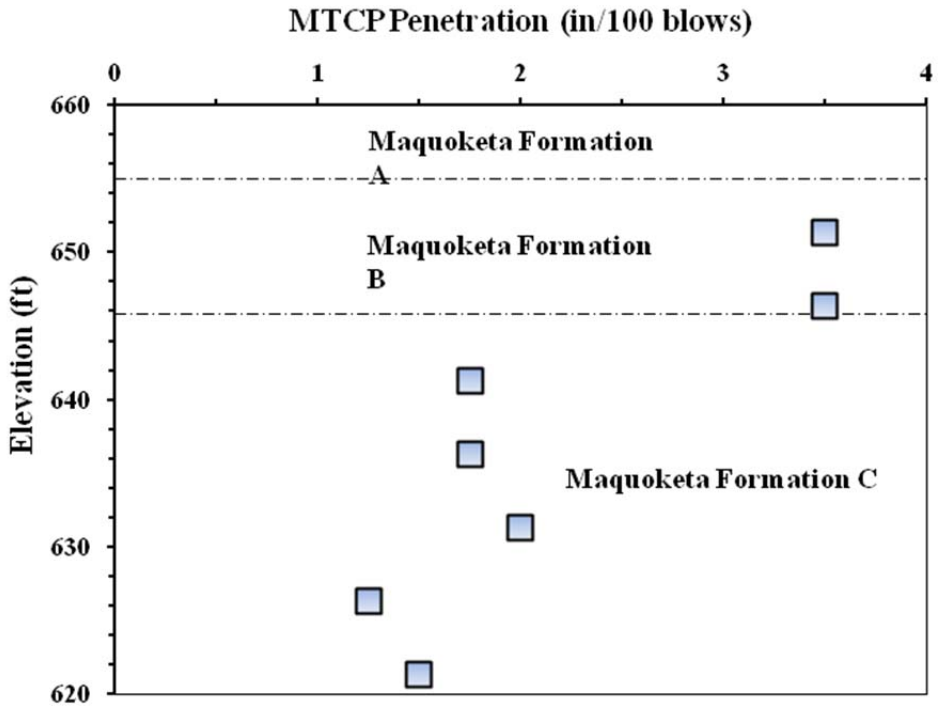

Figure 8.8- MTCP measurements used for example problem.

8.3.1 Design Using Proposed Method Based on Available $MTCP$ Measurements

The mean values for $MTCP$ are 3.5 for Stratum B and 1.65 for Stratum C. The standard deviation of the $MTCP$ measurements for Stratum B is 0.0 since both measurements are the same. The standard deviation of the $MTCP$ measurements for Stratum C is 0.29 in/100 blows. The standard deviation of the mean, or "model" value of $\overline{MTCP}$, is calculated following Equation 4.1. Since there are two $MTCP$ measurements in Stratum B and five $MTCP$ measurements in Stratum C, the empirical test quantity modifiers are 2.5 and 1.9 for Stratum B and Stratum C, respectively. The coefficients of variation for both strata are, thus, calculated as:

$$\sigma_{\overline{N_{eq}}-B} = \frac{0}{\sqrt{2}} = 0 \tag{8.29}$$

$$\sigma_{\overline{N_{eq}}-C} = \frac{0.29}{\sqrt{5}} = 0.13 \tag{8.30}$$

$$COV_{\overline{MTCP}-B} = \frac{\zeta \cdot \sigma_{\overline{N_{eq}}-B}}{\overline{N_{eq}}-B} = \frac{2.5 \cdot 0}{3.5} = 0, \text{ and} \tag{8.31}$$

$$COV_{\overline{N_{eq}}-C} = \frac{\zeta \cdot \sigma_{\overline{N_{eq}}-C}}{\overline{N_{eq}}-C} = \frac{1.9 \cdot 0.13}{1.7} = 0.15. \tag{8.32}$$

Using these coefficients of variation, the resistance factors for side resistance in Stratum B and Stratum C are, respectively, 0.20 and 0.18, as illustrated in Figure 8.9. Similarly, resistance factors for tip resistance are 0.56 and 0.48, respectively, for Stratum B and Stratum C as illustrated in Figure 8.10.

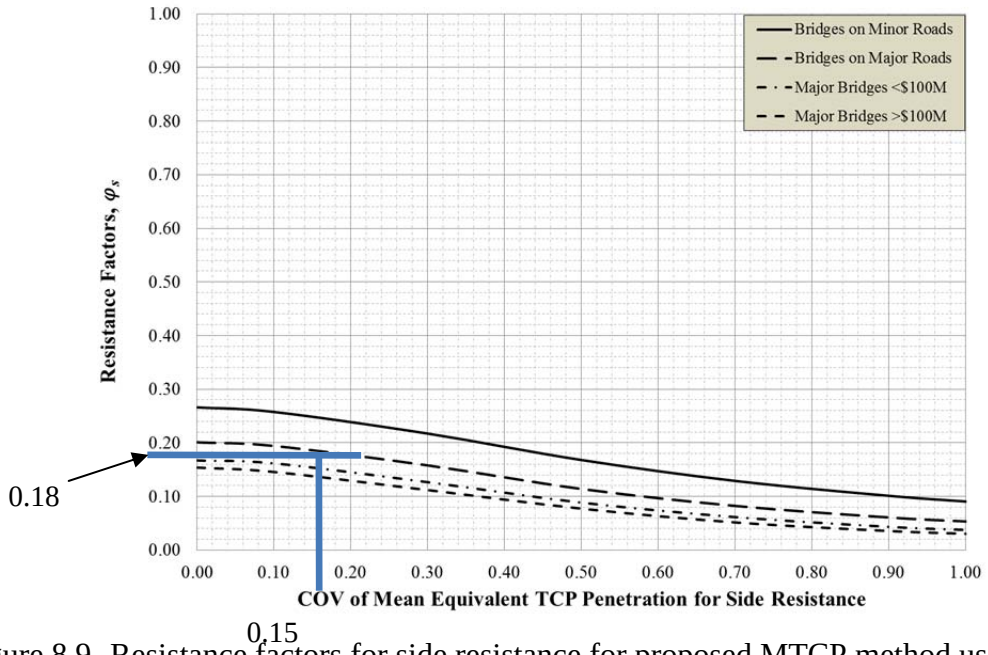

Figure 8.9- Resistance factors for side resistance for proposed MTCP method using available measurements. Lines shown reflect specific resistance factors established for Stratum B and Stratum C for example problem.

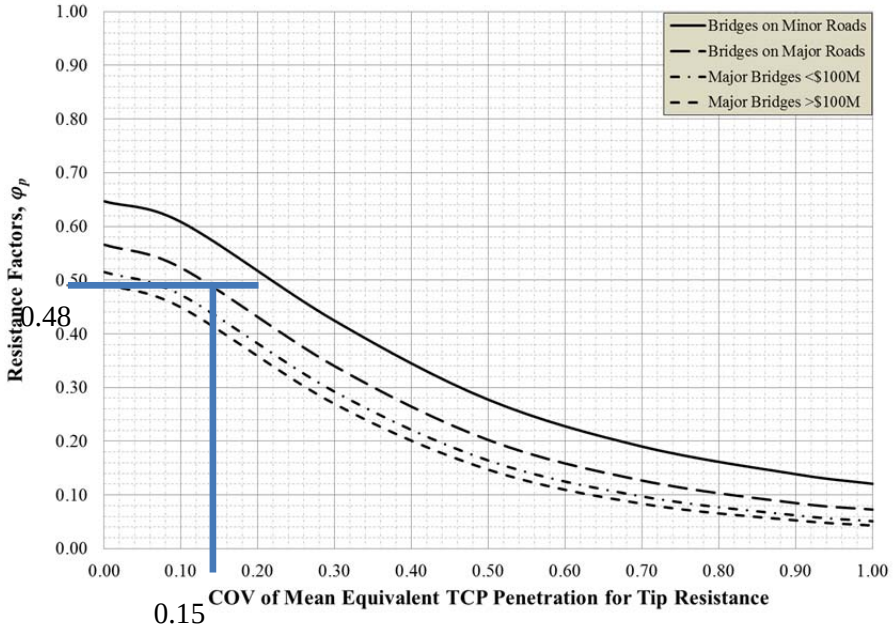

Figure 8.10- Resistance factors for tip resistance for proposed MTCP method using available measurements. Lines shown reflect specific resistance factors established for Stratum B and Stratum C for example problem.

The nominal unit side and tip resistance for Stratum B and Stratum C are calculated as:

$$q_{s-B} = 29 \cdot 3.5^{-1.14} = 7.0\ ksf, \tag{8.33}$$

$$q_{s-C} = 29 \cdot 1.7^{-1.14} = 15.8\ ksf, \tag{8.34}$$

$$q_{p-B} = 500 \cdot 3.5^{-1.22} = 108.4\ ksf, \text{ and} \tag{8.35}$$

$$q_{p-C} = 500 \cdot 1.7^{-1.22} = 261.7\ ksf. \tag{8.36}$$

Applying the resistance factors, the factored unit side and tip resistance are thus:

$$\phi_{s-B} \cdot q_{s-B} = 0.20 \cdot 7.0\ ksf = 1.4\ ksf \tag{8.37}$$

$$\phi_{s-C} \cdot q_{s-C} = 0.18 \cdot 15.8\ ksf = 2.8\ ksf \tag{8.38}$$

$$\phi_{p-B} \cdot q_{p-B} = 0.56 \cdot 108.4\ ksf = 60.7\ ksf \tag{8.39}$$

$$\phi_{p-C} \cdot q_{p-C} = 0.48 \cdot 261.7\ ksf = 125.6\ ksf \tag{8.40}$$

The factored total resistance was computed for shafts with diameters ranging from 3 to 5 feet, and lengths ranging from 8 to 23 feet. From these calculations, a 4 foot diameter, 15 feet long shaft produces a total factored resistance of 1754 kips, that just exceeds the total factored load. For this shaft, the factored side resistance in Stratum B was 176 kips while the factored tip resistance from Stratum C was 1578 kips. The estimated cost for a 4-foot diameter shaft is $600 per linear foot (Table 8.1), which leads to a total estimated cost of $9,000 per shaft.

8.3.2 Design Using Proposed Method with Greater Uncertainty in Measurements

Since the variability of the actual $MTCP$ measurements is quite low, a second design was performed using a coefficient of variation of 0.50 for the mean $MTCP$ value for both strata. The mean $MTCP$ value for each stratum was kept identical to the previous design (Section 8.3.1). Using these new coefficients of variation, the resistance factor for side resistance for both strata is 0.12, as illustrated in Figure 8.11. Similarly, the resistance factor for tip resistance for both strata is 0.20, as illustrated in Figure 8.12.

The nominal unit side and tip resistance for stratum B and C are again:

$$q_{s-B} = 29 \cdot 3.5^{-1.14} = 7.0\ ksf, \tag{8.41}$$

$$q_{s-C} = 29 \cdot 1.7^{-1.14} = 15.8\ ksf, \tag{8.42}$$

$$q_{p-B} = 500 \cdot 3.5^{-1.22} = 108.4\ ksf, \text{ and} \tag{8.43}$$

$$q_{p-C} = 500 \cdot 1.7^{-1.22} = 261.7\ ksf. \tag{8.44}$$

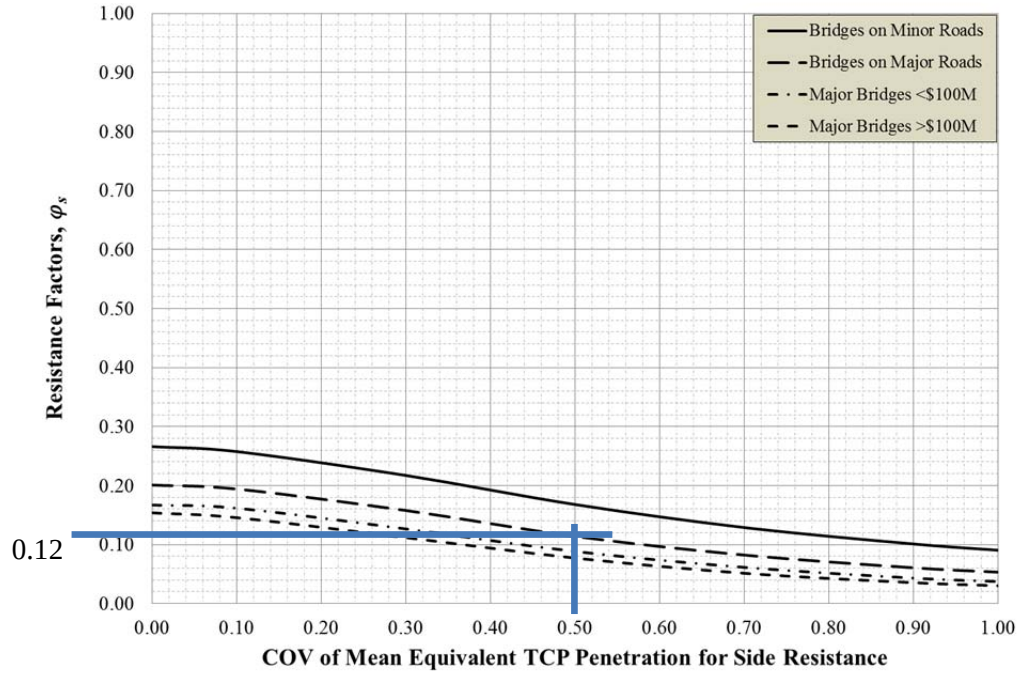

Figure 8.11- Resistance factors for side resistance for proposed MTCP method using greater coefficient of variation. Lines shown reflect specific resistance factors established for Stratum B and Stratum C for example problem.

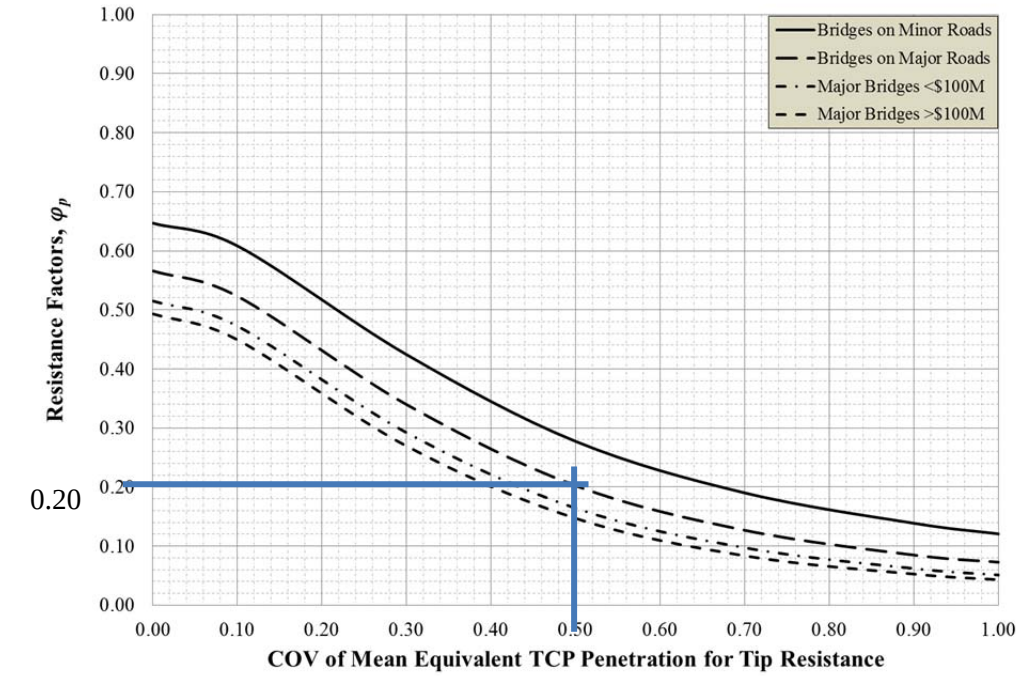

Figure 8.12- Resistance factors for tip resistance for proposed MTCP method using greater coefficient of variation. Lines shown reflect specific resistance factors established for Stratum B and Stratum C for example problem.

Using the revised resistance factors, the factored unit side and tip resistance are:

$$\phi_{s-B} \cdot q_{s-B} = 0.12 \cdot 7.0\ ksf = 0.8\ ksf \quad (8.45)$$

$$\phi_{s-C} \cdot q_{s-C} = 0.12 \cdot 15.8\ ksf = 1.9\ ksf \quad (8.46)$$

$$\phi_{p-B} \cdot q_{p-B} = 0.20 \cdot 108.4\ ksf = 21.7\ ksf \quad (8.47)$$

$$\phi_{p-C} \cdot q_{p-C} = 0.20 \cdot 261.7\ ksf = 52.3\ ksf \quad (8.48)$$

Using these revised values of factored unit side and tip resistance, a 6 foot diameter shaft with a length of 15 feet was found to have a factored total capacity of 1630 kips. The estimated cost for 6 foot diameter shafts (Table 8.1) is $1,000 per linear foot, which produces a total cost of $15,000 per shaft.

8.3.3 Design Using Nam and Vipulanandan Method

The design developed using the method proposed by Nam and Vipulanandan (2010) is based on allowable stress design (ASD) methods, which account for uncertainty through use of a factor of safety rather than through use of load and/or resistance factors. Since such methods to not produce shafts that achieve a specific target probability of failure, the comparisons made here only reflect the anticipated differences in construction costs, and not differences in costs associated with expected differences in performance.

As was the case for the previous calculations, the dead load and live load are taken to be:

DL = 700 kips

LL = 350 kips

So that the total design load, Q, is:

$$Q = DL + LL = 700^k + 350^k = 1050^k$$

The nominal unit side and tip resistance for stratum B and C are calculated as:

$$q_{s-B} = 26.95 * 3.5^{-1.07} = 7.1\ ksf, \tag{8.49}$$

$$q_{s-C} = 26.95 * 1.7^{-1.07} = 15.3\ ksf, \tag{8.50}$$

$$q_{p-B} = 500 * 3.5^{-0.79} = 185.9\ ksf, \text{ and} \tag{8.51}$$

$$q_{p-C} = 500 * 1.7^{-0.79} = 328.8\ ksf. \tag{8.52}$$

Based on the TxDOT Geotechnical Manual (Texas DOT, 2006), the allowable values of unit side and tip resistance are calculated by dividing the nominal unit side and tip resistance by factors of safety (FS) of 3.0 and 2.0, respectively. The allowable unit side and tip resistance are therefore calculated as:

$$\frac{q_{s-B}}{FS} = \frac{7.1\ ksf}{3.0} = 2.4\ ksf, \tag{8.53}$$

$$\frac{q_{s-C}}{FS} = \frac{15.3\ ksf}{3.0} = 5.1\ ksf, \tag{8.54}$$

$$\frac{q_{p-B}}{FS} = \frac{185.9\ ksf}{2.0} = 93.0\ ksf, \text{ and} \tag{8.55}$$

$$\frac{q_{p-C}}{FS} = \frac{328.8\ ksf}{2.0} = 164.4\ ksf. \tag{8.56}$$

Using these values for allowable unit resistance, a 3.0 feet diameter shaft with a length of 15 feet was found to have an allowable capacity of 1388 kips, which just exceeds the required value of 1050 kips. The estimated cost for a 3 foot diameter shaft (Table 8.1) is $400 per linear foot, for a total cost of $6,000 per shaft.

8.3.4 Comparison of Alternative Designs

Table 8.5 provides a summary of results for the three different designs using $MTCP$ measurements. As was the case for the SPT-based design methods, the shaft dimensions and estimated costs produced using the proposed method with different coefficients of variation differ substantially. Since both designs have similar reliability, this result demonstrates that the end product of the design is greatly affected by the coefficient of variation of the mean value for $MTCP$. This coefficient of variation depends on both the variability of the actual $MTCP$ measurements as well as the number of measurements available (true for all types of measurements). The variability of $MTCP$ for a given site is generally beyond the control of the designer, but designers often have substantial control over the number of measurements. Fortunately, the number of measurements has a significant effect on the coefficient of variation, often more so than the effect derived from site variability. As such, designers can directly influence the eventual cost for a project by comparing estimated costs for performing additional measurements with estimated costs for design with and without additional measurements (in a similar manner to that described for SPT measurements in Section 8.2).

As was the case for designs produced from SPT measurements in Section 8.2, the estimated costs derived from a "conventional" design method are substantially less than those derived from the proposed LRFD methods. However, it is again worth noting that such a design does not achieve the desired target reliability; thus, the "construction" cost savings that could be realized by using the conventional design method come with increased risks and increased chances for unacceptable performance.

Table 8.5- Comparison of shafts produced from alternative MTCP design methods for the example problem.

Shaft Characteristics	Proposed MTCP Method		Nam and Vipulanandan
	Actual Measurements	COV=0.5	
Diameter (ft)	4.0	6.0	3.0
Length (ft)	15	15	15
Cost ($)	9,000	15,000	6,000

8.4 Design Using Historical MoDOT Practice

Finally, historical methods used by MoDOT for designing drilled shafts in shale were applied to the example problem to compare designs from those methods with the results of designs performed using the proposed SPT- and MTCP-based methods. The historical method used by MoDOT prior to 2011 is based on results of uniaxial compression tests on intact rock core (MoDOT, 2009) and considers only side resistance (tip resistance is generally neglected). The uniaxial compressive strengths utilized in this example are based on an extensive series of uniaxial compression tests performed at the Frankford site. Based on these measurements, the mean uniaxial compressive strength for Stratum B is 8.0 ksf while the uniaxial compressive strength for Stratum C is 50.0 ksf.

As was the case for the previous calculations, the dead load and live load are taken to be:

DL = 700 kips

LL = 350 kips

so that the total design load, Q, is:

$$Q = DL + LL = 700^k + 350^k = 1050^k$$

The nominal unit side resistance for Stratum B and Stratum C are calculated from Equation 2.1 as:

$$q_{s-B} = 0.65 \cdot 1.0 \cdot 2.12 \cdot \sqrt{{}^{8.0}/_{2.12}} < 7.8 \cdot 2.12 \cdot \sqrt{{}^{576}/_{2.12}} \quad (8.57)$$

$$q_{s-B} = 2.7\ ksf\ < 272.6\ ksf$$

$$q_{s-C} = 0.65 \cdot 1.0 \cdot 2.12 \cdot \sqrt{{}^{50.0}/_{2.12}} = 6.7\ ksf \quad (8.58)$$

Applying a resistance factor of 0.55, as stipulated in MoDOT design guidance, the factored unit side resistance is:

$$\phi_{s-B} \cdot q_{s-B} = 0.55 \cdot 2.7\ ksf = 1.5\ ksf \quad (8.59)$$

$$\phi_{s-C} \cdot q_{s-B} = 0.55 \cdot 6.7\ ksf = 3.7\ ksf \quad (8.60)$$

Based on these values of factored unit side resistance, a 4.5 foot diameter shaft with a length of 40 feet was found to have a factored total resistance of 1520 kips, which just exceeds the required factored load of 1488 kips. The estimated cost for such a shaft is $700 per linear foot, or $24,500 per shaft.

Table 8.6 provides a summary comparison of results for the proposed methods described in this document and historical MoDOT design practice. The table clearly demonstrates that improved efficiency can be achieved by adopting the proposed design methods. Much of this efficiency can be attributed to use of both side and tip resistance for design of drilled shafts in shale. Some of the improved cost effectiveness may be attributed to the fact that the proposed methods will approximately achieve the desired target reliability while the historical method achieves some unknown reliability. The reliability for the historical methods is presumably greater than the target reliability

achieved for the proposed methods, but is highly variable depending on the scope of site characterization for the specific case.

Table 8.6- Comparison of shaft dimensions and costs from proposed methods and historical MoDOT design method.

Shaft Characteristics	Proposed SPT Method	Proposed MTCP Method	2009 MoDOT Method
Diameter (ft)	5.5 – 6.5	4 - 6	4.5
Length (ft)	15	15	40
Cost ($)	13,500 - 16,500	9,000 - 15,000	24,500

8.5 Summary

In this chapter, designs developed using several different design methods have been presented for a realistic example problem based on measurements at the Frankford load test site. The design methods used include the proposed methods for design based on SPT and MTCP measurements, the UCSB method for design using SPT measurements, the method proposed by Nam and Vipulanandan (2010) that uses TCP measurements, and the method used by MoDOT prior to 2011. The results of these analyses and comparison of construction cost estimates for the resulting shafts lead to several notable findings:

1. Estimated costs for shafts designed using the proposed methods are dependent on the number of measurements available and, to a lesser extent, on the variability of the design parameter measurements for a given site.
2. Estimated costs for shafts designed using the proposed methods are substantially less than estimated costs for shafts designed using historical

MoDOT practice. Much of the differences in costs is attributed to the fact that the proposed methods incorporate tip resistance for design while historical MoDOT practice has been to neglect tip resistance.

3. Estimated costs for shafts designed using the proposed methods are generally greater than estimated costs for shafts designed using two "conventional" design methods. However, it is important to note that the conventional design methods do not achieve the desired target reliability; thus, the construction cost savings that could be realized by using the conventional methods is offset by increased risk and increased likelihood of unacceptable performance.

Chapter 9 - Summary, Conclusions and Recommendations

9.1 Summary

Difficulty obtaining quality samples of shale materials for laboratory testing has led geotechnical engineers to consider use of in-situ test measurements as alternative predictors of the ultimate capacity of drilled shafts in shale. Specifically, the Standard Penetration Test (SPT) and the Texas Cone Penetration (TCP) test have been proposed and used for design of drilled shafts in shales. Use of such measurements generally requires that correlations among SPT and TCP measurements and ultimate unit side and tip resistance of drilled shafts be established. Use of such correlations within the framework of Load and Resistance Factor Design (LRFD) methods further requires knowledge regarding the variability and uncertainty associated with such correlations so that probabilistic calibrations can be performed. This document describes work performed to develop empirical methods for design of drilled shafts using SPT and TCP measurements in Missouri shales, including probabilistic calibration of resistance factors for use in the Missouri Department of Transportation's (MoDOT's) Engineering Policy Guide that serves as the basis for design of transportation infrastructure in the State of Missouri.

The present work to develop methods for design of drilled shafts in shale from SPT and TCP measurements included the following broad tasks:

1. conducting load tests on twenty-five full-scale drilled shafts constructed at two shale sites,

2. performing SPT and TCP test measurements at these two sites and five additional sites where load tests had previously been performed,
3. developing proposed relations for predicting the ultimate unit side and tip resistance for drilled shafts in shale from SPT and TCP measurements using regression analyses,
4. quantifying the variability and uncertainty in the proposed predictive relations using statistical analysis, and finally
5. establishing recommended resistance factors for the proposed design methods using probabilistic calibration methods.

The field load test program, described in Chapter 3, included load tests on ten shafts with diameters of 3 and 5 feet and lengths of 20 to 35 feet at one site near Frankford Missouri and fifteen 3-foot diameter shafts with lengths ranging from 30 to 50 feet at another site near Warrensburg Missouri. Standard Penetration Tests (SPT) and Modified Texas Cone Penetration (MTCP) tests were performed at each site to provide data for relating the measured ultimate unit side and tip resistance from the load tests to the in situ test measurements. These data were supplemented with results of other load tests performed for shafts in Missouri shales and in situ tests measurements conducted as part of the current work. Procedures used for the in situ tests were described in Chapter 3 while results of the in situ test measurements at each site were provided in Chapter 4.

Results of regression analyses used to develop the proposed relations for predicting ultimate unit side and tip resistance from SPT and TCP test measurements were presented in Chapters 5 and 6. Summary tables documenting the ultimate unit side and tip resistance measurements from the load tests performed at the Frankford and

Warrensburg sites were presented along with additional measurements from load tests performed by others at several sites across the state. The proposed predictive relations were presented in Chapter 5 while the analyses performed to quantify the variability and uncertainty in the proposed relations were described in Chapter 6.

Analyses performed to develop probabilistically calibrated resistance factors for use with the proposed design relations were described in Chapter 7. The resistance factors were developed to be dependent on the variability and uncertainty in the SPT and MTCP test measurements, which is a function of both the variability present in the in situ test measurements as well as the number of in situ test measurements performed within a given stratum. Separate resistance factors were also developed for four different roadway classifications, each having a different target probability of failure. An important result of the proposed resistance factors is that they will lead to achieving a consistent and appropriate reliability for drilled shafts when used with the proposed predictive relations. The resistance factors were presented in the form of charts for use in the MoDOT Engineering Policy Guide.

Finally, the proposed methods were applied to a practical example problem as described in Chapter 8 to illustrate application of the proposed methods. Results from the proposed methods were also compared to results obtained using several alternative design methods to illustrate the anticipated effect of adopting the proposed design methods compared to several relevant existing design methods.

9.2 Conclusions

The proposed design relations and associated resistance factors are recommended for design of drilled shafts from SPT and MTCP test measurements in shale. For design using SPT measurements, the ultimate unit tip resistance can be predicted from the mean value of N_{eq-60} as

$$q_p = 0.95 * \overline{N_{eq-60}} \quad (9.1)$$

and the ultimate unit side resistance can be similarly predicted as

$$q_s = \frac{\overline{N_{eq-60}}}{15} \quad (9.2)$$

Both of these relations are similar to those for the UCSB method proposed by Abu-Hejleh et al. (2003) if a factor of safety of 2.0 is assumed for the UCSB method (the UCSB method predicts "allowable" unit capacities so a factor of safety must be assumed for comparison with ultimate unit capacities).

For design using MTCP measurements, the ultimate unit tip resistance can be predicted from the mean value of $MTCP$ as

$$q_p = 500 \cdot \overline{MTCP}^{-1.22} \quad (9.3)$$

This relation produces estimates of ultimate unit tip resistance that are substantially greater than those predicted using either the existing Texas Department of Transportation (TXDOT) method (TXDOT, 2006) or the method proposed by Nam and Vipulanandan (2010). Similarly, the ultimate unit side resistance can be predicted from $MTCP$ measurements as

$$q_s = 29 \cdot \overline{MTCP}^{-1.14} \quad (9.4)$$

This relation produces estimates of ultimate unit side resistance that are similar to those produced using the method proposed by Nam and Vipulanandan (2010) but substantially lower than those predicted using the existing TXDOT method (TXDOT, 2006).

Recommended resistance factors for each of the proposed design relations were developed to achieve established target reliabilities for different roadway classifications and to be dependent on the variability and uncertainty present in the mean value of N_{eq-60} or $MTCP$, as represented by the coefficient of variation of the mean value of the parameters. This coefficient of variation is generally dependent on both the variability of N_{eq-60} or $MTCP$ measurements and on the number of available measurements. For a given site with given variability, the designer's primary influence on the coefficient of variation is through dictating the number of measurements, with the coefficient of variation being reduced substantially as the number of measurements increases.

There is substantial uncertainty in the proposed relations between SPT N_{eq-60} and the ultimate unit side and tip resistance. Predictions of ultimate unit side resistance from N_{eq-60} (Eq. 9.2) have a coefficient of variation of approximately 60 percent while predictions of ultimate unit tip resistance from N_{eq-60} (Eq. 9.1) have a coefficient of variation of approximately 50 percent. These results suggest that SPT measurements are generally not a precise or reliable predictor of ultimate unit side and tip resistance for drilled shafts in shale. Predictions of unit side resistance from $MTCP$ (Equation 9.4) also have a coefficient of variation of approximately 60 percent, which similarly suggests that MTCP measurements are not a terribly reliable predictor of unit side resistance for drilled shafts in shale.

In contrast, however, predictions of unit tip resistance from $MTCP$ (Equation 9.3) have a coefficient of variation of approximately 25 percent, which is substantially less than coefficients of variation for the other proposed relations and is similar to or less than coefficients of variation for many other design approaches. This suggests that $MTCP$ is generally a reliable predictor of unit tip resistance for drilled shafts in shale, that is as good, or better than many alternative predictors.

Recommended resistance factors to achieve established target probabilities of failure are generally reflective of the uncertainty present for the respective design relations, the selected target reliability, and the coefficient of variation of the respective design parameter (N_{eq-60} or $MTCP$). Recommended resistance factors for use with Equations 9.1, 9.2, and 9.4 are thus quite low, generally less than 0.35, whereas resistance factors recommended for use with Equation 9.3 are much greater, up to 0.65.

For each of the proposed relations, required resistance factors to achieve a given target reliability are greatest for low values of the coefficient of variation for the design parameter (i.e. when the design parameter is well established using a large number of measurements). Substantially lower resistance factors are required when the coefficient of variation for the design parameter is greater (i.e. when the design parameter is less well established using fewer measurements). However, the relatively large uncertainty associated with Equations 9.1, 9.2, and 9.4 tends to diminish the effect of the number of SPT or MTCP measurements because the fundamental design relation is so uncertain. As such, increasing the number of in situ test measurements will have a greater impact on design when using Equation 9.3 than when using the other proposed relations.

The proposed design relations and associated resistance factors provide a sound basis upon which to judge whether increasing the number of SPT and/or MTCP tests is likely to be cost effective for design of drilled shafts in shale using SPT or MTCP test measurements. Such evaluations can be accomplished by developing cost estimates for designs developed using the proposed methods considering different test quantities and comparing the potential cost savings to the expected cost for the expanded investigations. Such evaluations are similar to analyses presented in Chapter 8. While such evaluations are new and may have a "learning curve", it is anticipated that designers will rapidly develop good judgment regarding conditions where expanded investigations are likely to produce cost savings with relatively little experience using the proposed methods.

Finally, comparison of drilled shafts designed using the proposed methods with drilled shafts designed using historical MoDOT design procedures for a representative example problem suggest that use of the proposed methods will result in substantial cost savings compared to historical practice. Similar evaluations performed to compare the proposed methods to the UCSB method (Abu-Hejleh et al., 2005) and the method proposed by Nam and Vipulanandan (2010) suggest that the proposed methods will produce shafts that are more costly than would be produced using these alternative methods. However, it is important to note that the UCSB method and the method proposed by Nam and Vipulanandan do not achieve the target reliabilities established by MoDOT. Thus, while use of these alternative methods may produce lower construction costs, such savings will be offset by increased risk and increased likelihood of unacceptable performance.

9.3 Recommendations for Future Work

A number of recommendations for future work can be made based on experiences gained from this research. Several recommendations for future work are described here:

1. Because the proposed methods are empirical, it is always possible that consideration of additional measurements could suggest revisions or refinement of the findings of the present work. It is therefore recommended that SPT and MTCP measurements be performed at sites where future load tests are conducted in shale so that future evaluation of the proposed methods can occur.
2. Consideration should be given to developing appropriate methods for "site specific" calibration of design methods using SPT or TCP measurements. It is notable that the uncertainty in a "site specific" design method will inevitably be less than the uncertainty in the proposed methods, but will require site specific load testing.
3. The present work is based on "modified" Texas Cone Penetration tests that were performed using a conventional SPT hammer that differs from the hammer prescribed in the TXDOT Geotechnical Manual. The SPT hammer used has a similar theoretical hammer energy to the prescribed hammer so it seems unlikely that use of the prescribed hammer will substantially affect the finds of the present work. Nevertheless, a series of comparative tests using both the conventional SPT hammer and the prescribed hammer in the TXDOT standard should be performed to evaluate whether the "modified" TCP values used for the present work are practically identical to standard TCP measurements.

The resistance factors developed for side and tip resistance in this research were developed considering side and tip resistance independently as described in Chapter 7. Such resistance factors are appropriate when designing drilled shafts in conditions where shaft capacity is derived predominantly from either side or tip resistance. However, these same resistance factors will be conservative in cases where shafts derive substantial resistance from both side and tip resistance. Since such cases are relatively common and such cases provide an opportunity to realize additional cost savings, analyses should be performed to evaluate the potential cost savings that could be realized by more precisely considering shaft reliability when capacity is derived from both side and tip resistance. If such analyses demonstrate that potential cost savings are substantial, then work should be performed to develop practical methods to reliably account for the improved reliability when both side and tip resistance are substantial.

Appendix: Resistance Factors for Design of Drilled Shafts Using SPT and MTCP Measurements

Table A.1- Resistance factors for tip and side resistance determined from SPT measurements for Bridges on Minor Roads

COV	ϕ_s	ϕ_p
0.000	0.258	0.339
0.100	0.250	0.328
0.300	0.204	0.260
0.500	0.145	0.181
0.700	0.098	0.119
0.900	0.066	0.080
1.000	0.055	0.066

Table A.2- Resistance factors for tip and side resistance determined from SPT measurements for Bridges on Major Roads

COV	ϕ_s	ϕ_p
0.000	0.194	0.266
0.100	0.189	0.257
0.300	0.148	0.196
0.500	0.101	0.130
0.700	0.065	0.081
0.900	0.041	0.051
1.000	0.033	0.041

Table A.3- Resistance factors for tip and side resistance determined from SPT measurements for Major Bridges (<$100 million)

COV	ϕ_s	ϕ_p
0.000	0.162	0.228
0.100	0.154	0.215
0.300	0.120	0.162
0.500	0.078	0.102
0.700	0.048	0.061
0.900	0.030	0.038
1.000	0.024	0.030

Table A.4- Resistance factors for tip and side resistance determined from SPT measurements for Major Bridges (>$100 million)

COV	ϕ_s	ϕ_p
0.000	0.144	0.204
0.100	0.138	0.199
0.300	0.106	0.146
0.500	0.069	0.091
0.700	0.042	0.054
0.900	0.026	0.032
1.000	0.020	0.025

Table A.5- Resistance factors for tip resistance determined from MTCP measurements for a range in $MTCP$ values for Bridges on Minor Roads

COV	$TCP = 1$	$TCP = 4$	$TCP = 8$	AVG
0.000	0.601	0.699	0.641	0.647
0.100	0.567	0.656	0.602	0.608
0.300	0.405	0.446	0.422	0.424
0.500	0.266	0.289	0.277	0.277
0.700	0.183	0.197	0.190	0.190
0.900	0.133	0.143	0.140	0.139
1.000	0.117	0.124	0.120	0.121

Table A.6- Resistance factors for tip resistance determined from MTCP measurements for a range in $MTCP$ values for Bridges on Major Roads

COV	$TCP = 1$	$TCP = 4$	$TCP = 8$	AVG
0.000	0.522	0.619	0.557	0.566
0.100	0.483	0.568	0.517	0.523
0.300	0.322	0.359	0.337	0.339
0.500	0.194	0.212	0.201	0.202
0.700	0.123	0.133	0.124	0.127
0.900	0.083	0.087	0.084	0.085
1.000	0.070	0.075	0.073	0.073

Table A.7- Resistance factors for tip resistance determined from MTCP measurements for a range in $MTCP$ values for Major Bridges (<$100 million)

COV	$TCP = 1$	$TCP = 4$	$TCP = 8$	AVG
0.000	0.468	0.571	0.506	0.515
0.100	0.434	0.519	0.464	0.472
0.300	0.273	0.312	0.290	0.292
0.500	0.156	0.173	0.162	0.164
0.700	0.094	0.099	0.098	0.097
0.900	0.059	0.065	0.061	0.062
1.000	0.049	0.051	0.052	0.051

Table A.8- Resistance factors for tip resistance determined from MTCP measurements for a range in $MTCP$ values for Major Bridges (>$100 million)

COV	$TCP = 1$	$TCP = 4$	$TCP = 8$	AVG
0.000	0.447	0.547	0.486	0.493
0.100	0.413	0.493	0.442	0.449
0.300	0.253	0.285	0.269	0.269
0.500	0.141	0.152	0.147	0.147
0.700	0.083	0.086	0.081	0.083
0.900	0.050	0.053	0.054	0.053
1.000	0.042	0.044	0.043	0.043

Table A.9- Resistance factors for side resistance determined from MTCP measurements for a range in $MTCP$ values for Bridges on Minor Roads

COV	$TCP = 1$	$TCP = 4$	$TCP = 8$	AVG
0.000	0.258	0.275	0.266	0.266
0.100	0.251	0.266	0.256	0.258
0.300	0.212	0.223	0.216	0.217
0.500	0.163	0.172	0.168	0.168
0.700	0.126	0.131	0.130	0.129
0.900	0.100	0.103	0.100	0.101
1.000	0.088	0.092	0.091	0.090

Table A.10- Resistance factors for side resistance determined from MTCP measurements for a range in $MTCP$ values for Bridges on Major Roads

COV	$TCP = 1$	$TCP = 4$	$TCP = 8$	AVG
0.000	0.194	0.209	0.200	0.201
0.100	0.188	0.202	0.192	0.194
0.300	0.154	0.163	0.157	0.158
0.500	0.111	0.117	0.114	0.114
0.700	0.081	0.084	0.082	0.082
0.900	0.060	0.062	0.060	0.061
1.000	0.052	0.053	0.054	0.053

Table A.11- Resistance factors for side resistance determined from MTCP measurements for a range in $MTCP$ values for Major Bridges (<$100 million)

COV	$TCP = 1$	$TCP = 4$	$TCP = 8$	AVG
0.000	0.163	0.172	0.166	0.167
0.100	0.156	0.168	0.161	0.162
0.300	0.124	0.130	0.126	0.127
0.500	0.087	0.090	0.087	0.088
0.700	0.061	0.063	0.060	0.061
0.900	0.042	0.043	0.044	0.043
1.000	0.038	0.037	0.037	0.037

Table A.12- Resistance factors for side resistance determined from MTCP measurements for a range in $MTCP$ values for Major Bridges (>$100 million)

COV	$TCP = 1$	$TCP = 4$	$TCP = 8$	AVG
0.000	0.147	0.161	0.153	0.154
0.100	0.140	0.151	0.145	0.146
0.300	0.111	0.115	0.110	0.112
0.500	0.077	0.077	0.078	0.077
0.700	0.050	0.053	0.052	0.051
0.900	0.034	0.036	0.036	0.035
1.000	0.031	0.030	0.030	0.030

REFERENCES

AASHTO (1996), *Standard Specifications for Highway Bridges*, 16th edition, American Association of State Highway Transportation Officials, Washington, D.C.

AASHTO Standard T152 (2010), "Standard Method of Test for Air Content of Freshly Mixed Concrete by the Pressure Method", American Association of State Highway Transportation Officials, Washington, D.C.

AASHTO Standard T119M/T119 (2010), "Standard Method of Test for Slump of Hydraulic Cement Concrete", American Association of State Highway Transportation Officials, Washington, D.C.

Abu-Hejleh, N., M.W. O'Neill, D. Hannerman, and W.J. Attwool (2003), *Improvement of the Geotechnical Axial Design Methodology for Colorado's Drilled Shafts Socketed in Weak Rocks*, Report No. CDOT-DTD-R-2003-6, Colorado Department of Transportation – Research, Denver, Colorado.

Abu-Hejleh, N.M, M.W. O'Neill, D. Hannerman, and W.J. Attwool (2005) "Improvement of the Geotechnical Axial Design Methodology for Colorado's Drilled Shafts Socketed in Weak Rocks", *Transportation Research Record: Journal of the Transportation Research Board*, No. 1936, Transportation Research Board of the National Academies, Washington, D.C., 2005, pp 100-107.

Ang, A. H-S., W.H. Tang (1975), *Probability Concepts in Engineering Planning and Design*, 1st Ed., Wiley, New York.

ASTM C1621/C1621M (2009), "Standard Test Method for Passing Ability of Self Consolidating Concrete by J-Ring", ASTM International, Rev. B, West Conshohocken, PA.

ASTM D1586 (2008), "Standard Test Method for Standard Penetration Test (SPT) and Split-Barrel Sampling of Soils", ASTM International, West Conshohocken, PA.

Baecher, G.B., and J.T. Christian (2003), *Reliability and Statistics in Geotechnical Engineering*, John Wiley and Sons, 605 pp

Google Earth (2011a), 38º 56' 08.74" N and -92º 22' 17.03" E. Google Earth. May 3, 2010, August 13, 2011.

Google Earth (2011b), 38º 46' 12.76" N and -93º 42' 48.50" E. Google Earth. June 15, 2009, August 13, 2011.

Google Earth (2011c), 38º 08’ 58.34” N and -90º 56’ 47.11” E. Google Earth. May 3, 2010, October 29, 2011.

Google Earth (2011d), 39º 28’ 45.38” N and -91º 18’ 17.85” E. Google Earth. May 3, 2010, August 13, 2011.

Google Earth (2011e), 38º 46’ 24.72” N and -93º 41’ 19.73” E. Google Earth. June 15,2009, August 15, 2011.

Google Earth (2011f), 38º 56’ 19.13” N and -94º 31’ 56.16” E. Google Earth. May 3, 2010, August 15, 2011.

Google Earth (2011g), 38º 55’ 58.72” N and -94º 31’ 44.29” E. Google Earth. May 3, 2010, August 15, 2011.

Google Earth (2011h), 38º 11’ 46.57” N and -93º 52’ 17.39” E. Google Earth. June 15, 2009, August 16, 2011.

Google Earth (2011i), 39º 12’ 34.67” N and -93º 51’ 48.73” E. Google Earth. June 15, 2009, August 16, 2011.

Google Earth (2011j), 39º 06’ 33.30” N and -93º 34’ 51.58” E. Google Earth. May 3, 2010, August 17, 2011.

Google Earth (2011k), 39º 07’ 24.80” N and -94º 33’ 59.67” E. Google Earth. May 3, 2010, August 17, 2011.

Google Earth (2011l), 39º 12’ 53.42” N and -93º 30’ 42.64” E. Google Earth. February 11, 2005, August 17, 2011.

Google Earth (2011m), 39º 12’ 58.65” N and -93º 30’ 41.98” E. Google Earth. February 11, 2005, August 17, 2011.

Google Earth (2011n), 39º 32’ 34.32” N and -94º 43’ 07.41” E. Google Earth, June 5, 2011, June 30, 2012.

Google Earth (2011o), 39º 33’ 02.59” N and -94º 40’ 39.91” E. Google Earth. August 27, 2010, August 17, 2011.

Huaco, D.R., J.J. Bowders, and J.E. Loehr (2012), “Method to Develop Target Levels of Reliability for Design Using LRFD,” *Compendium of Papers for the 91st Annual Transportation Research Board Annual Meeting*, Washington, D.C., January 22-26, 2012 (CD-ROM).

Kulicki, J. M., Z. Prucz, C.M. Clancy, D.R. Mertz, and A.S. Nowak (2007), *Updating the calibration report for AASHTO LRFD code*, Final Rep. for National Cooperative Highway Research Program, Project No. NCHRP 20-7/186, 120 pp.

Loehr, J.E., J.J. Bowders, L. Ge, W.J. Likos, R. Luna, N. Maerz, B.L. Rosenblad, and R.W. Stephenson (2011), *Engineering Policy Guidelines for Design of Drilled Shafts*, Missouri Department of Transportation, Final Report for Project TRyy0922, Report cmr12003, 75 pp.

Miller, A. (2003), *Prediction of Ultimate Side Shear for Drilled Shafts in Missouri Shales*,
Masters Thesis , Department of Civil Engineering, University of Missouri, Columbia, Missouri.

MoDOT (2009), *Engineering Policy Guide*, Section 321, Missouri Department of Transportation, Web document, July 1, 2009.
<http://epg.modot.gov/index.php?title=Category:321_Geotechnical_Engineering>

MoDOT (2013), "Procedures for Estimation of Geotechnical Parameter Values and Coefficients of Variation", *Engineering Policy Guide*, Section 321.3, Missouri Department of Transportation, Web document, October 2, 2013
<http://epg.modot.gov/index.php?title=321.3_Procedures_for_Estimation_of_Geotechnical_Parameter_Values_and_Coefficients_of_Variation>.

Nam, M.S., and C. Vipulanandan (2010), "Relationship between Texas Cone Penetrometer Tests and Axial Resistances of Drilled Shafts Socketed in Clay Shale and Limestone," *Journal of Geotechnical and Geoenvironmental Engineering*, Vol. 136, No. 8, pp. 1161-1165.

O'Neill, M.W., and L.C. Reese (1999), *Drilled Shafts: Construction Procedures and Design Methods*, Federal Highway Administration, FHWA-IF-99-025, 758 pp.

Thompson, T.L. (1995), *The Stratigraphic Succession in Missouri (Revised - 1995)*, Missouri Department of Natural Resources, Division of Geology and Land Survey, Vol 40, 190 pp.

TXDOT (2006). *Texas Department of Transportation Geotechnical Manual*, Texas Department of Transportation, 57 pp.

TXDOT (1999). "Test Procedure for Texas Cone Penetration." TxDOT Designation: Tex-132-E

URS Corporation (2007), "Design Skin Friction and End-bearing of Drilled Shafts in Shale, I-64 Project", *Unpublished Memorandum*.